UNIVERSITÀ DEGLI STUDI
DI MILANO

SCHOOL OF AGRICULTURE ENVIRONMENT AND BIOENERGY, XXXII CYCLE

DEPARTMENT OF AGRICULTURAL AND ENVIRONMENTAL SCIENCE

Microbial electrochemical sensors for freshwater and wastewater monitoring

MATTEO TUCCI

Matr. n°R11555

Tutor: Dr. ANDREA SCHIEVANO

Co-tutors: PIERANGELA CRISTIANI

Prof. STEFANO BOCCHI

Coordinator: Prof. DANIELE BASSI

A.A. 2019

"Environmental pollution is an ***incurable disease****.*

It can only be prevented."

Barry Commoner, 1998

TABLE OF CONTENENTS:

ABBREVIATIONS

AC	=	Activated Carbon
BES	=	Bioelectrochemical systems
BOD	=	Biological Oxygen Demand
BQ	=	para-benzoquinone
CA	=	Chronoamperometry
CE	=	Counter Electrode
CN	=	Carbon Nanotubes
COD	=	Chemical Oxygen Demand
CV	=	Cyclic Voltammetry
DET	=	Direct Electron Transfer
EET	=	Extracellular Electron Transfer
GDL	=	Gas Diffusion Layer
LOD	=	Limit of Detection
LLOD	=	Lower Limit of Detection
MEC	=	Microbial electrolysis Cell
MES	=	Microbial Electrochemical System
MFC	=	Microbial Fuel Cell
MET	=	Mediated electron Transfer
NBS	=	Nature Based Solutions
ORR	=	Oxygen Reduction Reaction
PE	=	Population Equivalent

PSI = Photosystem I

PSII = Photosystem II

RE = Reference Electrode

SCE = Standard Calomel Electrode

sCOD = soluble COD

SEM = Scanning Electron Microscopy

TOC = Total Organic Carbon

ULOD = Upper Limit of Detection

WE = Working Electrode

WW = Wastewater

ABSTRACT

Freshwater is essential for socioeconomic development, health of the population and equilibrium of the ecosystem. However, pollution generated by human activities often degrade the quality of this vital resource. In order to address this problem with effective management strategies, continuous assessment of freshwater and wastewater status is necessary. Microbial electrochemical systems (MESs) are attracting increasing attention as sensing tools, due to their low-cost, sustainability, portability, generation of continuous on-line signal and low involvement of operators. In this dissertation, the implementation of MESs as sensors in two different environmental contexts is discussed: wastewater treatment monitoring and agriculture-related pollutants detection. Different prototypes were designed according to their specific application and their detection capabilities were investigated.

Regarding the monitoring of wastewater treatment process, floating Microbial Fuel Cells (MFCs) were tested as sensors for organic matter, a parameter that is currently measured with the labour-intensive and time-consuming BOD_5 test. The first prototype consisted of a floating frame holding two carbon cloth electrodes separated by a polypropylene felt and a clay layer. The biosensor was tested in the lab using real wastewater as both electrolyte and inoculum, and a calibration curve was obtained. However, when the device was tested in the plant of Carimate (CO), a strong influence of light irradiation on the signal was noticed. During a month of operations, a correspondence between the peaks of voltage and of the peaks of organic load was present, but the signal was delayed of about two days. To further understand the influence of different environmental factors on the current signal, a new device was conceived and compared with the previous configuration. This time the experimentation was carried out at the plant of Bresso Niguarda (MI). The new setup consisted in a cylindrical terracotta separator sealed at one end and held perpendicularly to the wastewater surface by a plastic floater. The carbon cloth anode was placed outside the cylinder, while a cathode of the same material was located inside. Light irradiation, temperature, sCOD and nitrates were continuously monitored for about 20 days. An automatic sampler was built to obtain wastewater samples every two hour every day. The correlation between the physical-chemical parameters and the cell voltages was quite poor, especially for the floating type, which was often subjected to the inversion of the electrodes potential. This was probably due to oxygen diffusion in the first layer of wastewater. The microbial

analysis of the biofilms confirmed this aspect, as aerobic strains (e.g. *Nocardicaceae*) were found on the anodes, and electrogenic bacteria usually present on anodes were found on the cathodes (i.e. *Geobacteriaceae*).

To monitor agriculture-related pollutants (i.e. herbicides), amperometric biosensors based on the inhibition of cyanobacterial photocurrent were studied. Many herbicide compounds are harmful to humans and the environment, and they are currently measured with classic analytic techniques (e.g. HPLC, GC-MS, etc.), which are expensive and time consuming. To build the first prototype, *Anabaena variabilis* cells were entrapped on a carbon felt electrodes using an alginate hydrogel, and p-benzoquinone was used as electron shuttle to sustain the electron transfer. With this device it was possible to obtain concentration-current calibration curves for two commonly used herbicides (i.e. diuron and atrazine), and the obtained linear range was suitable for environmental analysis. However, to build a long lasting device, a mediatorless configuration is preferable, as the redox mediator is cytotoxic and can undergo photodegradation. For this reason, a new biosensor was created: a paper-based electrode coated with carbon nanotube paint and a titanium nanolayer was used as substrate for the formation of a *Synechocystis wt.* biofilm. Whit this configuration, only a presence/absence inhibition signal could be obtained for atrazine and diuron, while the herbicide paraquat temporarily enhanced the electron transfer due to its redox mediator capabilities. Nevertheless, this biosensor was able to maintain its sensitivity even after it was kept in the fridge for 22 days, proving its potential as long-lasting device which can be easily stored or shipped after preparation.

These results demonstrated that microbial electrochemical sensors are a promising technology for sensing applications, with a great potential for the creation of a smart, diffuse grid of low-cost sensors for the continuous monitoring of water quality. However, further improvements are needed in order to reduce the response time, improve the sensitivity and discern between the influence of different environmental factors on the signal.

1. INTRODUCTION

1.1 Historical context

1.1.1 Water pollution, treatment and monitoring

Freshwater is essential for human health, socioeconomic development and the ecosystem. However, most of it is stored in groundwater and ice caps, and thus not immediately available [1]. Moreover, despite its constant regeneration through natural processes, freshwater is increasingly endangered by pollution. Once polluted, it is difficult and expensive to restore its pristine quality [2]. For this reasons, freshwater is a renewable yet scarce resource, and the concern for the deterioration of water supplies due to the impact of human activities is constantly rising. The unprecedented demographic growth, together with the change in the consumption pattern, is exacerbating these negative effects at an increasing scale (**Fig.1**).

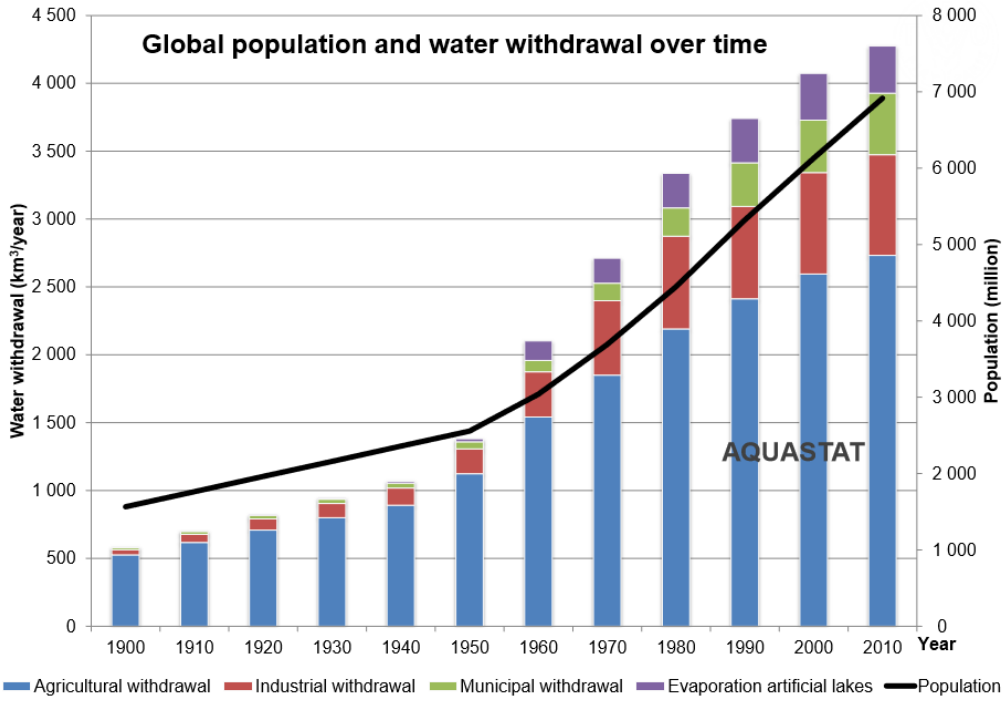

Figure 1 – Histogram of the growth of water consumption and population from 1900 to the present decade. The population growth is indicated with a black line. FAO – fao.org

According to "The United Nations World Water Development Report 2019: Leaving No One Behind" [3], global water demand is likely to rise at a constant rate until 2050. This will result in an increase

of water use about 20 - 30% above the current level, mainly due to the expansion of industrial and domestic sectors. Over 2 billion people already live in countries affected by high water stress, and nearly 4 billion people suffer serious water scarcity for at least one month per year (**Fig. 2**). As the demand for water grows and the effects of climate change intensify, those stress levels are likely to escalate.

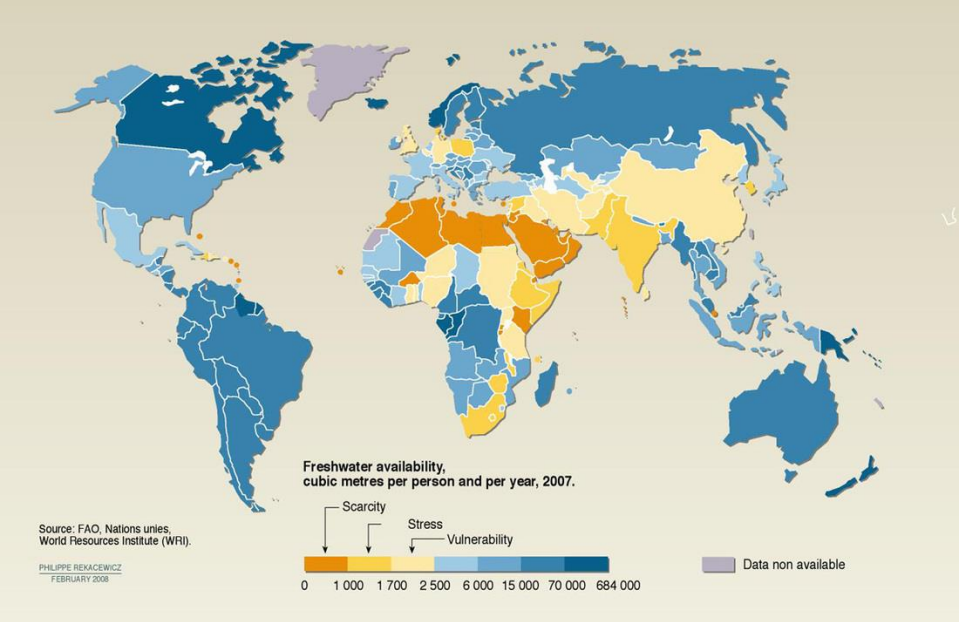

Figure 2 – Global map of the reshwater availability for the different states in 2007- FAO – fao.org

The major sources of water pollution are human settlements, industrial activities and intensive agriculture. About 80% of municipal wastewater is discharged directly into water bodies without any treatment, and industry is accountable for the release of millions of tonnes of heavy metals, solvents, toxic sludge and other contaminants per year [4]. Agriculture plays a major part in water pollution, as it is responsible for 70% of water withdrawal globally: in the process a huge amounts of pesticides, fertilizers, organic matter, drug residues, sediments and saline drainage are discharged into water bodies. All these contributes combined pose a serious threat for aquatic ecosystems, human health and productive activities [5]. Some of these pollutants tend to accumulate in the environment due to their slow degradation rates (e.g. pesticides, herbicides, heavy metals, etc.), and remain stored in plant, animal and human tissues, where their toxic impact is magnified [6].

In 2015, the United Nations General Assembly approved the 2030 Agenda for Sustainable Development, which consists of 17 Goals (SDGs) to be completed by the year 2030 (**Fig. 3**). Goal n°6

states: “Ensure availability and sustainable management of water and sanitation for all” [7]. According to the head of Water and Soil Laboratory at ATREE (Ashoka Trust for Research in Ecology and the Environment) Dr. Priyanka Jamwal, this goal is a key point of the entire Agenda, as its resolution would greatly affect every other sector in a positive way. In order to achieve goal n°6, especially regarding the targets 6.3, 6.5 and 6.6 (**Tab. 1**), an efficient water management system is needed. This can be only realized with constant assessment of water quality, the implementation of efficient infrastructures and effective wastewater treatment.

Figure 3. Sustainable Developement Goals for 2030 set by the United Nations – globalgoals.org

Table 1 - Targets 6.3, 6.5 and 6.6 from the Sustainable Development Goals (2015) – globalgoals.org

Target n°	Description
6.3	By 2030, improve water quality by reducing pollution, eliminating dumping and minimizing release of hazardous chemicals and materials, halving the proportion of untreated wastewater and substantially increasing recycling and safe reuse globally
6.5	By 2030, implement integrated water resources management at all levels, including through transboundary cooperation as appropriate
6.6	By 2020, protect and restore water-related ecosystems, including mountains, forests, wetlands, rivers, aquifers and lakes

Water treatment is a process aimed at purifying, disinfecting and protecting water against recontamination. It usually involves several chemical, physical and biological steps, depending on the typology and concentration of contaminants present in the water (**Fig. 4**). The most common methods rely on constant energy input (mainly electricity), which can be not practically feasible in most developing countries. In such places, low-tech solutions have also been implemented, but usually they are not scalable and sometimes do not guarantee the safety of water for drinking purposes [3]. Therefore, a key factor to ensure the system efficacy and the safety of the population is the constant monitoring of wastewater treatment process.

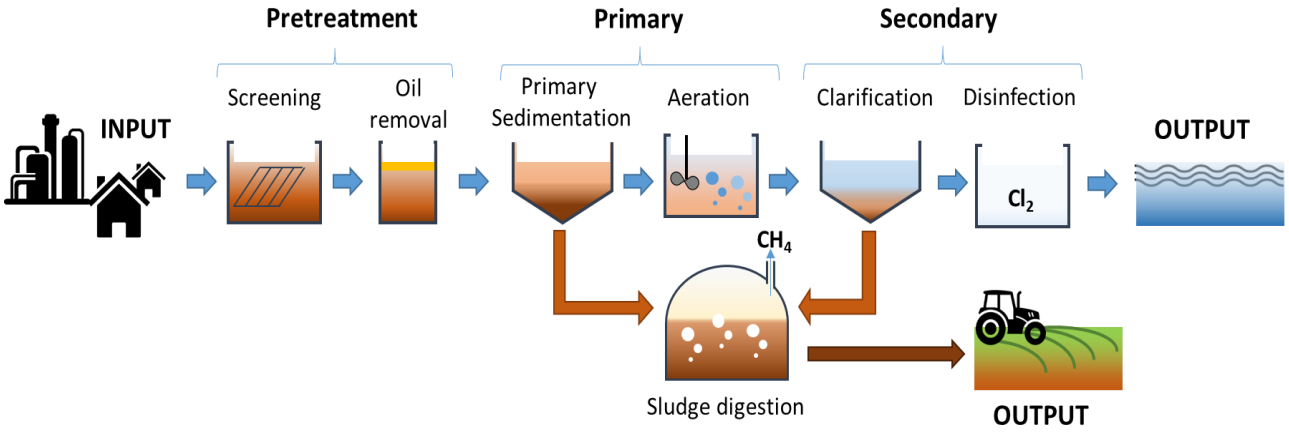

Figure 4 – Schematic representation of the different chemical, physical and biological steps of the wastewater treatment process

1.1.2 Environmental monitoring, nature-based solutions and smart sensors

Continuous and diffuse environmental monitoring is crucial to implement effective strategies to prevent and reduce pollution and preserve the ecosystem. Environmental monitoring means to observe the changes occurring in the environment due to natural cycles and anthropogenic impacts with scientific methods. The effects of pollution can have different scales in terms of time (i.e. chronic vs. acute) and spatial (i.e. local vs. global), therefore different sensing systems need to be used simultaneously to obtain information at multiple scales. Other than broad-scoped data collection, statistically based data processing and objective interpretations are needed to have an understanding of the quality of the environmental compartments [8].

In the present times, society is facing increasing challenges posed by unsustainable urbanisation, population growth, degradation and loss of natural capital and climate change. Such

problems have a strong impact on the ecosystem services, which consist in all the direct and indirect benefits provided by nature (e.g. climate regulation, water purification, soil fertilization, pollination, cultural and recreational services, etc.) that sustain the well-being of the human population [9]. A schematic representation of the different ecosystem service is presented in **figure 5**.

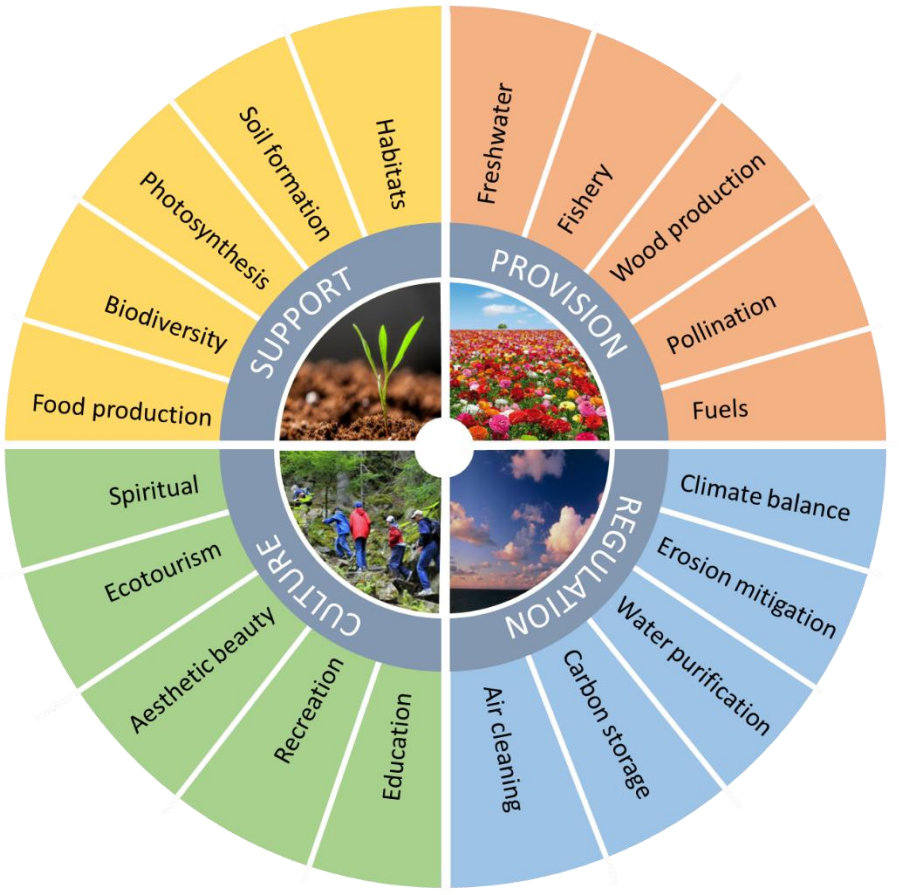

Figure 5 – Examples of ecosystem services divided in four categories: provision, support, culture and regulation

Thanks to a deeper understanding of the mechanisms of nature and its relationship with the anthropic environment, these issues can be addressed whit new approaches, for example utilizing Nature-based Solutions (NBS). NBS are sustainable methods inspired or supported by nature that can replace existing technologies: one approach consists in enhancing existing natural solutions, while the other aims to mimic how living organisms and communities cope with environmental stress [10]. This approach ensures the maintenance (or enhancement) of natural capital, together with the associated the ecosystem services, energy and resource-efficiency and resilience to change. However, in order to be successful, NBS must be specifically designed and adapted to local

conditions. Moreover, their efficacy needs to be constantly analysed, to ensure that quality of the provided service is maintained.

Another important novelty is the paradigm shift from sparse monitoring stations and costly short-term field measurements to integrated networks of on-line sensors. This new approach can provide continuous information regarding all the different aspects of the environment. Thanks to the computing capabilities of the modern era, processing and modelling of great amounts of data in real time is becoming more and more feasible [11]. However, the major problem related with ubiquitous sensing is represented by the acquisition of extensive amounts data which may have different accuracy, precision and quality. A different approach to diffuse sensing is represented by Smart Sensors, which are devices with an integrated processor that can give an informative output directly to the user [12]. This concept, combined with the Internet of Things can lead to the creation of Smart cities where the citizens are more involved and responsible in the management of environmental issues (**Fig. 6**)

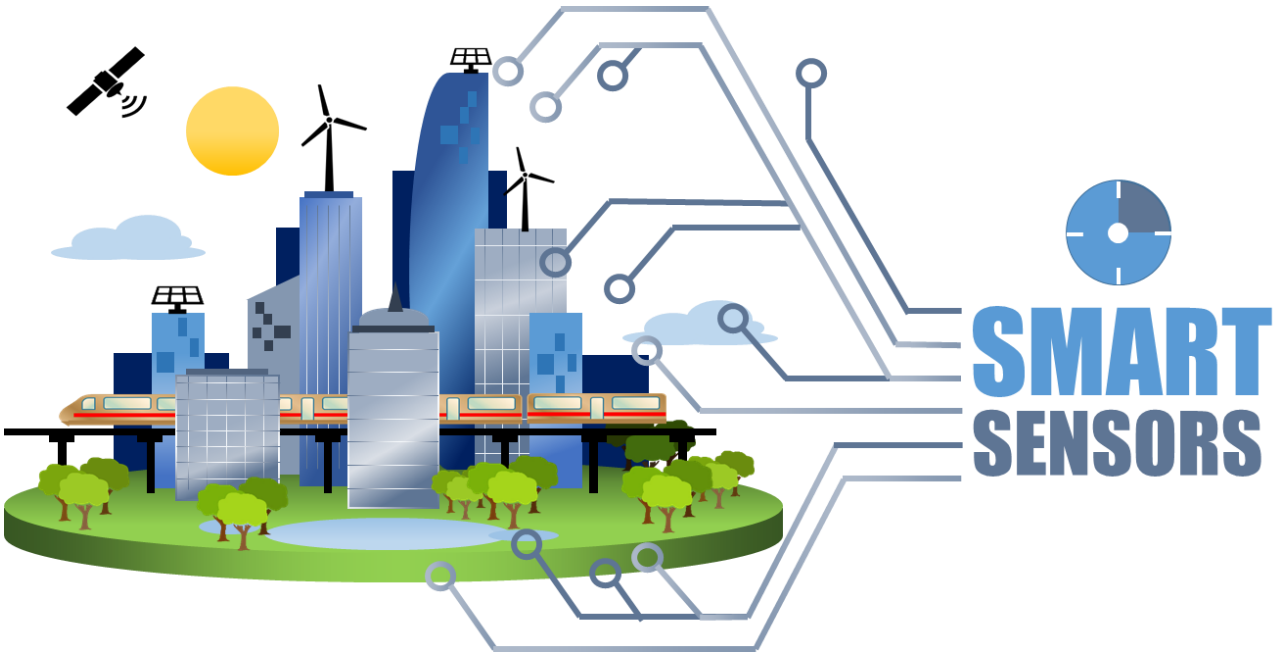

Figure 6 – Artwork representing a smart city, where the quality of the environment is constantly monitored with in real-time with smart sensors

Microbial electrochemical systems are a very promising technology the direction of Nature-Based Solutions for diffuse and on-line monitoring of environmental parameters. As the sensing element is a living organism, they can be easily integrated in natural systems [13]. Furthermore, their low-cost, sustainability, portability and low maintenance make them excellent candidate for

the creation of diffuse sensing network. As their output is already an electric signal (i.e. no transducer required), they can be easily integrated as smart sensors. The current that they produce can be even be harvested to power wireless data transmission system [14]. In this following chapters, the implementation of different kinds of microbial electrochemical systems (MESs) as water and wastewater quality sensors is discussed.

1.2 Organization of the dissertation

This dissertation is organized as follows: in the introduction the state of the art in microbial electrochemical systems is discussed, especially focusing on Microbial Fuel Cells (MFCs) and amperometric devices. The potential of their applications as sensors are examined in this part. Subsequently, the fundamentals of the experimental methods are presented. After that, the dissertation is divided in two sections: the first is dedicated to the application of floating MFC for monitoring wastewater treatment process and the second part refers to the study of microbial photo-electrochemical sensors for the detection of herbicides. General conclusions and perspectives are given at the end of the dissertation.

2 STATE OF THE ART

2.1 Microbial Electrochemical Systems (MESs)

The interest on Microbial Electrochemical Systems (MESs) has significantly boomed over the last twenty years, as it is clearly shown by the trend of publications on the subject (**Fig. 7**). They are part of the broader field of Bioectrochemical Systems (BESs), which comprises devices that employ bioelements other than microbes (e.g. plants, enzymes, photosystems, antibodies, etc.). This emerging technology represents a sustainable alternative to a variety of processes and applications, such as electricity production [15], wastewater treatment [16], high-value chemicals synthesis [17], nutrient recovery [18], fuel generation [19], desalination [20] and sensing [21].

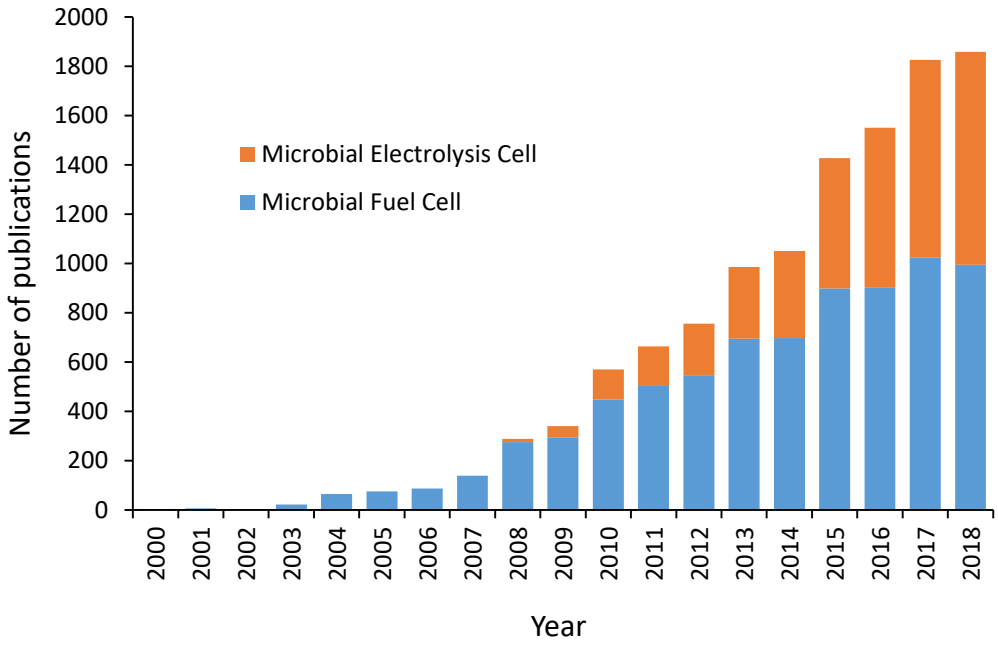

Figure 7 –Number of publications on Microbial Electrochemical Systems from the year 2000 to 2018, for the keywords "Microbial Fuel Cells" and "Microbial Electrolysis Cell" (Scopus database, March 2019). – scopus.com

MESs rely on the coupling of living electroactive microorganisms with an electrical circuit: microbes capable of extracellular electron transfer (EET) function as catalysts in one or more electrodic reactions [22]. The first experiment in which microbes were used to generate electricity was performed by Potter in 1911 [23]. Further configurations and applications were experimented ever since, with important progress on the comprehension of electron transfer mechanisms,

implementation of novel, low-cost and durable electrode and materials and development of efficient bio-electrocatalytic interfaces [24]. However, there is still a large margin for improvement and optimization before MESs can compete with existing technologies for most applications [25].

In MESs, oxidation occurs in the anodic compartment, and the generated electrons are transferred via external electrical circuit to the cathode, where the reduction reaction happens. Due to the electric potential gradient, protons and other cations generated at the anode tend to migrate to the anodic compartment, while anions tend to go in the opposite direction. The anode is called bioanode when the anodic reaction is catalysed by microbes, and biocathode is the term referred to the cathode when the cathodic reaction is biotic (**Fig. 8**).

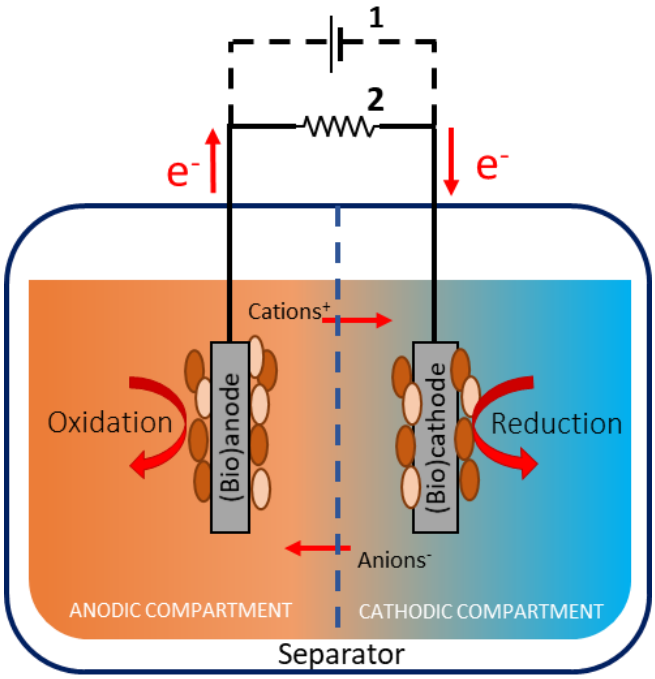

Figure 8 – Schematic representation of a microbial electrochemical device: if power is applied to the system it is called Microbial Electrolysis Cell (1), whether if the device generates power across a resistance it is referred to as Microbial Fuel Cell (2)

When electrical energy is produced across a resistance, these systems are termed Microbial Fuel Cells (MFCs). Conversely, when power is supplied to the system in order to thermodynamically force non-spontaneous reactions, those systems take the name of Microbial Electrolysis Cells (MECs). A more detailed description of the mechanisms is provided in the following sections.

2.2 *Microbial Fuel Cells*

2.2.1 MFC definition and principles

MFCs are certainly the most studied system among BESs [24]. A MFC is a bio-catalysed electrochemical device able to convert chemical energy in electrical energy through a cascade of redox reactions [26]. The simplest configuration is composed by two chambers (**Fig. 9**): in the anodic chamber, microorganisms oxidize organic substrates using the anode as electron acceptor, and then the electrons are transferred via an external circuit to the cathode, where the reduction semi-reaction happens. The final electron acceptor is usually oxygen, that is reduced to H_2O in the Oxygen Reduction Reaction (ORR). The two chambers are separated by a membrane (or a porous separator) that allows the exchange of ions. As batteries and fuel cells, this technology aims at physically separate the oxidation and the reduction processes in order to produce energy. The driving force for the bioelectrogenic activity is the potential difference existing between the two compartments: reducing conditions in the anode chamber and oxidizing in the cathodic one [26].

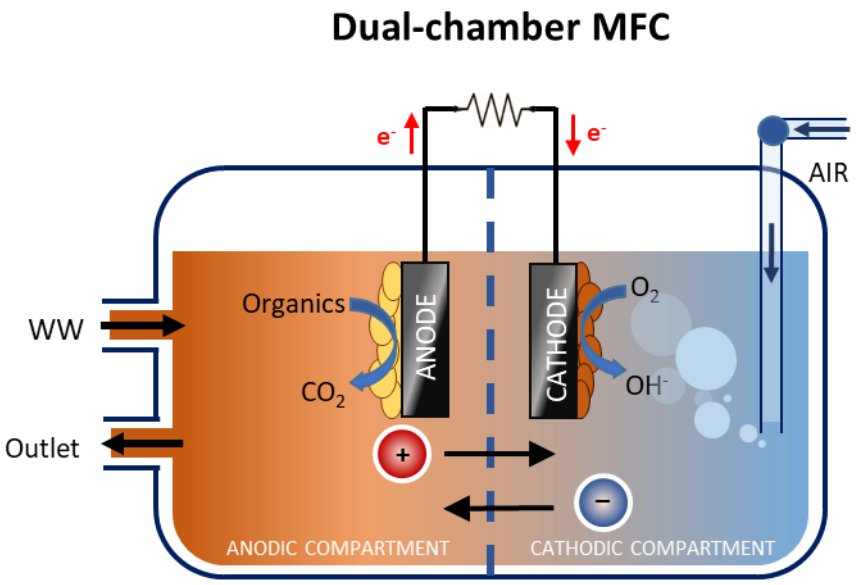

Figure 9 – Schematic representation of a dual-chamber MFC. Wastewater (WW) is the source of organic matter for the anodic chamber, and atmospheric oxygen is pumped into the cathodic chamber to serve as electron acceptor. Electrons originated from the bio-oxidation of organic matter at the anode travel through the external circuit to reach the cathode, where they participate in the oxygen reduction reaction. The anodic biofilm is represented with yellow circles and the cathodic biofilm is represented with brown circles. A membrane (or separator) divide the two compartments while allowing the exchange of ions.

The microbial communities adhering to the electrode surfaces form a biofilm, which is a surface-associated congregation of microbial cells. The major component that keeps the biofilm bound together is an extracellular polymeric matrix composed mainly of polysaccharides [27]. In most MFCs, the biofilms are formed by spontaneous colonization of the electrodes operated by the microorganisms present in the inoculum. Due to the natural selection process, the species able to exchange electrons with the electrode are favoured, and become more abundant in the immediate proximity of the conductive surface [28]. It has been observed that MFCs that employ mixed cultures can achieve significantly higher power densities compared to the ones with pure cultures [29]. This is probably due to the interspecies electron transfer occurring in the bacterial syntrophic associations, that allows a more efficient use of the energy obtained from various substrates. Indeed, one of the main features of MFCs is their ability to utilize a wide range of organic matter as substrate to produce energy, ranging from simple molecules (glucose, acetate, lactate etc.) to complex substrates (cellulose, molasses, starch, etc.), as well as the mixed organics contained in wastewater, domestic wastes, agricultural wastes (dairies, manure, fruit pulp etc.), and other types of fermentable substrates [24]. When wastes are used in MFCs, the benefits of renewable electricity generation are combined with simultaneous pollution remediation, resulting in an eco-friendly process with positive impact on the environment [26].

However, in most of the studies conducted on MFC, the main substrate used as electron donor in the anodic reaction is acetate (**Eq. 1**). This is because it is the end product of many metabolic pathways (e.g. acetic fermentation from ethanol, Entner-Doudoroff route from glucose, acidogenesis from proteins, saccharides and lipids, etc.), thus readily available to the microbes [24]. Additionally, it is highly soluble in water and stable at room temperature, as it is unaffected by undesirable microbial reactions such as methanogenesis and fermentation [30].

Anodic reaction: $CH_3COOH + 2H_2O \rightarrow 2CO_2 + 8H^+ + 8e^-$ $E^0_{Anode} = -0.29$ V (Equation 1)

Oxygen is the most common electron acceptor for the cathodic reaction (**Eq. 2**), due to its ubiquitous presence and its high oxidation potential (E°= +1.23V at pH=0), which makes it energetically favourable. At pH 7 we have:

Cathodic reaction: $2O_2 + 8H^+ + 8e^- \rightarrow 4H_2O$ $E^0_{Cathode} = +0.81$V (Equation 2)

Coupling the two reactions (**Eq. 1 and 2**) we obtain:

Cell reaction: $CH_3COOH + 2O_2 \rightarrow 2CO_2 + 2H_2O$ $E^0_{Cell} = +1.10V$ (Equation 3)

The cell potential E^0_{Cell} (or electromotive force, *emf*) e is calculated as the difference between the standard reduction potentials:

Cell potential: $E^o_{Cell} = E^o_{Cathode} - E^o_{Anode}$ (Equation 4)

As the cell potential is positive, the electricity generation from these reactions is spontaneous. Nevertheless, the ORR has a low reaction rate due to its high overpotential even in presence of effective catalysts (i.e. Pt) [31]. This aspect is considered one of the major bottlenecks for energy production with MFC and other fuel cells that use oxygen as final electron acceptor.

Interestingly, if the kinetics of ORR were fast on the materials present on the earth's crust, many oxidation reactions would take place spontaneously: fast metal corrosion, deterioration of non-metallic materials and oxidative stress on living organisms, which would lead to quicker ageing and death [32].

2.2.2 Air-cathode MFC

A very common alternative to the two-chamber MFC is the single-chamber air-cathode MFC. This setup consists of just one compartment: the cathode is placed on a wall of the chamber, with one side facing the same solution as the anode and the other one exposed to the outside air (**Fig. 10**). As the two electrodes are in contact with the same solution and no polymeric membrane is present between them, protons produced by the anodic reaction can diffuse freely toward the cathodic compartment. Also, the cathode is subjected to bacterial colonization, becoming a biocathode. The electroactive biofilm that is formed in this way shows a highly stratified structure [33]. This is due to the high oxygen gradient that is generated in the proximity of the cathodic surface: the aerobic bacteria growing on the cathodic surface consume O_2 diffusing from the air side, allowing anaerobic microorganisms to thrive on the solution side [34]. Therefore, the cathodic biofilm is able to prevent oxygen from reaching the bioanode and preserves anaerobic conditions in its vicinity. In this way, short-circuit phenomena that can decrease of the electric output of the cell

are avoided [35]. This aspect is proven by the presence of a high pH gradient (from 8.5 to 6) within the biofilm itself [36].

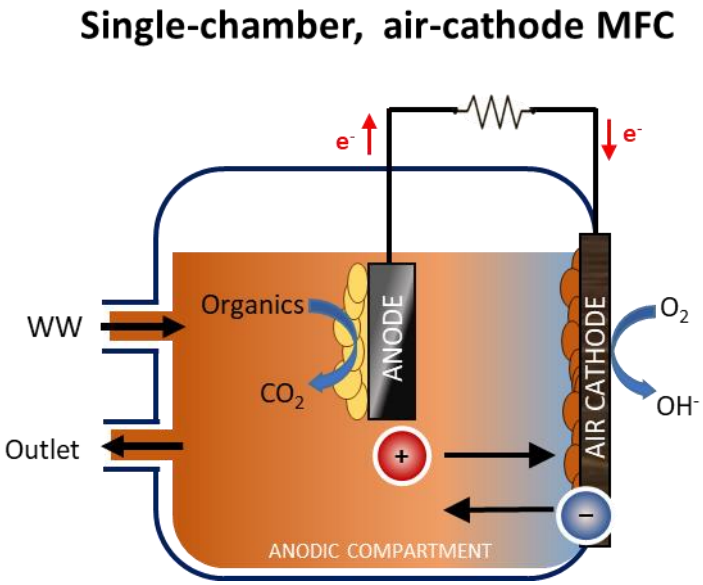

Figure 10 - Schematic representation of a single-chamber, air-cathode MFC. Wastewater (WW) is the source of organic matter for the anodic chamber, and atmospheric oxygen diffuses from the porous cathode into the electrolyte to function as electron acceptor. There is no separation between the two electrodes, and the anaerobic conditions at the anode are ensured by the oxygen consumption operated by the cathodic biofilm.

The absence of ionic-exchange membranes to separate the two compartments offer several advantages: it strongly reduces the cost of the device and avoids the high ohmic resistance generated by this kind of separator [37]. Moreover, polymeric membranes are subjected to performance losses overtime due to biofouling: the surface undergoes microbial colonization which results in ion diffusion limitations [38,39].

2.2.3 Direct and indirect electron transfer

There are two main mechanisms of EET between bacterial cells and the electrodic surface: direct electron transfer (DET) and mediated electron transfer (MET).

DET occurs through physical contact between the outer membrane of the bacterial cell with the electrodic surface, in absence of diffusional redox species [40]. Since the cell membrane is non-conductive, membrane-bound proteins able to transfer electrons from inside the bacterial cell to an

outer solid electron acceptor are necessary for the DET to happen. The structures identified so far are outer-membrane c-type cytochromes (**Fig. 11A**) and conductive pili or nanowires (**Fig. 11B**).

C-type cytochromes are multi-heme proteins which serve as electron carrier in several electron transport chains. Some sediment inhabiting bacteria, such as *Geobacter*, *Rhodoferax* and *Shewanella,* have evolved outer-surface cytochromes c in order to be able to use solid terminal electron acceptors present in minerals, like iron(III) [41]. In MFCs, the electrode substitutes the solid electron acceptor of mineral origin [40]. This mechanism has been demonstrated in experiments involving *Geobacter sulfurreducens*, where the wild type was compared with mutants with the cytochrome c encoding gene deleted or overexpressed [42].

The presence of conductive pili in electroactive microorganisms was recently reported by the Lovley research group [43]. They consist in electronically conductive filaments made proteins that facilitate long-range extracellular electron transfer and even interspecies electron transfer. Two different mechanism have been identified: electron transfer in *Shewanella oneidensis* nanowires is obtained by electron hopping/tunnelling between cytochromes present on the filaments, while the conductive pili of *Geobacter sulfurreducens* have metallic-like conductivity, which can be attributed to overlapping pi–pi orbitals of aromatic amino acids [44].

MET relies on the presence of dissolved low-molecular redox species that shuttle electrons across the bacterial membrane and to the solid electrode. When the redox mediator is produced by the bacteria as a result of its metabolism, the MET is defined endogenous (**Fig. 11C**). For example, *Pseudomonas aeruginosa* can produce a pigment called pyocianine and *Shewanella oneidensis* release a quinone-based mediator (2-amino-3-dicarboxy-1,4 naphthoquinone), which have been identified as responsible for the respective electrochemical activity [24].

Exogenous redox mediators have been the object of many electrochemical studies since 1980s [45]. In this approach, artificial mediators like thionine, neutral red, viologens, iron chelates, phenazines, phenothiazines, phenoxazines and quinones are added in solution to support electron transfer (**Fig. 11D**). However, as in most applications a continuous or semi-continuous input of the fuel source is required, the electron shuttle has to be constantly added, increasing operational costs. In addition, many of these compounds are toxic to humans and dangerous for the environment [42].

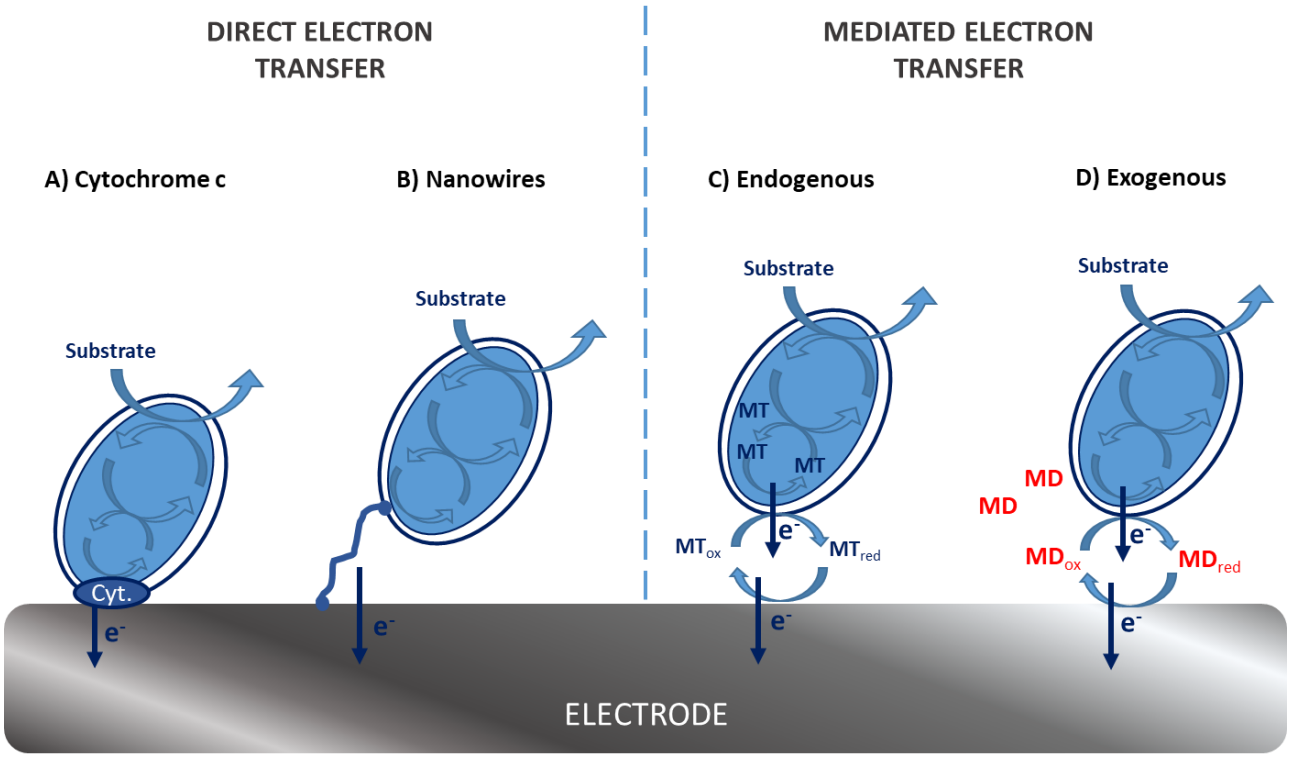

Figure 11 – Schematic representation of the different mechanism of electron transfer from a microorganism to a solid electrode: Direct Electron Transfer trough A) pili or B) cytochromes, and Mediated Electron Transfer trough C) endogenous metabolites produced by the microbes (MT), and D) through exogenous redox mediators (MD).

2.2.4 Electrodic materials and geometries

In MFCs, the anodic reaction is catalysed by microbes. To improve the interaction between the electroactive biofilm and the electrodic surface, the anodic material should be: electrical resistant to corrosion, highly conductive, mechanically strong, biocompatible, environmentally friendly and low-cost [24]. Two main categories of materials have been used for anodes in MFCs: carbon-based and metallic. Due to their low cost, good biocompatibility and resistance to corrosion, carbon-based materials are the most frequently used. Unfortunately, they possess relatively low electrical conductivity and mechanical strength, which limits their application at large scales, while for small-scale systems (e.g. biosensors) they are often the best option [46]. On the contrary, metallic electrodes show good mechanical strength and conductivity. However, the application of noble metals such as gold and platinum is limited by their high cost, while other metals like copper and nickel have a low level of biocompatibility. Indeed, copper and nickel electrodes can release ions that can be poisonous for microbes [24]. SS-based materials are cheaper than carbon, but their biocompatibility needs to be improved before use, for example by coating or surface

functionalization [46]. The characteristics of the anodic materials used in MFCs are summarized in **Figure 12**.

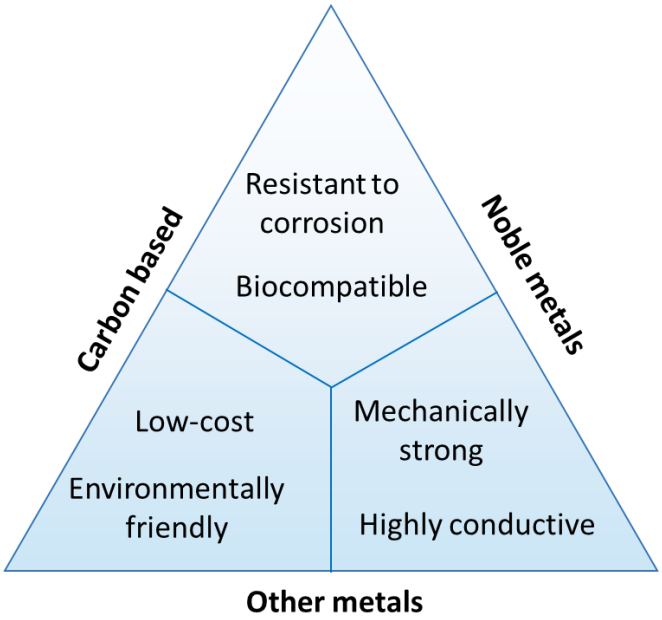

Figure 12 – General properties of the anodic materials used in MFCs: carbon based materials are biocompatible and resistant to corrosion like the noble metals, but in addition they are cheap and more environmentally friendly. All metals are mechanically resistant and highly conductive with respect to the carbon based materials. However non-noble metals can be affected by corrosion and they have biocompatibility issues.

Anodic materials can be of two main geometries: planar configuration (e.g. plate, rod, paper, veil, cloth, and mesh) and porous three-dimensional structure (e.g. foam, granular bed, felt and brush). Due to their lower costs, defined surface area and uniformity of surface properties, planar electrodes are preferable for the biosensor application where a high power output is not needed. In addition, a plane surface makes the biofilm visualization by microscopic techniques easier, making this configuration suitable for fundamental research on microbe–electrode interactions.

Conversely, 3-D electrodes offer high surface area for the colonization of electro-active biofilms, which improves the power production of the device [46].

Examples of carbon-based anodic material are shown in **figure 13A**, divided in planar and 3-D configurations. **Figure 13B** presents some examples of metallic materials.

A)

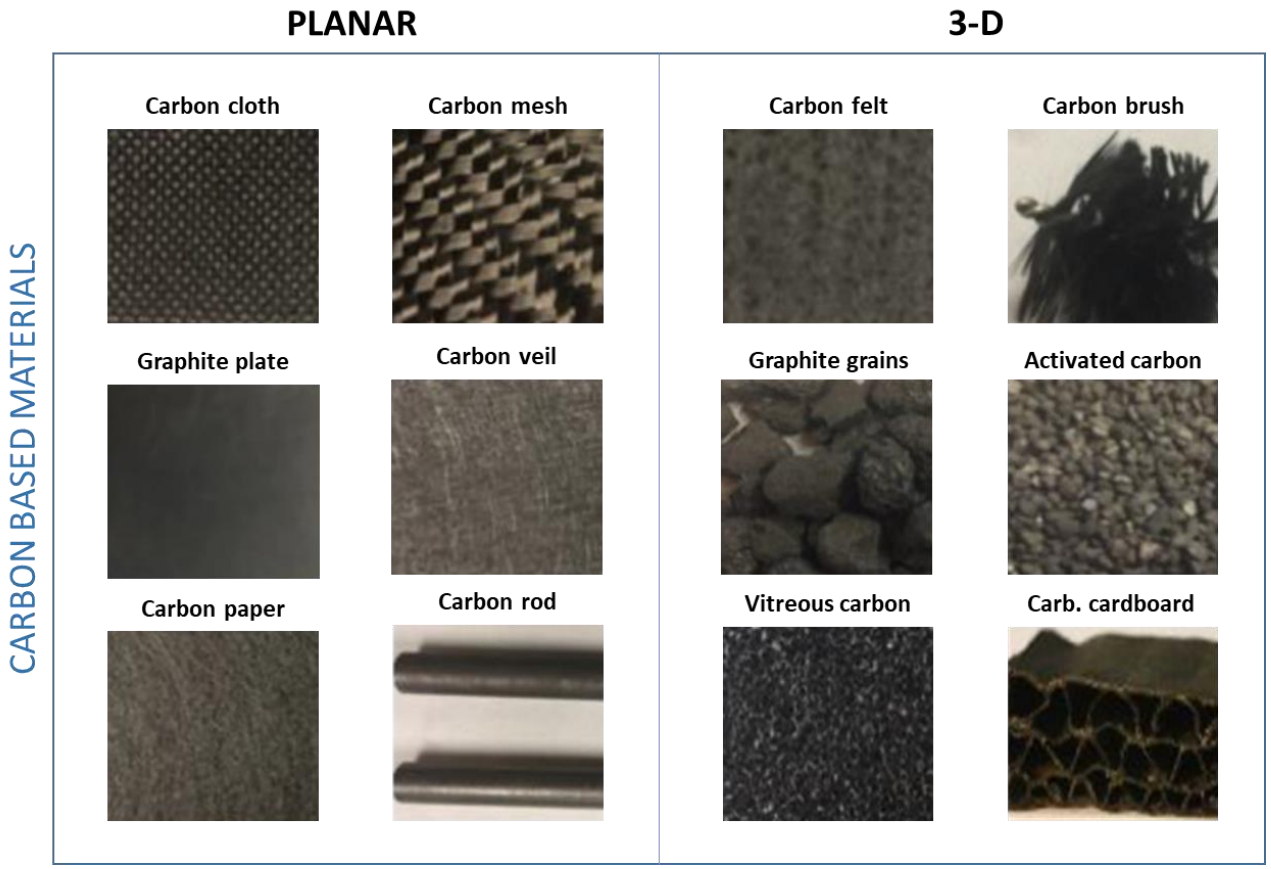

B)

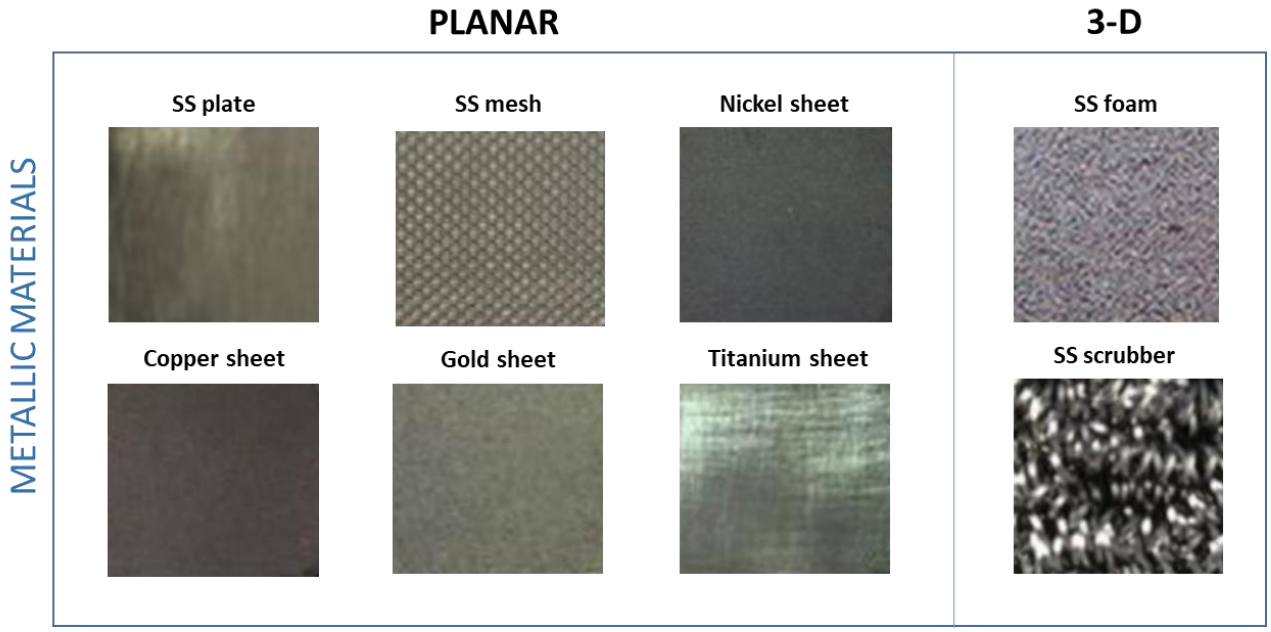

Figure 13 – A) Carbon-based and B) metallic materials used for electrodes in MFCs, divided in planar configuration and 3-D configuration.

The materials used for the cathodes can be similar to the ones described for the anodes [47]. However, as the ORR occurring at the cathode presents kinetic limitations due to its high overpotential, the choice of the catalyst is critical for the device performances [46]. Cathodic catalysts can be abiotic (e.g. platinum, activated carbon, etc.) or biotic (e.g. enzymes, bacteria, etc.).

Abiotic catalysts are mainly divided in three different types: platinum-based, carbon-based or made of non-precious metals. The first group comprises materials containing platinum, which has been widely used in MFCs especially because of its predominant role in more mature technologies such as fuel cells. However, the high price and the risk of poisoning by the anions present in wastewater (i.e. sulphur) represent important drawbacks for its application.

The second group comprises materials like graphene, carbon nanotubes (CN), activated carbon (AC), carbon black, etc., which are generally cheaper and more stable than the first group even in harsh conditions. AC is by far the most used in cathode fabrication. Santoro et al. optimized the procedure to create the AC-based catalytic layer: AC is be mixed with a binder (i.e. PTFE) and then pressed on the current collector surface at about 150-200°C and 1400psi [48].

Finally, the last group includes materials containing transition metals like Mn, Fe, Co and Ni. These materials have a significant production cost, due to the high temperature and specific precursors needed. On the other hand, they can outperform Pt-based materials in alkaline conditions and they are unaffected by heavy polluted environments [46].

Regarding biologic catalysts, enzymes such as laccase and bilirubin oxidase can be immobilized on the electrode surface to catalyse the ORR. This approach entails few disadvantages, mainly due to the complexity and cost associated with purification steps and immobilization techniques [32]. Moreover, enzymes are fragile once outside of a living cell. Conversely, microbial biofilms are inexpensive, robust, durable and autonomously colonize the electrode. In addition, bacterial biocathodes can outperform Pt-based abiotic cathodes, as reported Jang et al. [49]

2.2.5 MFCs as multipurpose sensing tool

In the recent years, the application of MFC to sensing purposes is attracting increasing interest from the scientific community. Indeed, MFCs are being studied as water quality assessment tools both in quantitative and qualitative way [50]. The underlying principle is that a variation in the concentration of the target bioactive chemical (i.e. analyte) affects the current response of the device [21]. For example, MFCs have been employed to monitor biochemical oxygen demand (BOD)

[51–57], dissolved oxygen [58], volatile fatty acids (VFAs) [59,60], heavy metals [50,55,61,62] and pesticides [63].

Most studies on MFC-based sensors focused on the monitoring of BOD, which is a parameter that indicates the amount of biodegradable organic matter dissolved in water. Presently, the most common method for BOD analysis is the BOD_5 test. Nevertheless, there are several analytical and operational limitations associated with this method, like questionable accuracy and irreproducibility, and it requires skilled personnel to perform the analysis [53]. Additionally, the five days needed for the test to be completed make this method not effective for real-time monitoring and in conditions where rapid feedback is necessary [51]. On the contrary, MFCs can provide a real-time on-line signal relative to the BOD content in water [64]. Since organic substances are the substrate for the anodic reaction, the anodic biofilm serves as sensing element of the device. The aim is to establish a linear relationship between the BOD and the current output of the MFC [65]: within a certain range, the current (i.e. flux of electrons) is directly proportional to the rate of the bio-catalysed reactions occurring on the electrodic surface (**Fig. 14**) [51]. When the concentration of substrate is low, there is no significant difference between the signal and the background noise. As the concentration increase, more and more organic molecules are oxidized by the electroactive biofilm, thus more electrons are transferred to the anode and the current increases. After a certain threshold, however, the substrate saturates the biofilm, thus an increase in concentration does not cause an increase in the current, which tends to a plateau.

The correlation between BOD and current is also exemplified in **Fig. 15A**: when an increase in the BOD concentration occurs in solution, a corresponding rise in the generated current can be noticed. As the organic matter is consumed, the current decreases until the original condition is restored. It is important to keep in mind that, for this correlation to happen, the cathodic half-reaction cannot be limiting the current production, as the overall output of the MFC is determined by both half-reactions. Moreover, parameters like pH, salinity and temperature need to remain constant, as they can strongly affect the bacterial metabolism and the performances of the device, creating disturbances in the signal [66,67]. Indeed, simultaneous changes in conditions may lead to false warnings or lack of response. For this reason, the effects of such factors on the MFCs performance need to be properly understood and controlled [63].

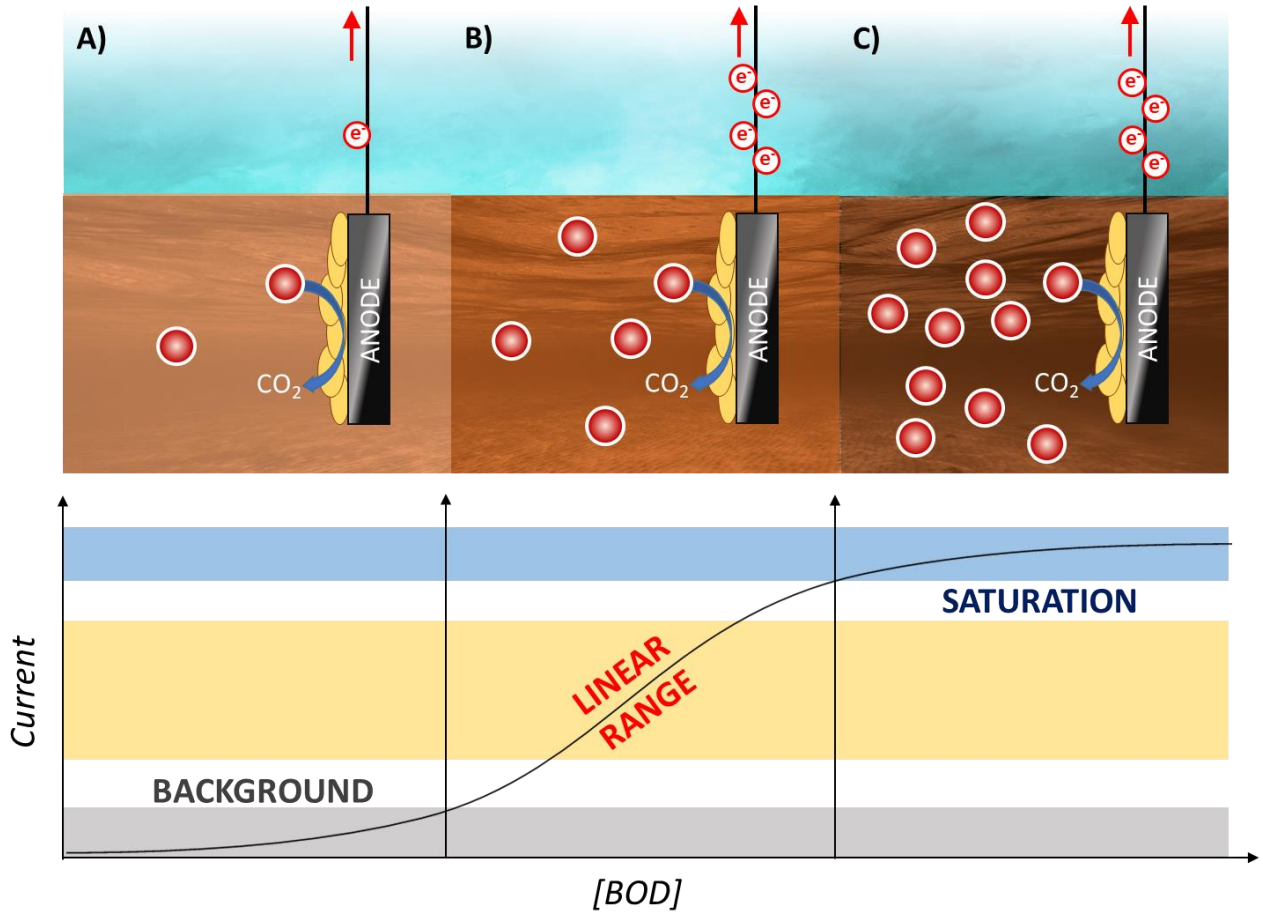

Figure 14 – Representation of the signal variation of a MFC-based sensor at increasing concentrations of BOD in solution. When the concentration is too low (A), the signal it is too low to be distinguished from the background noise. In the linear range (B), an increase in BOD concentration results in an increase in the current, as more molecules can react on the anodic surface, hence producing more electrons. After a certain threshold however, all the active sites of the biofilm are saturated, which means that an increase in concentration will not increase the current.

MFCs can also be used as toxicity sensors (**Fig. 15B**). Toxic substances like heavy metals, surfactants, volatile organic compounds and pesticides are generally measured with analytical methods like high-performance liquid chromatography (HPLC), atomic absorption spectroscopy (AAS) and gas chromatography-mass spectrometry (GC-MS). These techniques are very accurate and precise in measuring pollutants [68]. However, they are often expensive and time-consuming, and they involve sample pre-treatment, complex equipment and highly-trained operators [68], making them unsuitable for on-line in-situ testing [21]. MFCs offer a low-cost and simpler alternative to these methods. Indeed, the presence of toxic compounds can inhibit the metabolism of microbial communities growing on the electrodes or even cause their death. As a result, the amount of electrogenic bio-catalysed reactions decreases, thus the current output drops [65]. These kind of sensors can also be referred as “shock sensors”, where shock is the sudden increase of the

contaminant load in solution [21]. It is important to underline that in this case the MFC has to operate always under saturating conditions. In this way, the current variations generated by changes in the concentration of substrate (i.e. organic matter) are avoided [21].

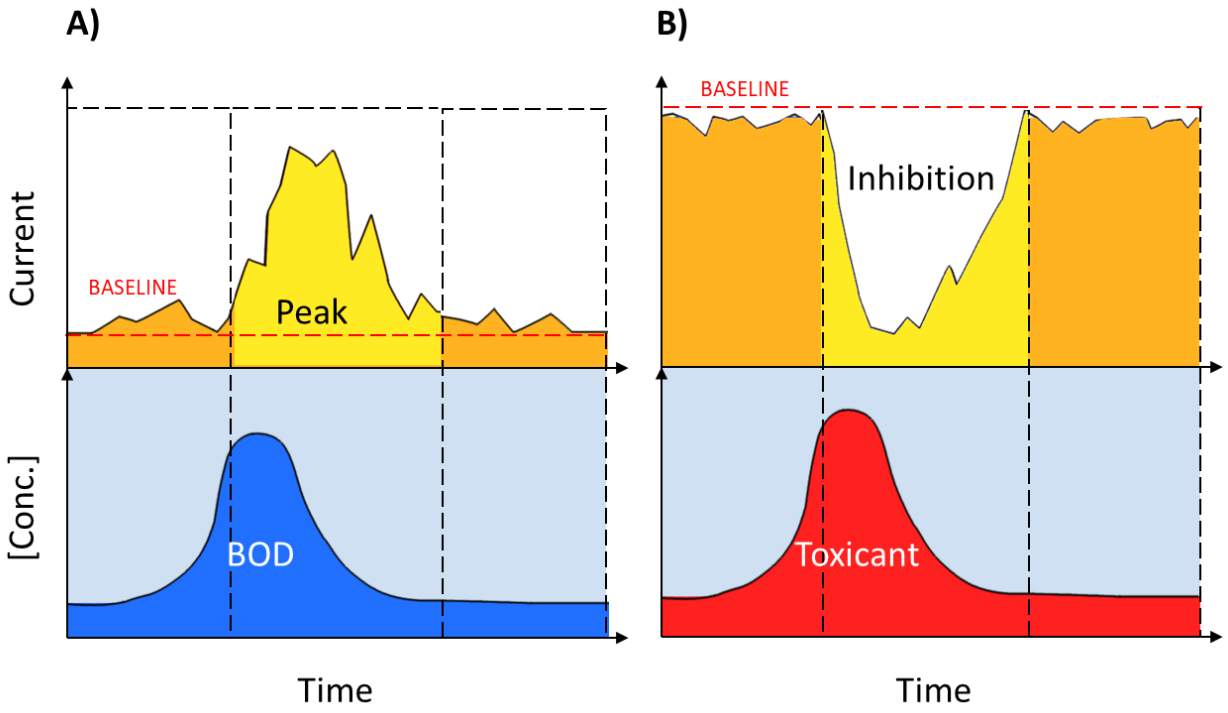

Figure 15 – Qualitative representation of the current response of a MFC when a change in the electrolyte composition occurs: in the case of an increase of BOD, the current will follow the increase if the system is not in saturated conditions. As the organic matter is consumed, the current decreases again to the background level (A); in the case of a spike of toxicant, the current drops from its baseline. When the concentration of toxicant decrease, the system can recover until the original condition is restored (B). A shock event could also be a variation of other conditions like temperature, pH and conductivity.

Another application of microbial electrochemical sensors is the monitoring of biofouling, (i.e. biofilm development) on metallic surfaces. Indeed, biofilms can promote interfacial physico-chemical reactions on metallic materials, resulting in biocorrosion and undesirable changes in material properties [69]. Therefore, biofouling can cause important damages in industrial plants, for example to cooling systems [70]. The different phases of the biofilm attachment on a metallic surface are shown in **figure 16**.

In 2003, Cristiani *et al.* developed a system to monitor biofilm settlement based on quasi-galvanostatic polarization directly applied to stainless-steel industrial pipelines using a zinc connected to a resistor [71]. In this way, the biofilm formation causes an increase in the ohmic drop

between the stainless-steel element and the zinc anode, which is the signal that indicates the need for antifouling treatment to prevent pipelines corrosion. A similar system was also applied to monitor biofilm development in soil [72].

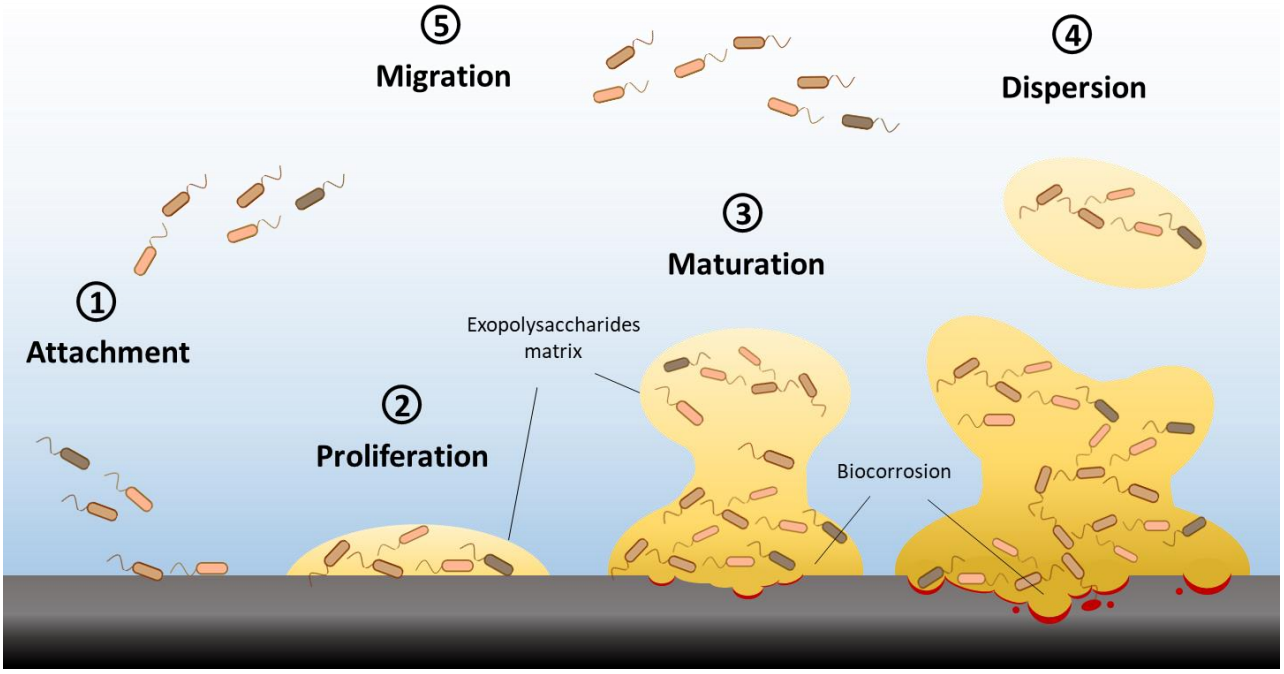

Figure 16 – Cycle of biofilm formation on metallic surfaces: initially few cells can attach to the surface (1), then they proliferate and form a micro-colony by excreting polysaccharides (exopolysaccharides matrix) that enhance the adhesion (2). As the colony reach maturation, different layers of microorganisms grow on the surface (3), and their metabolic processes can lead to the corrosion of the metal (biocorrosion). When the colony has reached the maximum thickness, due to mechanical stress some parts gets detached (4), which lead to the dispersion of some of the microbes. Those microbes can then migrate to colonize other surfaces (5).

2.2.6 Advantages and limitations of MFC-based biosensors

As introduced in the previous sections, MFCs are devices that can produce electrical power from organic wastes and atmospheric oxygen. When they are used as biosensors, the electric current generated serves as signal. These features of MFCs imply several advantages over other types of biosensors.

First of all, these devices do not need any external power input, as they are sources of energy themselves. Therefore, they can be applied in off-grid remote places [57] or in areas of third-world countries where the electricity is not easily available [73]. In addition, being self-powered makes them environmentally sustainable and reduces the operational costs. The energy produced could even be gathered to power other complementary sensors (e.g. redox, dissolved oxygen, pH, etc.) [14]. As the occurrence of pollutants in the feeding stream is directly recorded as electrical response

from the system, they do not require any additional transducer to operate [64]. Furthermore, the signal provided by this kind of sensors is continuous and has quick response time [55], enabling for on-line real-time monitoring of the water quality [65]. Another important aspect is that they do not require the use of purified chemicals, which can be toxic and/or increase the operational costs [74].

Since the biofilm is originated directly from the environmental matrices at which the electrodes are exposed (e.g. wastewater, sediments, sludge, etc.), there is no need for artificial inoculum [75], thus the bioreceptor is inexpensive and do not require being cultured in laboratory.

MFCs have also proven to be robust systems able to function over long-term periods of operations with little to no maintenance [53].

As stated in the previous section, MFCs are sensitive to a variety of toxic compounds. In this way they can be applied as non-specific early-warning system in environmental matrices where different kinds of pollutants can be present (e.g. water bodies) [76].

Several researchers focused their studies on biocompatible and low cost materials for MFCs, such as terracotta [77], paper wastes [78], natural rubber [79], lingo-cellulosic materials (e.g. *Arundo donax* cane) [80], etc. In this way, the construction of these devices can be sustainable both from an economic and ecologic point of view. Moreover, Di Lorenzo research group focused on the development of miniaturized 3D-printed MFC sensors [51,63]. This can be greatly increase the portability of the device and the possibility of working on-site. A summary of the advantages of MFC-based sensor, divided in operational, economic and ecologic, is presented in **Fig. 17**.

Currently, several limitations still affect the implementation of MFCs as water quality sensors. The first issue is related to the sensor performances: lots of studies focus on further lowering the detection limit, increasing the detection range and improving the sensitivity. Nevertheless, the detection limit of MFCs-based sensors hardly ever meets the water quality standards [75]. A recent study showed that the detection limit of these sensors is mainly hindered by the mass-transfer barrier constituted by the biofilm [81]. Additionally, whole bacterial cells are generally less sensitive than other bioreceptors (e.g. enzymes, DNA, photosystems, antibodies), because of the diffusional limitations created by the membranes of the living organism [75].

Another major challenge for real-world applications of these systems is the signal interference caused by simultaneous variations of BOD and toxicity levels [82]. Indeed, when the bioanode is used as sensing element, a variation in the BOD concentration can mask or even counterbalance the response to toxicants, causing a false signal [75]. Employing the biocathode as

sensing element may be more effective for toxicity monitoring, as it is not affected by the BOD variations [83].

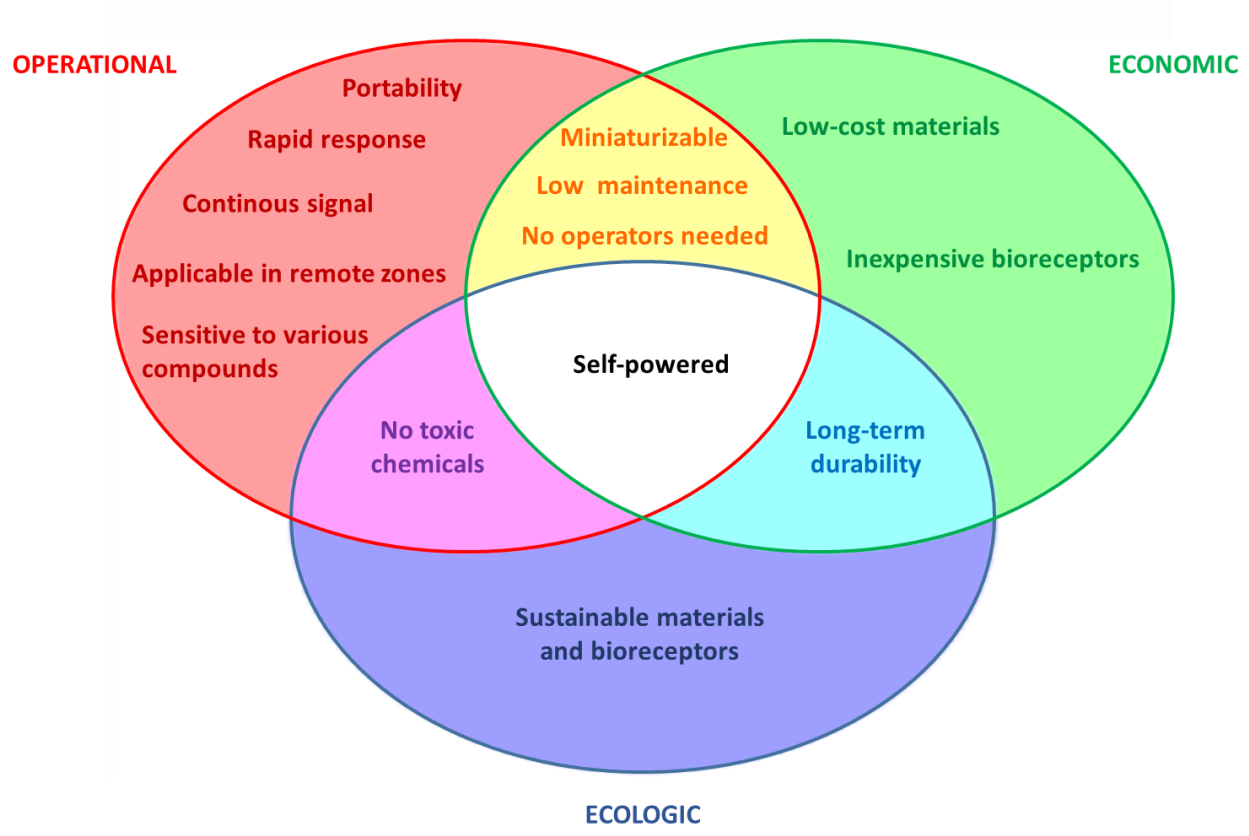

Figure 17 – Advantages of MFC-based sensors over the conventional analytic methods, grouped as operational, economic and ecologic

As mentioned before, the signal of MFCs-biosensor is affected by variations in environmental conditions like temperature, pH and salinity. Recently, Chouler et al. proposed a systematic study on these kind of operational disturbances applying the factorial design of experiment (FDOE) to discern between the different parameters and analyse their individual and synergistic effects [63]. However, further research should address the application of the sensor to real scenarios.

Finally, Grattieri et al. pointed out that, for industrial applications, MFCs require too much time to recover their pristine conditions after a toxic shock [21].

2.3 Photo-bioelectrochemical sensors

2.3.1 Amperometric biosensors

Unlike MFC-based sensors that spontaneously produce the current signal due to the redox gradient between the two electrodes, amperometric biosensors require an energy input to function. Indeed, a fixed potential is applied to the biosensor electrode in order to force thermodynamically unfavorable reactions. The first amperometric biosensor was created by Clark in 1956, which consisted in an enzymatic oxygen sensor for medical application [84]. Since then, the field of electrochemical biosensing expanded quickly, with research and commercial applications in quality control, drug screening, disease diagnosis and treatment, and environmental monitoring [85].

Amperometric biosensors are constituted by two closely associated elements: a biological recognition element (i.e. bioreceptor) and an electrochemical transducer (i.e. electrode). They provide a measure of the current generated by the biocatalyzed electrochemical reactions occurring on the electrodic surface [86]. As previously described for the BOD monitoring with MFC-based sensors, the measured current is directly correlated with the rate of consumption/production of the electroactive specie, thus to its concentration in the bulk solution. Amperometric measurements are conducted with a three-electrodes setup, which is depicted in **Fig. 18.**

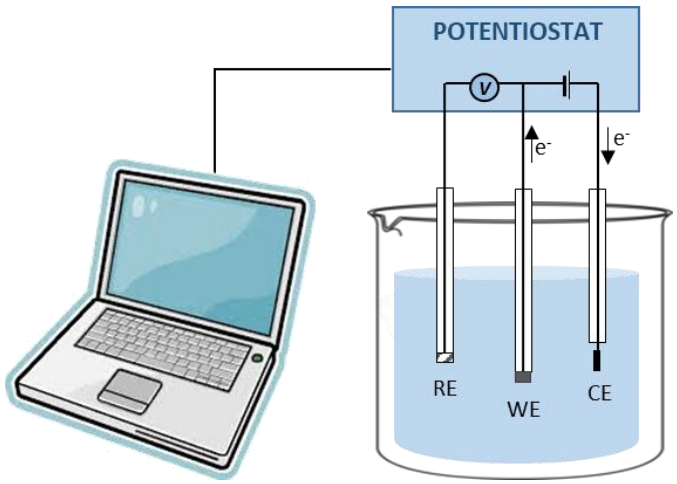

Figure 18 – Schematic representation of the three-electrode setup. The imposed potential on the WE is set against a RE and controlled by the potentiostat. The generated current pass between WE and CE and it is recorded by the potentiostat.

The reaction of interest occurs on the Working Electrode (WE), which is the biosensor. For the reaction to happen, a potential is applied to the WE by means of a potentiostat. This potential

is measured against a Reference Electrode (RE), which maintains its fixed potential due to its stable composition. To close the electric circuit, a counter reaction needs to take place. Thus, a third electrode named Counter Electrode (CE) is necessary. The current flows between the WE and CE and it is recorded by the potentiostat. The current is usually recorded in function of time, hence the electrochemical technique used is called chronoamperometry [87]. A more detailed explanation on these concepts can be found in the following chapter: "Fundamentals of the techniques".

2.3.2 Photo-bioelectrochemical systems

Photo-bioelectrochemical systems combine photosynthetic microorganisms (e.g. algae, cyanobacteria) or subcellular units (e.g. chloroplasts, thylakoid membranes, photosystems) with electrochemical devices.

Photosynthetic organisms perform the light-induced oxidation of water as first step of the photosynthetic process (**Eq. 5**). As molecular oxygen is the by-product of this process, it is called oxygenic photosynthesis. In the equation, light energy or photon energy is indicated with *hv.*

Water oxidation: $H_2O \xrightarrow{h\nu} \frac{1}{2}O_2 + 2H^+ + 2e^-$ (Equation 5)

Photosynthetic microorganisms possess organelles named thylakoids. Within the thylakoid membrane, protein complexes called photosystems contain pigments able to absorb light energy. The electrons obtained by the oxidation of water are initially transferred to the pigment P680 present in Photosystem II (PSII). When this pigment becomes excited by light energy, it initiates an electron-transport chain, which consists in a cascade of redox reaction between intermediate cofactors where the pigment P700 inside Photosystem I (PSI) is the final electron acceptor. This pigment can also be photo-excited, generating another electron-transport chain that ultimately reduces NADP+ to NADPH (**Fig. 19**). 680 and 700 are the respective adsorption wavelength of the two pigments expressed in nm [88].

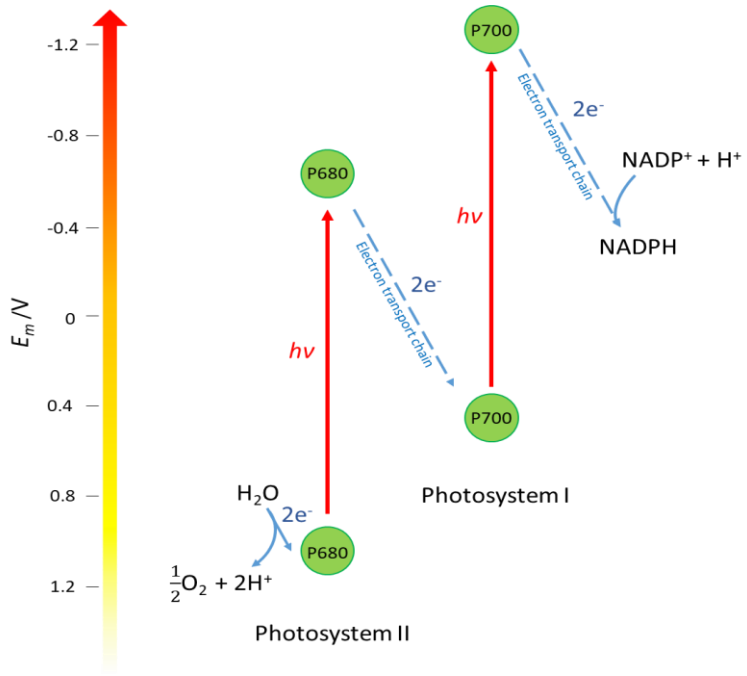

Figure 19 - Z shaped energy diagram representing the electron transfer in the oxygenic photosynthetic process. The vertical axis represents the reduction potentials of the chemical species. When the chlorophyll pigments P680 (PS II) and P700 (PSI) are excited by light, their energy level increase, initiating an electron transport chain. In this way, water is able to donate electrons to the NADPH despite the higher reduction potential.

In bioelectrochemical systems, a solid electrode (i.e. anode) is the final electron acceptor of the photosynthetic activity. Between those systems, the most studied devices are known as biophotovoltaics [89], where oxygenic photosynthetic organisms or subcellular photosynthetic components are used to harvest light energy and generate electric power (**Fig. 20**). As the produced current is generated from light energy, it is termed photocurrent.

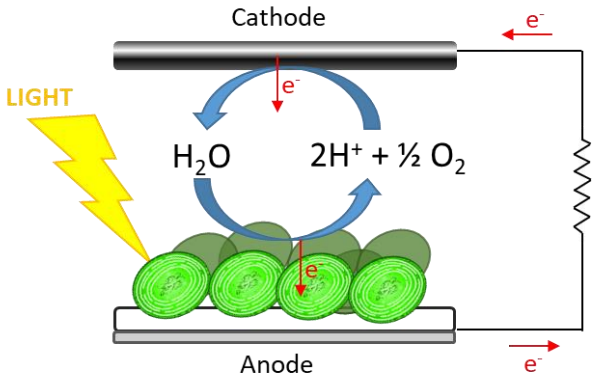

Figure 20 – Scheme of a biophotovoltaic system: in presence of light, water is oxidised at the anode and the electrons travel via external circuit to the cathode, where the inverse reaction occurs.

These systems have the unique advantage of producing electrical energy solely from water and light, in absence of any organic substrate. Nevertheless, the electrical power produced by photosynthetic materials is still too low for energy applications [21]. One of the reasons behind this problem is the poor understanding of the mechanisms of extracellular electron transfer by phototrophs [90]. Studies about quinone-based redox molecules to enhance the electron transfer [91], implementation of redox polymers [92], and screening of bacterial species can be found in literature [90], but a deeper understanding from the fundamental point of view is still lacking.

Since high power production is not needed for sensing purposes, photo-bioelectrochemical sensor represent a promising application of this technology. For example, they can be used to continuously monitor the presence of herbicides in water bodies.

2.3.3 Herbicides and photocurrent inhibition

Herbicides are a variety of phytotoxic chemicals used to manage weeds in agricultural and non-agricultural systems, and constitute approximately 40% of all applied pesticides worldwide [93]. However, accordingly to the properties of the molecules, they can raise environmental and safety issues. In fact, many of them are reported to be endocrine disruptors [94] or have carcinogenic or teratogenic effects on several species of animals [95]. Moreover, they can damage non-target plants in edge-of-field habitats [96], and some of them are persistent in the environment, especially in groundwater [97]. Herbicides can be classified by mechanism of action: in **table 2** is reported the classification system made by the Herbicide Resistance Action Committee, which is adopted worldwide except USA, Canada and Australia [98].

Table 2 - Herbicides categorized by mechanism of action according to the HRAC classification system

HRAC Group	Type of action
A	Acetyl CoA carboxylase (ACCase) inhibitors
B	Acetolactate synthase (ALS) inhibitors
C	Photosystem II inhibitors
D	PSI Electron Diverter
E	Protoporphyrinogen oxidase (PPO) inhibitors
F	Carotenoid biosynthesis inhibitors HPPD inhibitors

	DOXP inhibitors
G	EPSP synthase inhibitors
H	Glutamine synthase inhibitors
I	DHP synthase inhibitors
K	Microtubule inhibitors Mitosis inhibitors Long chain fatty acid inhibitors
L	Cellulose inhibitors
M	Uncouplers
N	Lipid Inhibitors
P	Auxin transport inhibitors
Z	Nucleic acid inhibitors Antimicrotubule mitotic disrupter Cell elongation inhibitors

Photosynthesis inhibitors are between the most used herbicides worldwide, and they can be grouped by site of action (**Fig. 21**): PSII inhibitors (e.g. atrazine, diuron, metribuzin, bromoxinil, etc., Group C), PSI electron diverters (e.g. paraquat and diquat, Group D) and oxidative phosporilation uncouplers (e.g. dinoseb and dinoterb, Group M).

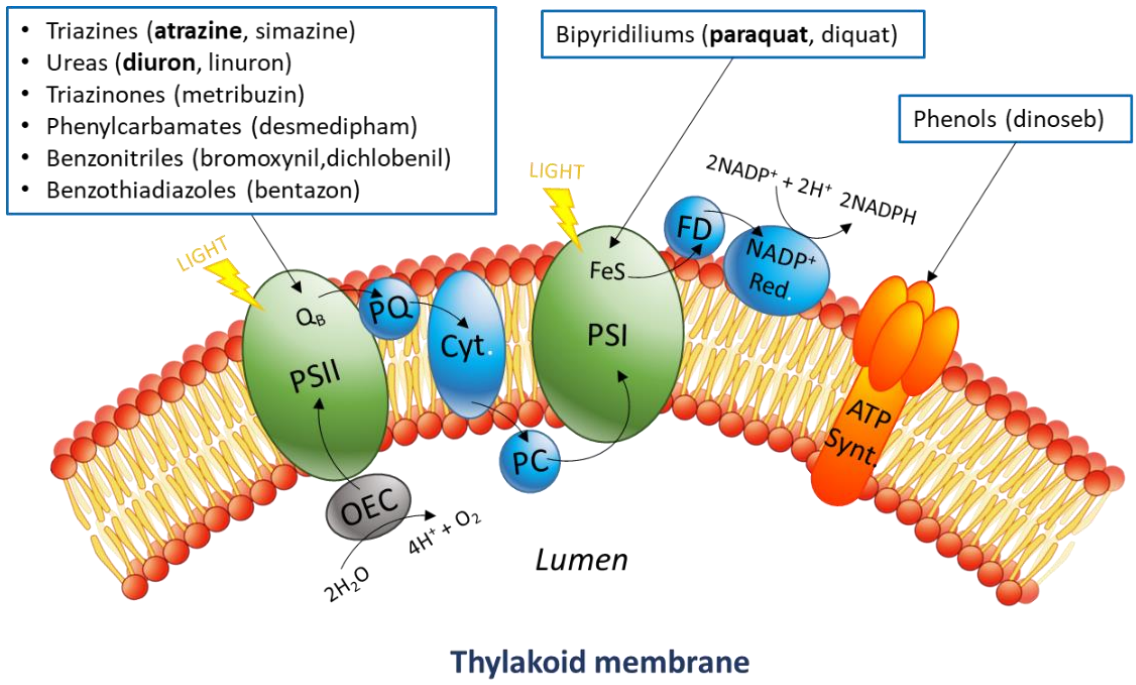

Figure 21 – Schematic representation of the photosynthetic transport chain in the thylakoid membrane. Water oxidation happens inside the membrane (lumen) and is part of a cascade of redox reactions between the different protein complexes and intermediates

present on the membrane. Depending on their chemical properties, different photosynthesis inhibitors target different active sites, causing the interruption of the electron flow (PSI and PSII) or blocking the production of ATP (ATP Synthase).

Compared with classic analytical methods (e.g. HPLC, GC-MS, AAS), electrochemical sensing is faster, simple to use, cost-effective, and portable, thus more suitable for on-line and in-situ monitoring [21]. Moreover, it can give information about the physiological impact of bioactive compounds and how they affect the metabolism of living organisms [6]. In this case, when the photosynthetic electron transport chain is interrupted by the presence of inhibitors, the produced photocurrent drops immediately, as electrons are no longer transferred to the anodic electrode (**Fig. 22**)

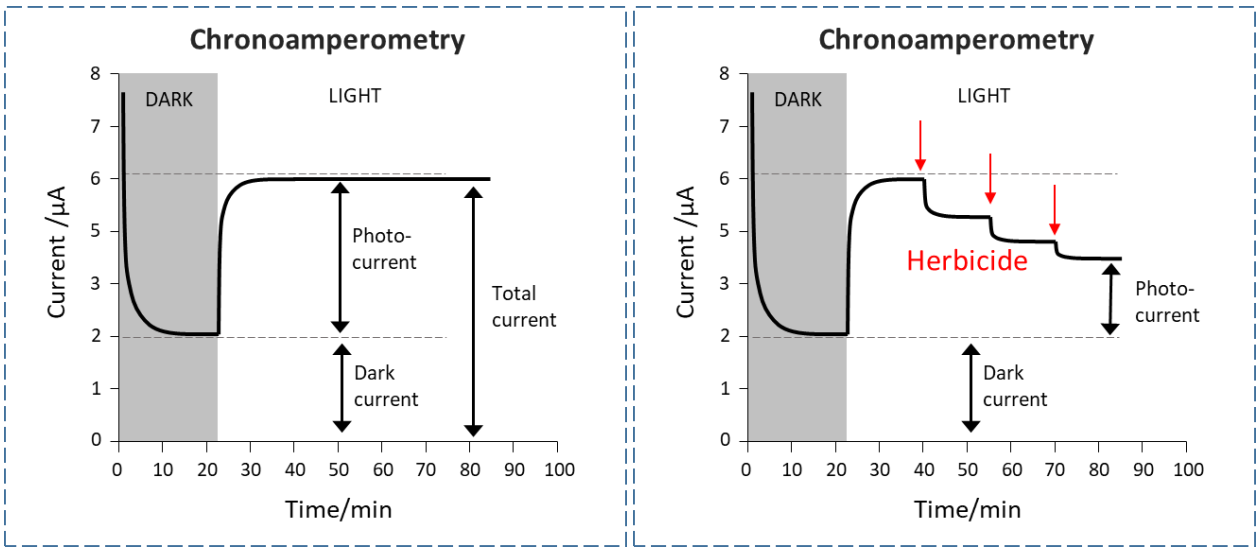

Figure 22 – Effect of photosynthesys-inhibiting herbicides on the photocurrent of a photo-bioelectrochemical sensor. Dark current is the background level of current obtained in absence of illumination, while and photocurrent is obtained under illumination. When the target herbicide is injected in solution, the photocurrent drops in a concentration-dependent manner.

3 AIM OF THE WORK

The inspiration of the work conducted during the three years of my PhD was based on the question: “What are the challenges for actual field applications of environmental sensors based on microbial electrochemical systems?”. The main focus of the experimentation, in fact, has been how to address the substantial issues that arise when mechanisms and devices studied in the lab are applied in the environment. Indeed, the environment is a highly complex system with constantly changing factors and sometimes unpredictable outcomes. In order to be applicable, new technologies need also to be carefully planned starting from the design of the device, involving low-cost solutions, sustainable materials, and relatively simple preparations.

From these starting points, the main goals of the experimentation were:

- Carry on experimentation in the field or at least mimic real conditions as much as possible
- Analyse the impact of environmental conditions on the signal of the devices
- Minimize the use of pure and/or toxic chemicals
- Create long-lasting devices
- Obtain a reliable signal in terms of sensitivity, selectivity and stability

In this dissertation, all these points have been addressed and the outcomes have been analysed, aiming to increase the knowledge in the promising field of MES-based sensing.

4 FUNDAMENTALS OF THE TECHNIQUES

4.1 Electrochemical techniques

From: *M. Tucci. Electrochemical micro biosensor for glucose analysis: application in complex matrix., MSc Thesis, University of Milan-Bicocca, 2016* [99]

Electrochemical analyses involve techniques that investigate the charge transport across the interface between chemical phases, usually solid (electrode) and liquid (electrolyte), but it can also involve the gas phase. The charge is transported through the electrolyte by the movement of ions and through the electrode by the movement of electrons. There are two main factors that affect the charge transfer: the mass transfer in the solution and the electron transfer at the electrode surface. In **figure 23**, those mechanisms are represented for a generic reaction of a dissolved oxidized specie O and its reduced form R.

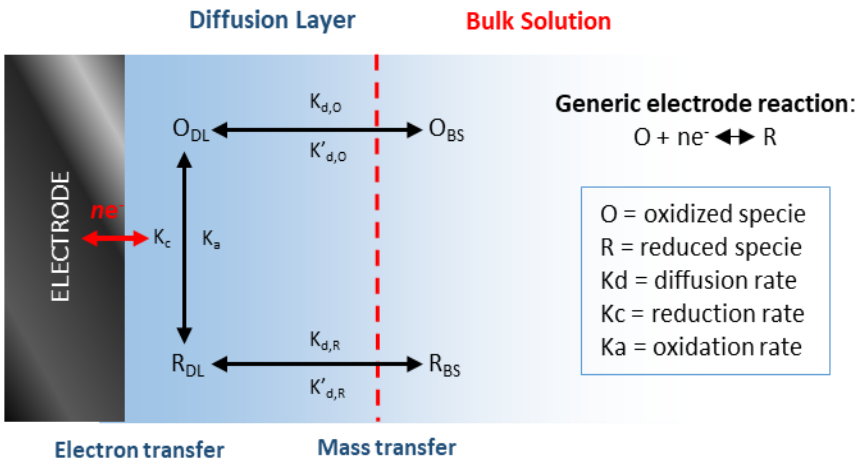

Figure 23 Model of the driving processes at the electrode surface: mass transfer and electron transfer. Adsorption and other intermediate reactions are not considered

The mass transfer, which is the transport of electroactive species across the solution, depends on migration (electric field), diffusion (concentration gradient) and convection (hydrodynamic transport). On the other hand, the electron transfer is due to the potential of the electrode and to the specific reactions involved. In addition, other processes can influence the charge transfer:

intermediate reactions occurring before the electron transfer and adsorption/desorption or crystallization at the surface of the electrode [87].

4.1.1 Faradic and non-faradic processes

There are two kinds of processes that can occur at electrode surface when a potential step is applied: faradaic and non-faradaic. Non-faradaic processes do not involve any charge transfer across the electrode/electrolyte interface, which means that no redox reactions are taking places at the electrode surface. Those reactions are thermodynamically or kinetically unfavorable at a given potential. Non-faradaic processes include adsorption/desorption, ions migration through the solution and change in the structure of the electrode solution interface. In this cases, the electrode/solution interface can be assimilated to a capacitor, as the charge will tend to accumulate on one side of the interfacial region and disperse on the other. For this reason, the current originated from these phenomena is referred to as capacitive current. Faradaic processes comprise oxidation or reduction reactions on the electrode surface, where charge (i.e. electrons) is transferred across the solid/liquid interface. Such reactions are governed by Faraday's law (**Eq. 6**), which states that "the amount of chemical reaction caused by the flow of current is proportional to the amount of electricity passed" [87].

$$m = \frac{Q\,M}{F\,z} \qquad \text{(Equation 6)}$$

In this equation, *m* is the mass of the substance liberated at an electrode in grams, *Q* is the total electric charge passed through the substance, *F* is the Faraday constant, *M* is the molar mass of the substance and *z* is the number of electrons transferred per ion. In order to be feasible, faradic processes require a significantly higher electron energy as compared to the theoretical thermodynamic values. The potential difference between the theoretical number and the potential actually needed to drive a given reaction at a certain rate is termed overpotential.

The background limits of an electrochemical experiment are the potentials at which a faradic current is observed having the WE immersed in a solution containing only the supporting electrolyte. When the potential is moved to more extreme values than the background limits, the constituents of the electrolyte solution react on the electrode, causing a sharp current increase of current due to their high concentrations [87].

4.1.2 Three-electrode electrochemical cell

An electrochemical cell can be defined as two electrodes, a Working Electrode (WE) and a Reference Electrode (RE), separated by an electrolyte phase [87]. The WE is the electrode where the reaction of interest occurs, whether the RE is an electrode with a constant composition and a fixed potential. The potential of the WE is measured against the potential of the RE. If the experiment implies a current flow, another electrode, called Counter Electrode (CE), is added to the setup This electrode forms with the WE an electric circuit in which the current flows (**Fig. 24A**). The potentiostat is an analytic instrument that can apply a selected potential to the WE and, at the same time, measure the potential difference ΔV between the WE and the RE. The applied potential causes the current i to pass between the CE and the WE, which is also measured by the potentiostat (**Fig. 24B**).

A) **B)**

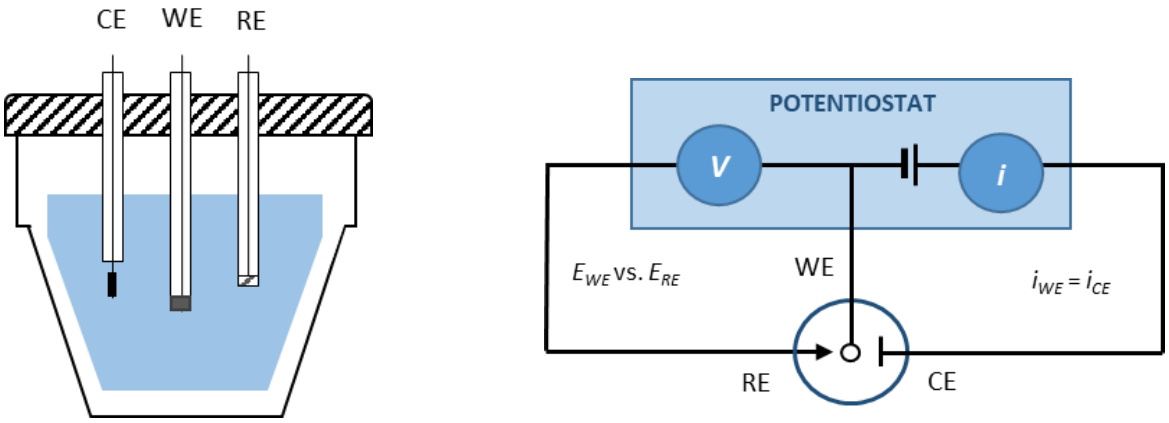

Figure 24 – Schematic representation of a three electrode system: a potentiostat is able to apply a potential difference between the WE and the RE and measure the resulting current between WE and CE.

The tip of the RE needs to be very close to the WE in order to reduce as much as possible the ohmic drop caused by the resistance of the solution. The CE, instead, should be distanced from the WE so that the counter reactions do not affect the behavior of the WE: if the compounds produced on the CE surface reach the WE, they may cause interfering reactions. For this reason, the CE is often placed in a separate compartment [87]. The three electrode setup is used to perform most

electrochemical techniques, such as chronoamperometry linear-sweep voltammetry and cyclic voltammetry.

4.1.3 Chronoamperometry

Chronoamperometry (CA) is a technique that consists in applying a fixed potential step to the WE in order to observe possible electrochemical reactions generated at that condition (**Fig. 25A**). The current response is measured and plotted as a function of time (**Fig. 25B**) [100].

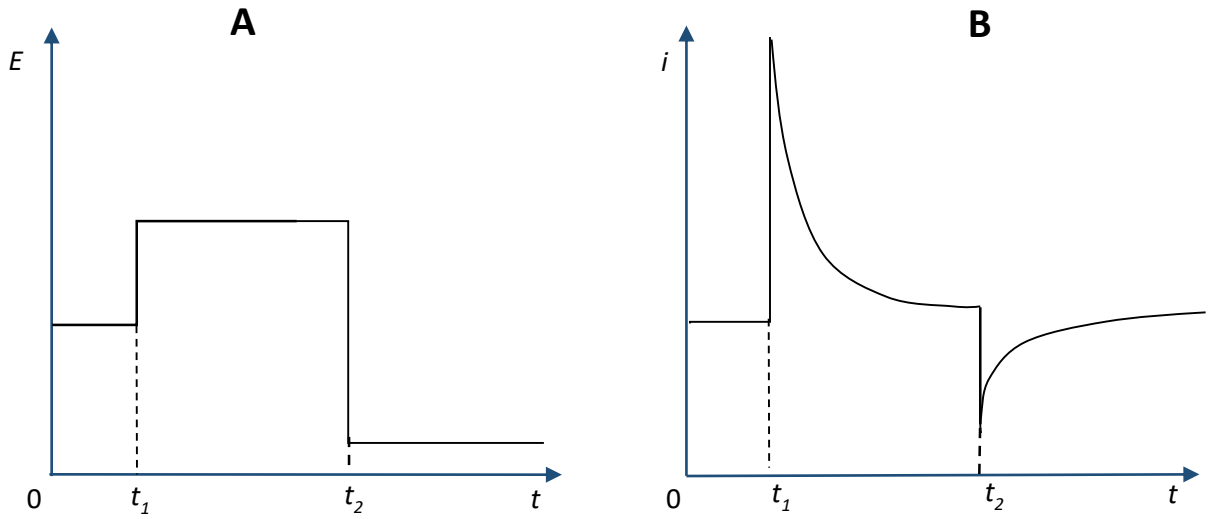

Figure 25 - Qualitative representation of a theoretical chronoamperometry. A) excitation waveform, B) corresponding chronoamperogram

If the WE potential was in a region where no faradaic processes were occurring, and is set into a region where the potential causes any electrochemical reaction to happen, a sharp variation in the current response can be observed (t_1, t_2). This happens because the molecules electroactive compound(s) present in the proximity of the electrode surface are quickly oxidized or reduced, accordingly to the chosen potential step. As those molecules react, a gradient of concentration is generated in the solution, which causes other molecules of the same compound(s) to diffuse toward the WE and react as they reach its surface. As the electroactive specie is consumed, the current decreases due to lack of reactant [87].

4.1.4 Linear-sweep voltammetry

A linear sweep voltammetry (i.e. polarization curve) is a potentiodynamic electrochemical technique: the potential is varied linearly with time (voltage ramp, **Fig. 26A**), and the potentiostat measure the current flowing between the WE and the CE. In this way a current vs. potential plot can be obtained (**Fig. 26B**).

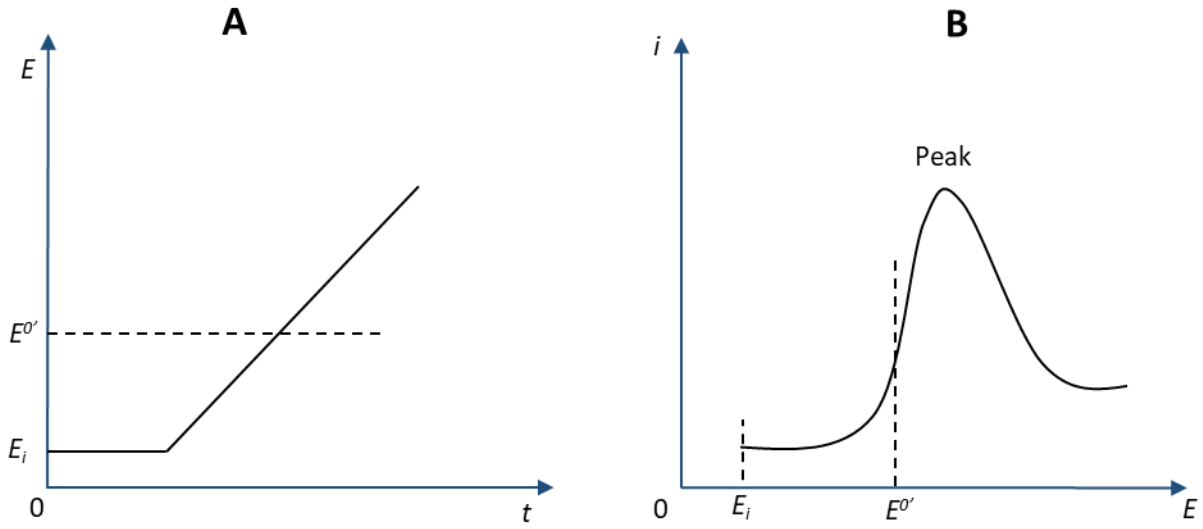

Figure 26 – Qualitative representation of a theoretical liner sweep voltammetry. A) excitation waveform, B) corresponding polarization curve

In the case depicted in **figure 26**, only non-faradaic currents flow at the initial potential E_i. Then the imposed potential start to increase, and when it reaches the vicinity of the formal potential $E°'$ (i.e. reaction potential at the given conditions of pH, T, ionic strength and concentration) for the involved specie, the reaction begins and a current flow starts. As the potential continues to grow, the concentration of the compound at the electrode surface drops, while the flux of molecules towards the electrode increases due to the electric gradient, and so does the current. When the potential pass E°', the concentration at the surface becomes close zero, and the mass transfer of the compound in direction of the surface reaches a maximum rate. After that, the current declines due to the depletion of the compound in the solution surrounding the electrode. Hence a peak in the current-potential curve can be observed.

4.1.5 Cyclic voltammetry

In a cyclic voltammetry (CV) the potential applied to the WE varies at a constant rate between two vertices. The first ramp of potential is called forward scan, and when the potential moves in the opposite direction it is called reverse scan (**Fig. 27A**). The current flowing between the WE and the CE is measured and recorded by the potentiostat, and it is represented in a current vs. potential plot (**Fig. 27B**). If a current peak is present in the chosen potential range, it means that a redox reaction is taking place at the electrode surface.

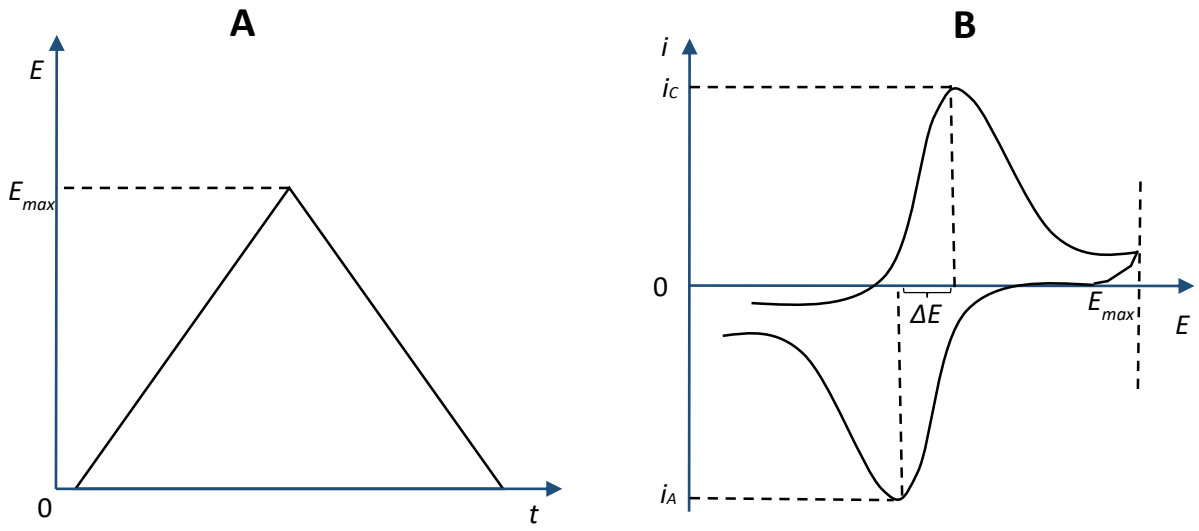

Figure 27 - Qualitative representation of a theoretical cyclic voltammetry. A) excitation waveform, B) corresponding voltammogram for a reversible redox reaction

Usually, in a CV experiment multiple cycles are performed, in order to allow the system to reach a steady state. When this condition is obtained, if the height of the anodic peak i_A and the cathodic peak i_C are equal, the involved reaction is chemically reversible. In addition, the reaction is electrochemically reversible if the difference between the potential of the two peaks ΔE is less than 57 mV. This conclusion can be demonstrated using the Nernst equation (**Eq. 7**). Multi-cycle CV are also used to observe a chemical change of the solution and/or the electrode over time, until the system reaches the equilibrium [100].

$$E = E° + \frac{R\,T}{n\,F}\,ln\,\frac{a_{ox}}{a_{red}} \qquad \text{(Equation 7)}$$

The terms of the Nernst equation are: the cell potential at the given absolute temperature (i.e. electromotive force) *E;* the standard cell potential $E°_{cell}$; the universal gas constant *R*; the absolute temperature *T*; chemical activity for the relevant species *a*; the Faraday constant *F;* the number of moles of electrons transferred in the cell reaction *z*.

4.2 Sensing and validation of the method

4.2.1 Chemical sensor definition

A chemical sensor is a device that transforms a chemical information in a useful analytical signal [101]. The chemical information can be about a chemical specie, a reaction or a physical property of the whole system, such as adsorbance, refractive index, conductivity, temperature, mass change, etc. The two major constituents of a chemical sensors are a chemical recognition system, called receptor, and a physiochemical transducer. The receptor is the element that transforms the chemical information in a form of energy, while a transducer is the part capable of converting the energy generated by the receptor into an analytical signal [101]. When a sensor employs a biologic element as receptor it is called biosensor. Biological receptors can range from multicellular organisms to subcellular units (e.g. enzymes, antibodies, photosystems, etc.).

In electrochemical sensors, the transducer is constituted by an electrode, and the signal is a property of the electrochemical system, such as current, voltage, impedance, etc. The signal can be measured by an analytic instrument, and then it is converted into a digital output [86]. A flow chart of the steps needed for a measure of is represented in the figure below (**Fig. 28**), and a theoretical microbial electrochemical sensor is presented as example.

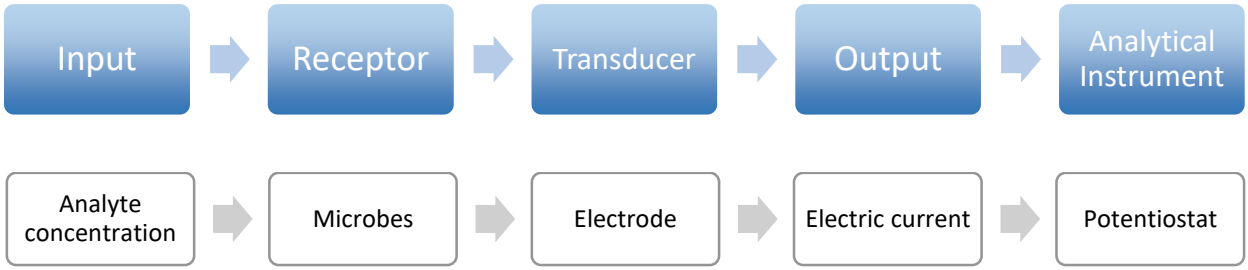

Figure 28 - Flow chart representing the elements necessary for a measurement (Blue boxes). A generic microbial electrochemical sensor is used as example (white boxes)

4.2.2 Sensor calibration

According to analytical chemistry, calibration is the process aimed at establishing an "unequivocal mathematical relationship between the measured physical quantity and the analyte concentration" [102]. The measurable physical quantity, which is the output of the sensor, is called response signal (i.e. current in the case of amperometric sensors). The general relationship that correlates the intensity of the signal (y) and the analyte concentration in the sample (c) can be described by the following equation:

$$y = F(c) + e_y \qquad \text{(Equation 8)}$$

where *F(c)* is the calibration function and e_y represent the error on the response measurement [103]. Due to its convenience, the most common calibration function is the direct proportionality relationship:

$$y = ac \qquad \text{(Equation 9)}$$

The factor a represents the sensitivity of the sensor, and it can be calculated with relationship the expressed in **equation 10**. The higher is the value, the more sensitive is the sensor towards the selected analyte.

$$a = \frac{d_y}{d_c} \qquad \text{(Equation 10)}$$

According to the characteristics and properties of sensor setup (e.g. bioreceptor, transducer, working conditions, etc.), the range of substrate concentrations in which the linear relationship is valid (i.e. linear range) can be of a certain width [86]. A wider linear range allows a higher applicability of the sensor. Below or above this range, a nonlinear correlation could be established, until there is no correlation between the analyte and the signal. The Lower Limit of Detection (LLOD) of a chemical sensor is defined as the lowest concentration of analyte that can be distinguished from the absence of that substance (i.e. blank value) within a defined confidence limit [103]. It can be obtained with the signal-to-noise approach [104] using the relationship expressed in **equation 11**, where σ is the standard deviation of the measure of the lowest concentration and a is the slope of the calibration curve:

$$LLOD = \frac{3\sigma}{a} \qquad \text{(Equation 11)}$$

Conversely, the Upper Limit of Detection (ULOD), is the highest concentration of analyte that can be distinguished from the saturation condition within a defined confidence limit. These concepts are exemplified in **figure 29**, where a theoretical response signal of a sensor is plotted against the analyte concentration.

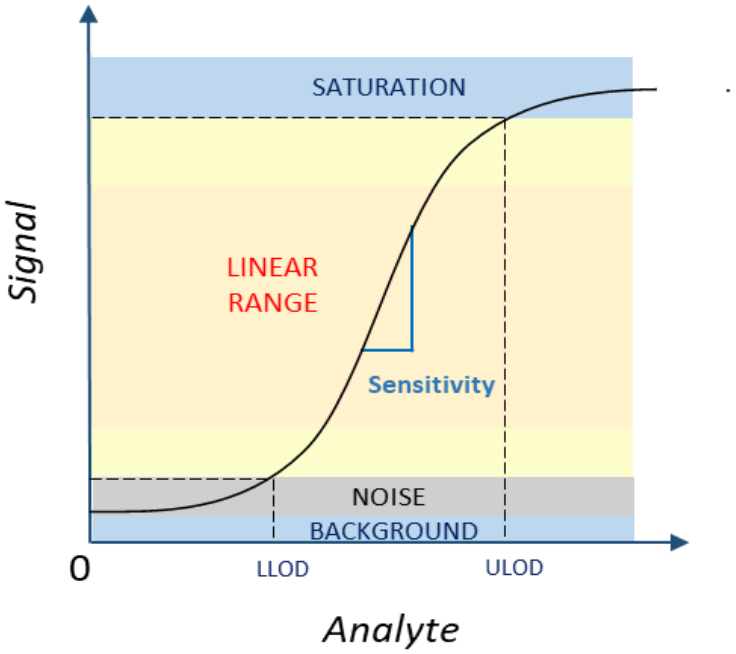

Figure 29 – Theoretical response of a sensor towards an analyte: when the concentration of analyte is below the LLOD, the signal of the sensor is undistinguishable from the background level. For greater amounts of analyte, the correlation between signal and analyte can be considered linear within a certain range. Then, after a certain concentration, corresponding to the ULOD, the sensor gets saturated and the signal tends to a plateau.

4.2.3 Figures of merit of the sensor

Besides the sensitivity, the linear range and the limits of detection, there are other parameters, or figures of merit, to evaluate performances of a chemical sensor.

A very important aspect to take in to account is the selectivity, which indicates how good is the sensor at discriminate a particular analyte from other substances that may be present in the sample, which can interfere with the signal [103]. This term is different from specificity, as the latter is absolute and refers to the ability to respond only to one particular substance (e.g. antibodies with

antigens). However, due to the similarity between analytes or to the lack of receptors that are exclusive to the target substance, specificity is often not achievable, making selective sensing the best option available [105]. On the other hand, arrays of non-specific sensor can still be able to discern between analytes, in the so called "chemical nose/tongue" approach, where multidimensional data can be used as a "fingerprint" of the analyte: a unique set of different measures that individuate a single substance [105]. Moreover, non-specific sensors can be useful as screening tools able to detect a broad variety of analytes. In this way they can be used as preliminary step to the implementation of more refined techniques.

Trueness, precision and accuracy and are also very important parameters to assess the performance of a sensor. In a set of measurements, the term trueness refers to the closeness of the obtained measure to a given value or standard (e.g. known concentration of analyte). It is a measure of the systematic errors that can impact on the measuring process, and it can be expressed as bias, which is the difference between the average of the set of measure and the true value. On the other hand, precision concerns the closeness of the obtained values to each other, thus it is an evaluation of the random errors and the statistical variability of the measurement. Its quantitative expression is the standard deviation from the average. Accuracy is the combination of these two factors, and it evaluates of the overall uncertainty of the measure [106]. The representation of these concepts is shown in **figure 30**.

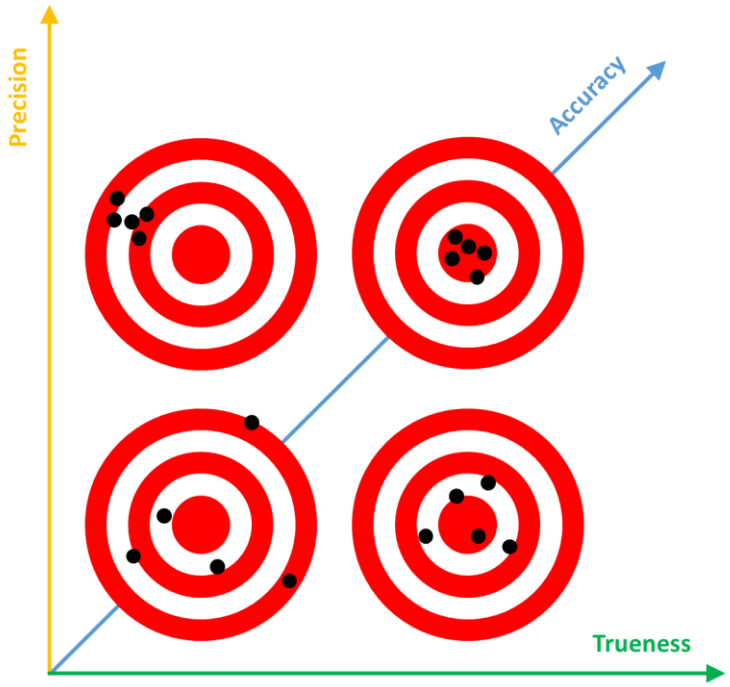

Figure 30 – Representation of the concepts of trueness, precision and accuracy. The true value is represented by the centre of the target, and the measurements are represented with black dots.

The response time is another critical characteristic of a chemical sensor: it can be defined as the time passed between the moment when the analyte is added to the solution and the moment when the sensor response can be considered stable [103]. This time gap is influenced by the analyte speed of diffusion towards the receptor, which mainly depends on the stirring of the solution and the presence of diffusional barriers. Also, the characteristics of the receptor, like the rate of activity and the affinity towards the analyte, play a key role in the velocity of response [86]. Clearly, sensors with shorter response time are preferable.

4.2.4 Durability of the sensor

In order to be reliable and cost effective, a sensor should be durable and consistent overtime. This aspect can be summarized in two factors: stability and lifetime. The operational stability can be defined as the drift of the signal obtained on the same concentration of analyte over a period of time [86]. It is determined by the characteristic of the receptor (e.g. fragility, lifetime, self-repairing capabilities, homeostasis) and the operational conditions at which the sensor is exposed (e.g. pH, temperature, sample composition, solvents, fouling, clogging, etc.). Moreover, the way in which the sensor is stored can greatly affect its long-term stability.

The lifetime of the sensor, on the other hand, refers to the overall time span in which the sensor can be operated. It depends on the stability but also on the materials and construction technique used to build the sensor.

5 MFC FOR WASTEWATER MONITORING

5.1 BOD monitoring in wastewater treatment plant

From: M. Tucci, A. Goglio, A. Schievano, P. Cristiani. Floating MFC for BOD monitoring in real time: field test in a wastewater treatment plant. Proceedings of the 7th European Fuel Cell Piero Lunghi Conference (2107) [107]

5.1.1 SCIENTIFIC BACKGROUND

The Biological Oxygen Demand (BOD) measurement is a key factor for the wastewater treatment process. Currently the BOD_5 test is the most widely used. However, this method has some analytical and operational limitations, such as questionable accuracy and irreproducibility, labour intensity and time consumption. Therefore, this method is not effective for process control and real-time monitoring where rapid feedback is needed [51].

Since the current or the charge generated from a Microbial Fuel Cell (MFC) are proportional to the concentration of fuel used under non saturated conditions [108], Microbial Fuel Cells (MFCs) are attracting increasing attention as a tool for on-line BOD monitoring. Over the years, very different set-up and configurations have been developed for this purpose [54,56,57,109]. However, very few of them seem to focus on a real wastewater treatment application, as in most cases they employ pure chemicals as substrates, artificial electrolytes, gas sparging, controlled temperature and ion exchange membranes, which can undergo biofouling. Here, a low-cost, online, self-powered MFC-based sensor for BOD is presented, and its application in a real wastewater treatment plant is discussed.

5.1.2 MATERIALS AND METHODS

Cell construction

The structure of the sensor consisted in a polystyrene floating frame, holding identical plane electrodes made of carbon cloth (SAATI P10) separated by a clay layer and an insulating polypropylene felt (**Fig. 31A**). The submerged anode (13x10 cm) and the air cathode (16x16 cm) are connected to a circuit with 100Ω of external load. The anaerobic biofilm on the anode surface oxidize the organic matter present in the anoxic wastewater, while the oxygen reduction reaction

(ORR) occurs at the air-exposed cathode (**Fig. 31B**). This simple and low-cost construction allows an easy applicability in a real plant in multiple copies, with an estimated overall price of 1.70€ for the construction of one cell.

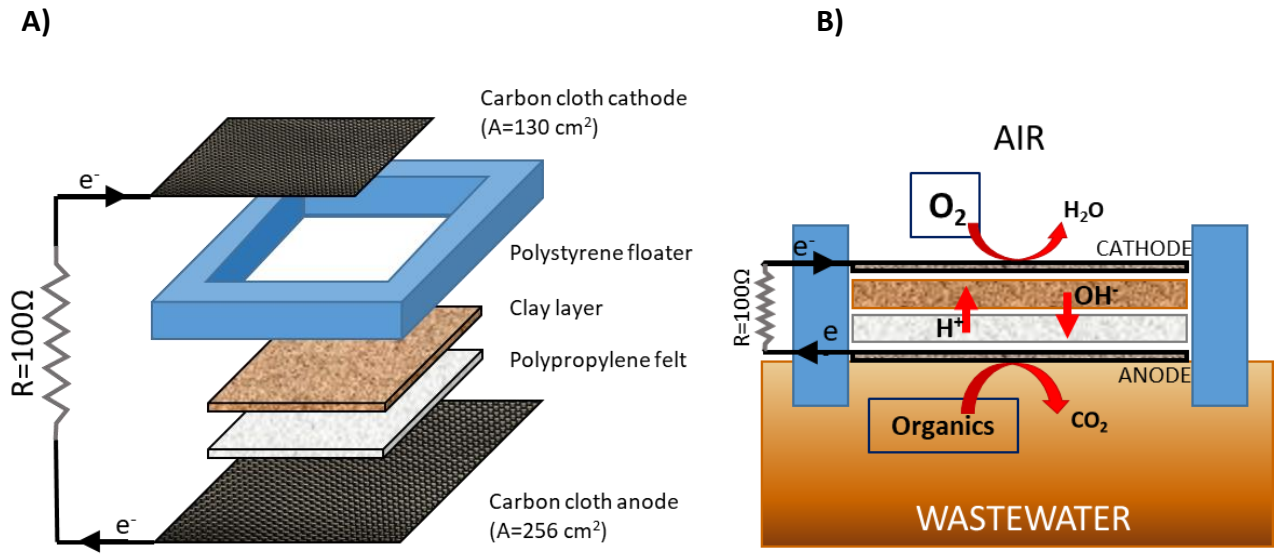

Figure 31 – Schematic representation of the structure of the floating MFC prototype (A) and of the reactions (B)

Calibration in laboratory

Two cells constructed as previously described were placed in a stirred 40L tank and fed with acetate as the sole carbon source. Raw wastewater was collected from the wastewater treatment plant of Carimate (CO, Italy) and used as both inoculum and electrolyte. Calibrations were performed by subsequent addition of sodium acetate (Sigma Aldrich). Liquid samples were collected from the tank during the experiments for the chemical analysis.

Wastewater treatment plant

The wastewater treatment plant of Carimate treats about 5.000.000 m^3/year of urban wastewater (70.221 population equivalent, PE) and 1.000.000 m^3/year of industrial wastewater. Six identical cells constructed as previously described were placed directly in the tank of the plant, where anaerobic denitrification occurs. The exact point is indicated on the map of the plant shown in **figure 32C**. Samples of the wastewater were collected nearby the cells for the chemical analysis. **Figure 32A and B** show pictures taken during the operations.

A)

B)

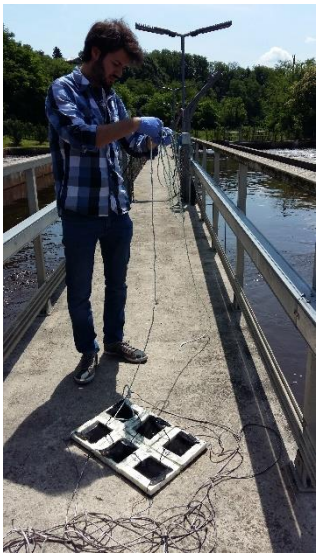

C)

Figure 32 – Pictures taken during the field trials A) and B), map of the wastewater treatment palnt of Carimate (CO) C). The exact point in the denitrification tank where the cells were placed is indicated with a red pointer.

Measurements

The Total Organic Carbon (TOC) and the Total Inorganic Carbon (TIC) were continuously monitored with Sievers 820 Portable Total Organic Carbon Analyzer. The potential difference across the resistance (R) of every MFC was acquired every 6 min via a multichannel Data Logger (Graphtech midi Logger GL820). The generated current (I) was calculated by the equation I = V/R, where I is the current flowing through the external resistance. Polarization curves were measured by linear sweep voltammetry using a platinum counter electrode and Ag/AgCl in KCl 3 M a reference electrode. The measure was conducted with a portable potentiostat (Ivium, CompactStat). The soluble Chemical Oxygen Demand (sCOD) of the wastewater samples was measured by a spectrophotometric method. Each sample was filtered with syringe filters (Sartorius, 0,45µm porosity), and then added to HT-COD cuvette test (Hach Lange Gmbh), and digested at 175 ºC for 15 min (Lange HT 200 S). After cooling, the COD value was read by an UV- spectrophotometer (Lange DR 3900).

5.1.3 RESULTS AND DISCUSSION

Figure 33 shows the current trend of two cells and sCOD when subsequent additions of acetate were performed. The increase and decrease of sCOD are followed by the current with a very short response time. The linear correlation between the current signal and the concentration of sCOD is shown in the inset: the range varies between between 13 and 34 ppm and the obtained R^2 is 0.88.

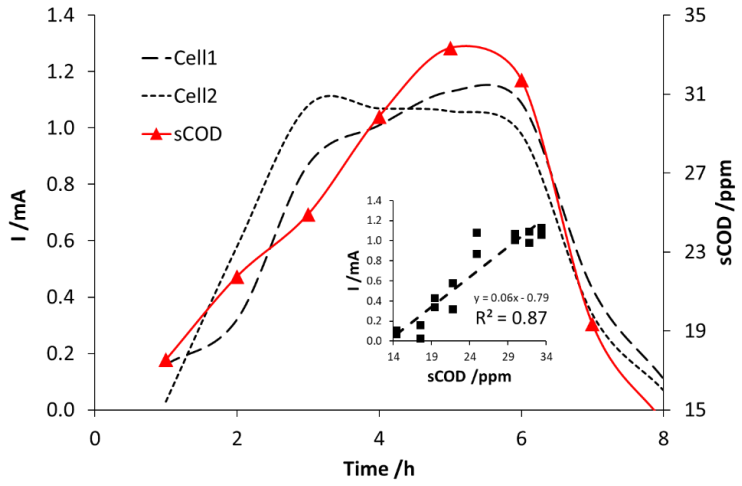

Figure 33 - Trends of current of two MFCs and sCOD during subsequent addition of acetate. Linear correlation between current and sCOD (inset).

For higher concentration of sCOD the linear relationship is lost, until the system is completely saturated and the current reaches a plateau around 100 ppm (**Fig. 34**).

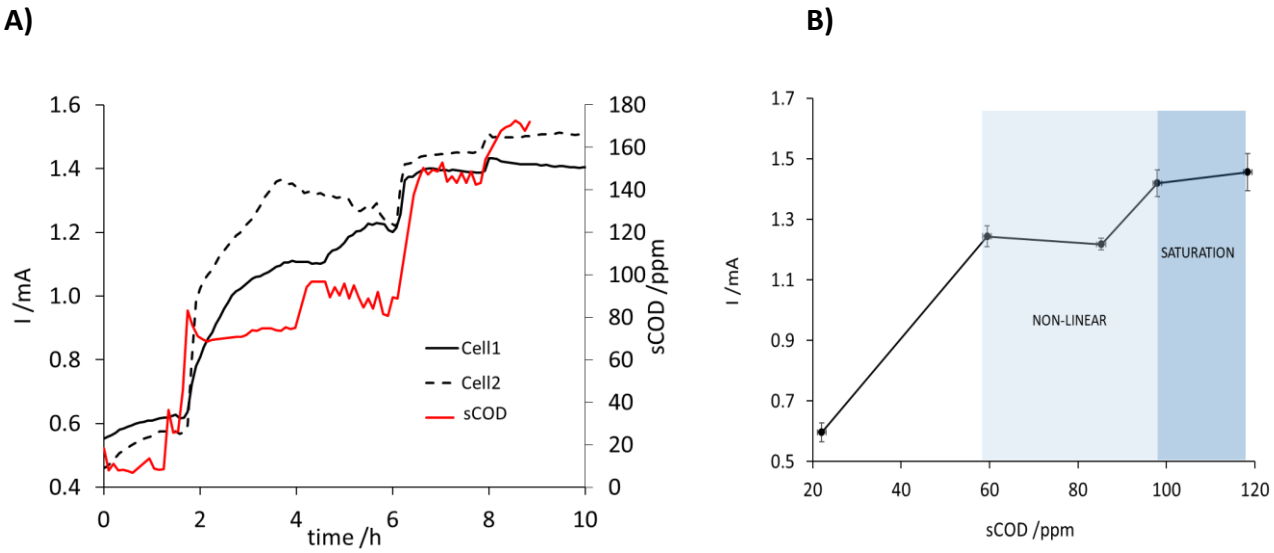

Figure 34 - Trends of current of two MFCs and sCOD during subsequent addition of acetate (A). Current vs. sCOD calibration curve of the average of the two cells showing the saturation effect (B).

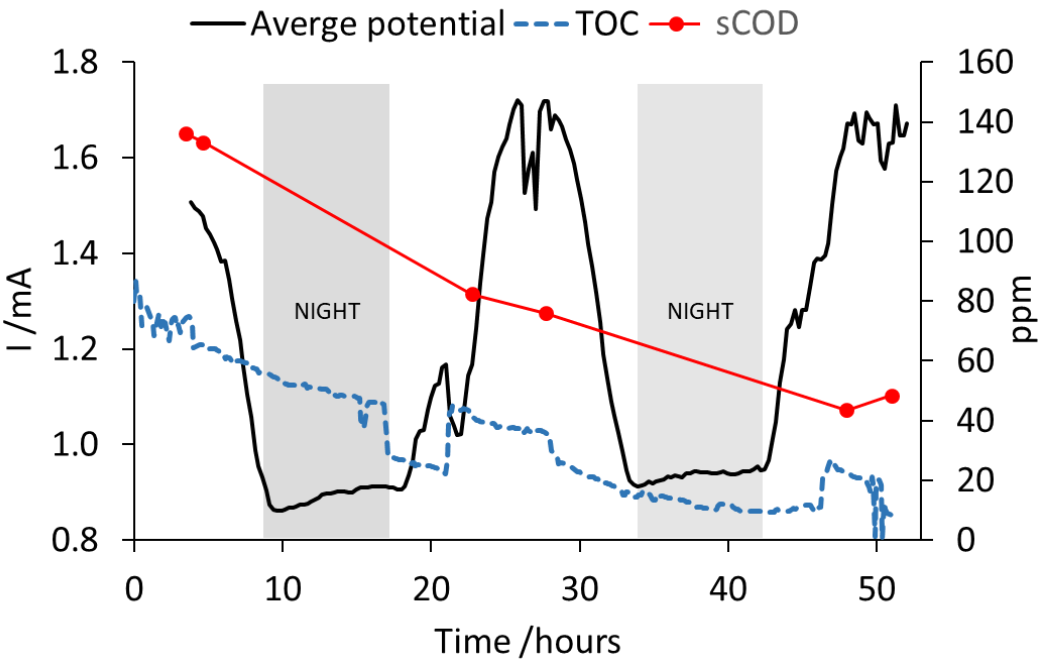

Figure 35 – Trend of current, TOC and sCOD recorded over a period of three days.The current is an average of three replicates and is stongly influenced by the daily illumination cycle, with no noticeable correspondance with the organic load present in the wastewater.

Initially, the six floating MFC were tested for three days in the denitrification tank of the plant. However, the variation of the organic matter in the wastewater, measured both as COD and TOC, seems not correlated with the current trend (**Fig. 35**). Instead, the trend shows the presence of peaks in correspondence with the maximum illumination of daylight. This phenomenon was observed also in a longer trial, which was conducted over a period of 30 days (**Fig. 36**). Indeed, the current trend is characterized by daily peaks related to the periods of illumination of the cathodic surface. In order to exclude this interference, the moving average of the current was calculated (period 100, solid line), and this time it can be noticed how its trend follows the increase and decrease of the soluble COD (diamonds). However, a delay between the peaks is present, which is probably due to the presence of recalcitrant organic compounds in the wastewater. Indeed, the degradation of these compounds operated by the anodic biofilm is normally much slower than the sole acetate.

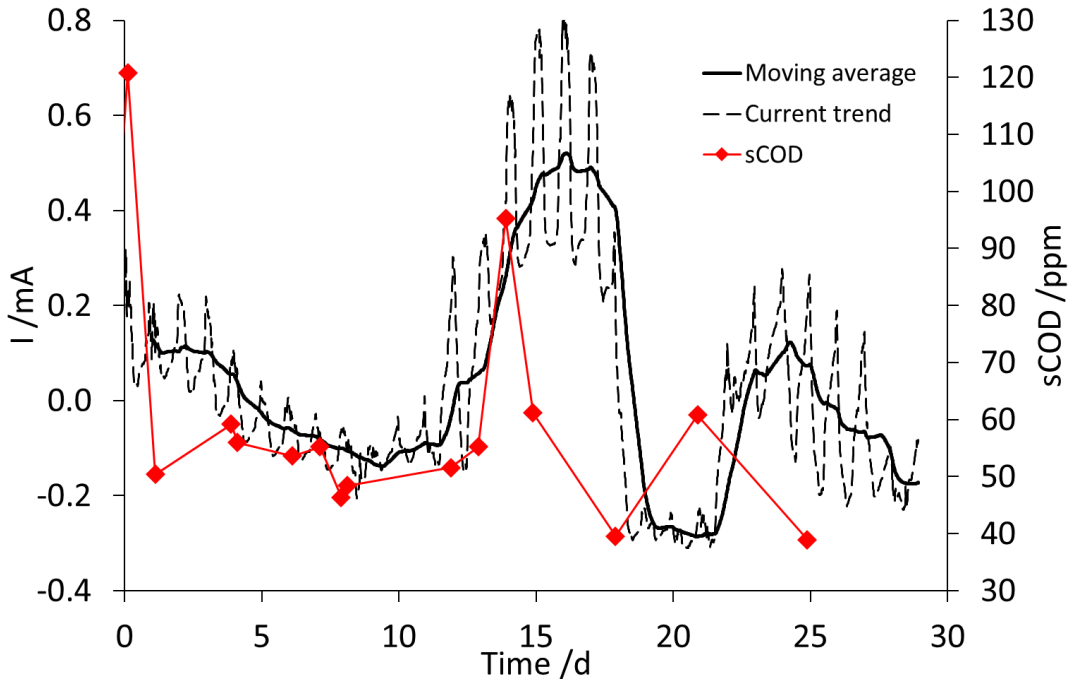

Figure 36 – Trends of average current output of the six floating MFC and measured sCOD concentration in the denitrification tank over a period of 30 days. The peaks of organic load are followed by peaks in the voltage trend with a delay of about two days.

Another critical aspect of this setup is related to the cathodic performance, as shown by the polarization curves in **figure 37**. As expected, the anodic curves display a strong correlation with the sCOD, whether no variation can be noticed on the cathode performance at the three different

concentrations. However, the current that can pass through the cathode is much lower than the one that can be generated at the anode. For this reason, the cathode inefficiency seems to generate a bottleneck effect on the sensor performance, as it limits the current of the overall system, and thus the sensitivity of the anode. The lack of a catalyst for oxygen reduction, together with the fact that the area of anodes and cathodes are very similar, could provide a good explanation of this behaviour. If the goal is to keep a low price and sustainable materials, a solution to this problem could be the increase of the anode/cathode surface ratio, instead of employing expensive catalysts.

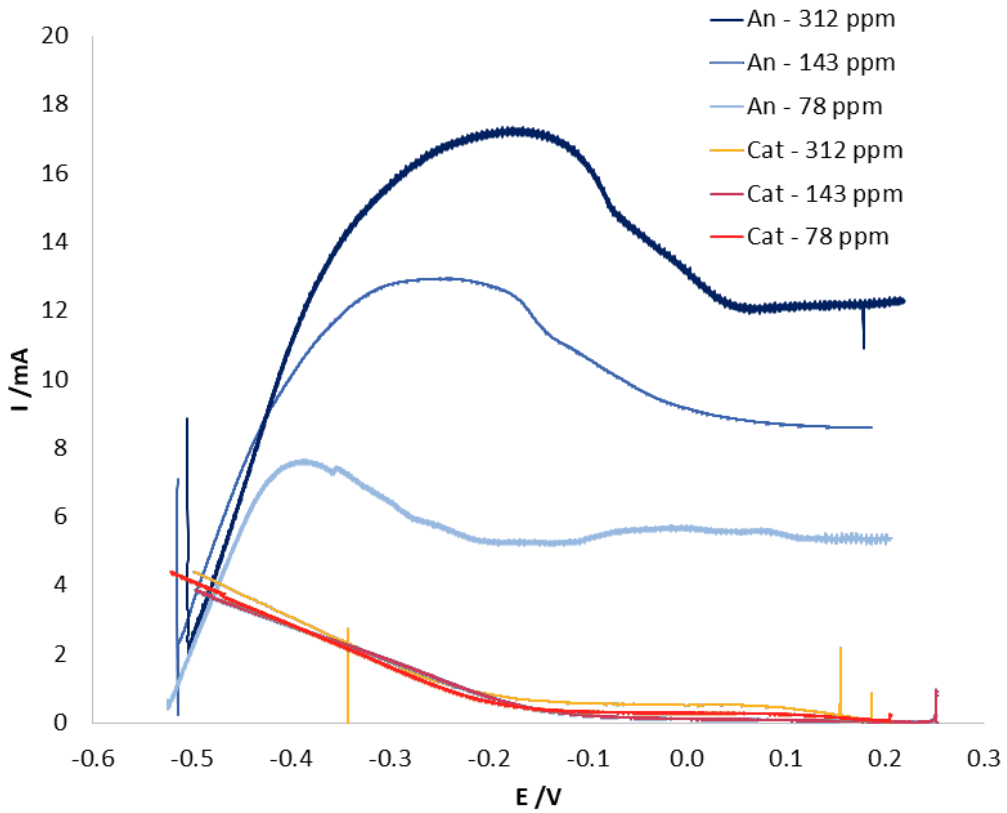

Figure 37 – Anodic and cathodic polarization curves of the floating MFC at different concentrations of sCOD

5.1.4 CONCLUSION

A new prototype of floating membraneless MFC-based sensors for BOD monitoring has been successfully calibrated and operated in a real wastewater treatment plant. A correspondence between the peaks of current and sCOD has been observed, which is encouraging in view of a possible future application. Further investigations should address the decrease of the impact of environmental factors (e.g. light, temperature, precipitations, etc.) on the current signal as well as reducing the response time, studying the influence of recalcitrant compounds and enhance the

sensibility of the sensor. Moreover, the performance of the cathode needs to be enhanced, for example by increasing the active surface of the cathode and increasing the anode/cathode surface ratio.

5.1.5 AKNOWLEDGEMENTS

The author acknowledges Sud Seveso Servizi S.p.a. for the chance to perform the experiment in the wastewater treatment plant of Carimate (CO), and Paolo Bonelli and Fausto Otero, for the support in the construction of the voltage acquisition system.

5.2 Impact of physical-chemical factors on MFC-based sensor for wastewater monitoring

From: M. Tucci, E. Barontini, A. Schievano, M. Papacchini, A. Espinoza-Tofalos, A. Franzetti, P. Cristiani. Influence of environmental factors on MFC-based sensor for wastewater monitoring. Proceedings of the 8th European Fuel Cell Piero Lunghi Conference (2109)

5.2.1 SCIENTIFIC BACKGROUND

In many recent studies, the current generated by Microbial Fuel Cells (MFCs) has been evaluated as signal for wastewater monitoring, since various physical-chemical factors (e.g. BOD, dissolved oxygen, temperature etc.) can affect the microbial metabolism and thus the cell performance [66,67]. Moreover, these systems require minimum maintenance and do not need external power source, so they are especially suitable for remote sites and diffuse environmental monitoring. However, few attempts have been made to study this technology in real field applications. An interesting approach to this subject is represented by floating MFCs located directly in the tank of a wastewater treatment plant: oxidation of the organic matter present in the wastewater occurs at the submerged anode, while oxygen is reduced at the air-cathode [107]. In this kind of systems, a clear understanding of the parameters that can influence the current output is necessary to analyse the signal. For instance, light variation is an environmental condition that can have a strong influence on the system in direct and indirect ways (e.g. temperature change, enhancement of photosynthetic organisms, etc.). The oscillation of power produced in flat MFC during the circadian cycle was recently reported, especially for flat MFC of small geometry [13]. Also, the variability of the wastewater composition can strongly affect the MFCs performance: for example, the presence of recalcitrant organic compounds, level of oxygenation, nitrate content etc., can create disturbances in the current signal [65]. Herein, the impact of light and other physical-chemical factors on the microbial communities and the performances of floating MFCs has been investigated.

5.2.2 MATERIALS AND METHODS

Cell construction

Two types of cells were placed in the denitrification tank of the wastewater treatment plant of Bresso-Niguarda (MI): one constituted by a planar frame and the other with a ceramic cylinder. Regarding the first type (**Fig. 38A**), the construction of the cell was similar to the prototype described in the previous chapter. This time, however, no clay layer was put between the electrodes, and both the anodes and cathodes were 10 x 10 cm. The second type consisted in a terracotta cylinder that functioned both as rigid structure and separator between the electrodes. A floater ensured that the cylinder remained afloat perpendicularly to the wastewater surface. One end of the tube was sealed and the other was in communication with the atmospheric air. A plain carbon cloth anode (5x15 cm) was fixed outside of the tube, while a carbon cloth cathode (18x20 cm) functionalized with carbon nanotube paint was placed inside the cylinder (**Fig. 38B**). A plastic cone was placed on the top of the tube in order to protect the cathode from sunlight and allow the passage of air. The voltage was continuously measured across a resistance of 100Ω for the first type and 500Ω for the second type using a multichannel Data Logger (Graphtech midi Logger GL820). For each type, two groups of triplicates were constructed and operated.

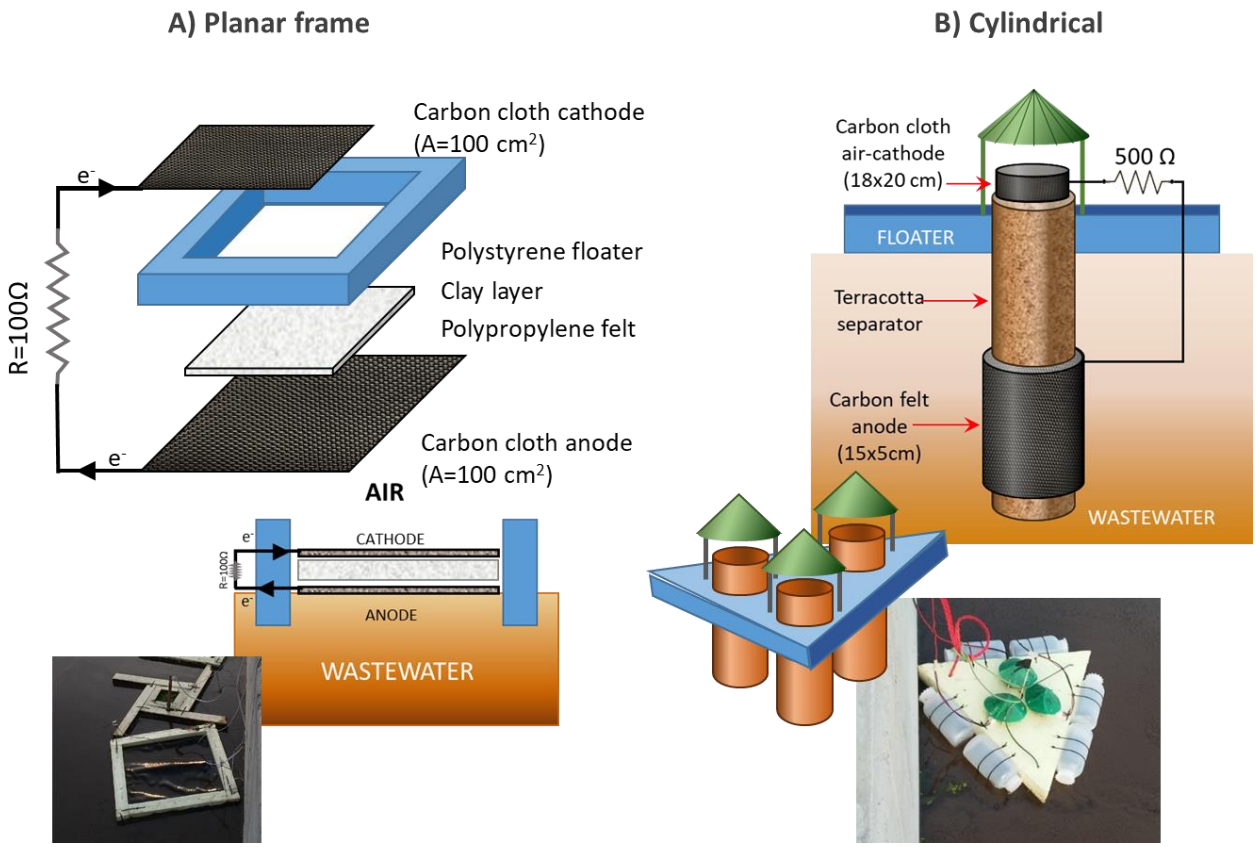

Figure 38 – Two types of cells used for the experimentation: A) a floating planar frame holding two carbon cloth electrodes separated by polypropylene felt, B) a terracotta cylinder that separates the inner cathode from the outer anode held by a floater. The cross section, a 3D scheme and a picture are shown for each type.

Wastewater treatment plant

The experimental activities were conducted at the wastewater treatment plant of Bresso-Niguarda (MI), group CAP Amiacque (**Fig. 39A**). This plant is situated in the urban area of Milan and treats urban wastewater for about 173000 PE. The plant is involved in several collaborations with University of Milan, University of Milan-Bicocca and Politecnico di Milano for the development of an innovative and sustainable wastewater cycle, including the cultivation of microalgae and the production of biogas, in the direction of a biorefinery framework. **Figure 39B** shows a picture of the cells placed in the denitrification tank of the plant, and in **figure 39C** a picture taken during the construction of the electric setup is depicted.

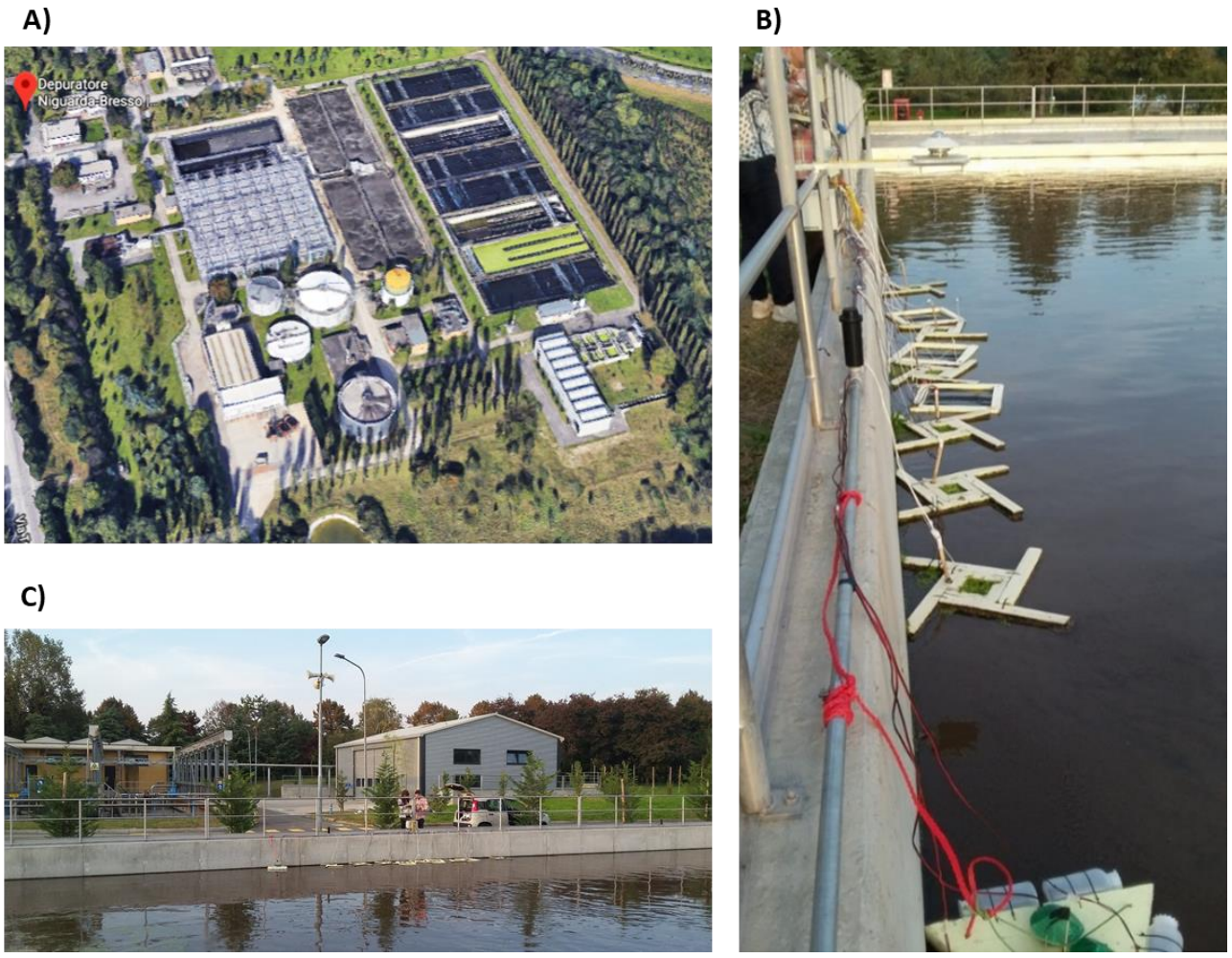

Figure 39 – A) aerial view of the wastewater treatment plant of Bresso-Niguarda, B) Floating MFCs employed for the experiment in the denitrification tank, C) picture taken during the setting up of the data-logger

Physical-chemical measurements

Solar irradiance and temperature were continuously monitored using a pyranometer (Kipp&Zonen, **Fig. 40**), and a thermometer (Dallas Semiconductor) respectively. A vertical profile of redox potential and dissolved oxygen was obtained for the first 50cm of water, using submergible probes (AMEL).

Figure 40 – Pyranometer placed over the denitrification tank of the wastewater treatment plant

An automatic sampler was built in order to continuously collect wastewater sample from the denitrification tank. It was constituted by a circular wooden structure holding 12 identical vessels (**Fig. 41B and C**), each of them provided with a funnel in which was placed filter paper shaped as a cone (**Fig. 41E**). The wastewater was collected by means of a submersible pump. The tube of the pump was connected to a rotating arm that directed the output stream on the different vessels. The pump and the rotating arm were synchronized by an automatic system controlled with Arduino (**Fig. 41A and F**) in such a way that the arm would move the tube from one vessel to the next every two hours (**Fig. 41F**), thus collecting 12 samples per day. After being re-filtered (syringe filters Sartorius, 0,45 µm porosity), the samples were analysed in terms of soluble COD and nitrate content using a spectrophotometer. For COD measurement, an aliquot was added to HT-COD cuvette test (Hach Lange, LCK 1414), and digested at 175 °C for 15 min (Lange HT 200 S). After cooling, the COD value was read by an UV- spectrophotometer (Lange DR 3900). The nitrate was also determined using a cuvette test (Hach Lange, LCK 339) and the concentration value was measured using the same UV-spectrophotometer.

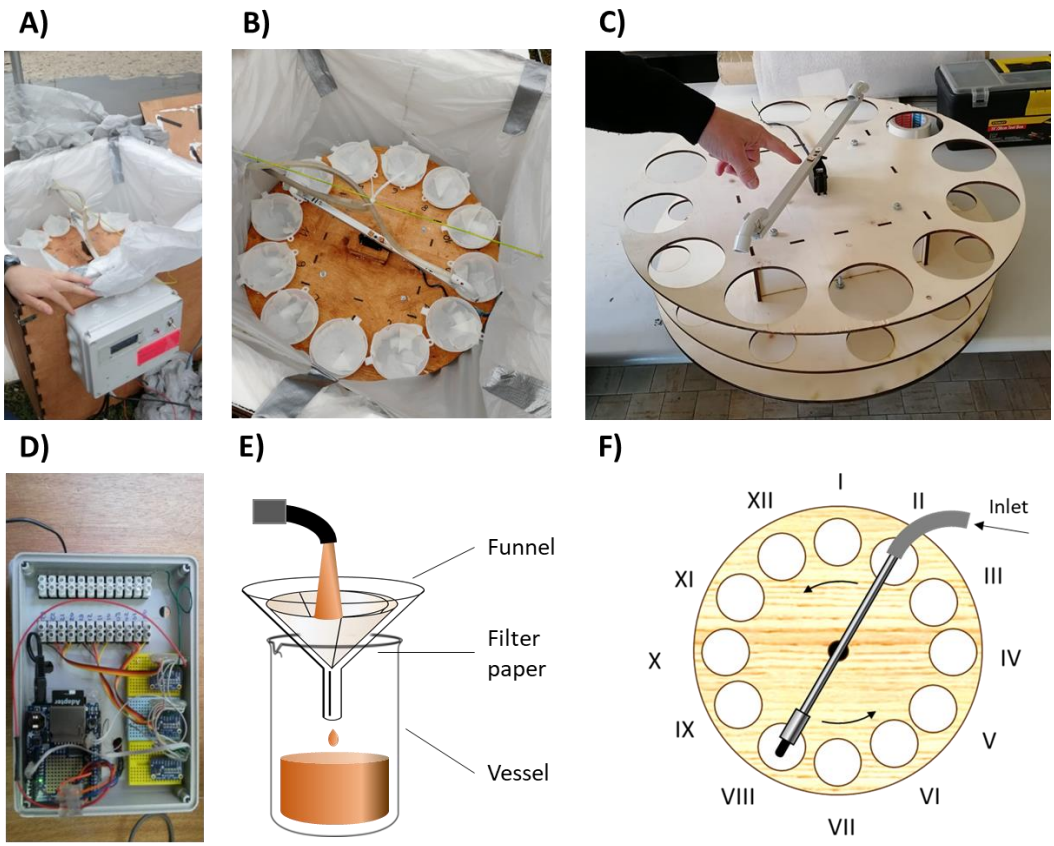

Figure 41 – A) and B) pictures of the automatic sampler used for the experimentations. C) Picture taken during the construction of the sampler. D) Digital control system of the pump and the rotating arm. E) Scheme of the sampling technique: the wastewater is collected by a funnel containing filter paper, which then percolates into a vessel. F) Scheme of the rotating arm that moves over the 12 different vessel during 24h cycles.

Microbial characterization

Biofilm samples at anodes and at cathodes, and a liquid sample from the bulk of the wastewater tank were collected for microbial analysis. The taxonomic characterization of the bacterial communities was performed by Illumina sequencing of the 16S rRNA gene. Total bacterial DNA was extracted according to the manufacturer's instructions using the FastDNA Spin for Soil kit (MP Biomedicals, Solon, OH, USA). The amplification of the V5-V6 hypervariable regions of the 16S rRNA gene was carried out as described by Daghio et al. [110]. Forward and reverse reads were merged with perfect overlapping and quality filtered with default parameters using UPARSE pipeline [111] and the obtained sequences were taxonomically classified by RDP classifier (confidence >80%) [112]. To analyse the ecologic diversity of the different microbial populations, a Non-metric Multidimensional Scaling analysis was performed: the different bacterial populations were ordinated based on a distance or dissimilarity matrix obtained through iterative runs of the NDMS algorithm [113].

5.2.3 RESULTS AND DISCUSSION

Physical-chemical analysis

The trends of solar irradiance, temperature, cell potential, nitrate and sCOD content in the wastewater over 20 days between the months of April and May 2019 are reported in **figure 43**.

An evident correspondence between the peaks of illumination and the peaks of temperature measured at the wastewater surface can be observed, as the sunlight irradiation during the day heats the wastewater surface. The content of nitrates remains below 2mg/l for most of the selected period, while sCOD trend shows a continuous fluctuation in the range 10 - 100mg/l. No clear correlation can be observed between the voltage trends of the cells and the other physical-chemical factors. The signals of all MFCs are noisy, with sharp peaks and lows. In addition, the voltage of the planar MFCs is most of the times negative, which means that the potential of the two electrodes becomes inverted, having the electrode exposed to air working as anode and the submerged electrode behaving as cathode. This effect is probably due to the presence of dissolved oxygen in the first centimetres of wastewater (**Fig. 42**), which increases the redox potential of the solution and hinders the formation of an anaerobic anodic biofilm. Indeed, the anodes of the planar prototype are immersed only for a couple of cm in the wastewater, thus they can be strongly affected by this factor.

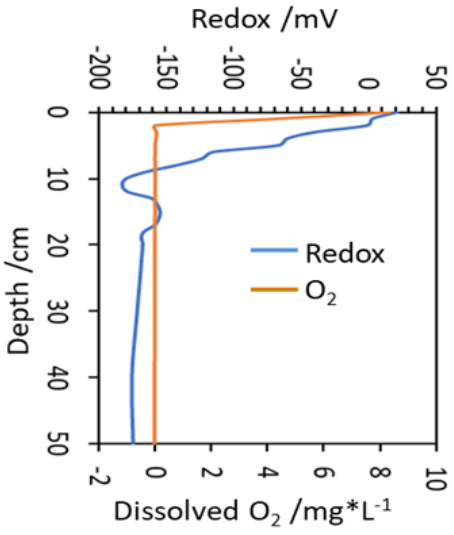

Figure 42 – Vertical profile of redox potential and dissolved oxygen in the first 50cm of wastewater in the denitrification tank. While oxygen seems to be quickly depleted in the first 3 cm from the wastewater surface, the redox potential decreases within the upper 10 cm.

Conversely, the anodes of the ceramic type are immersed deeper in the tank (~ 10 cm below the wastewater surface), and for this reason they are less influenced. The inversion occurs only for one group of cells (Cylindrical 1) and only for short time intervals.

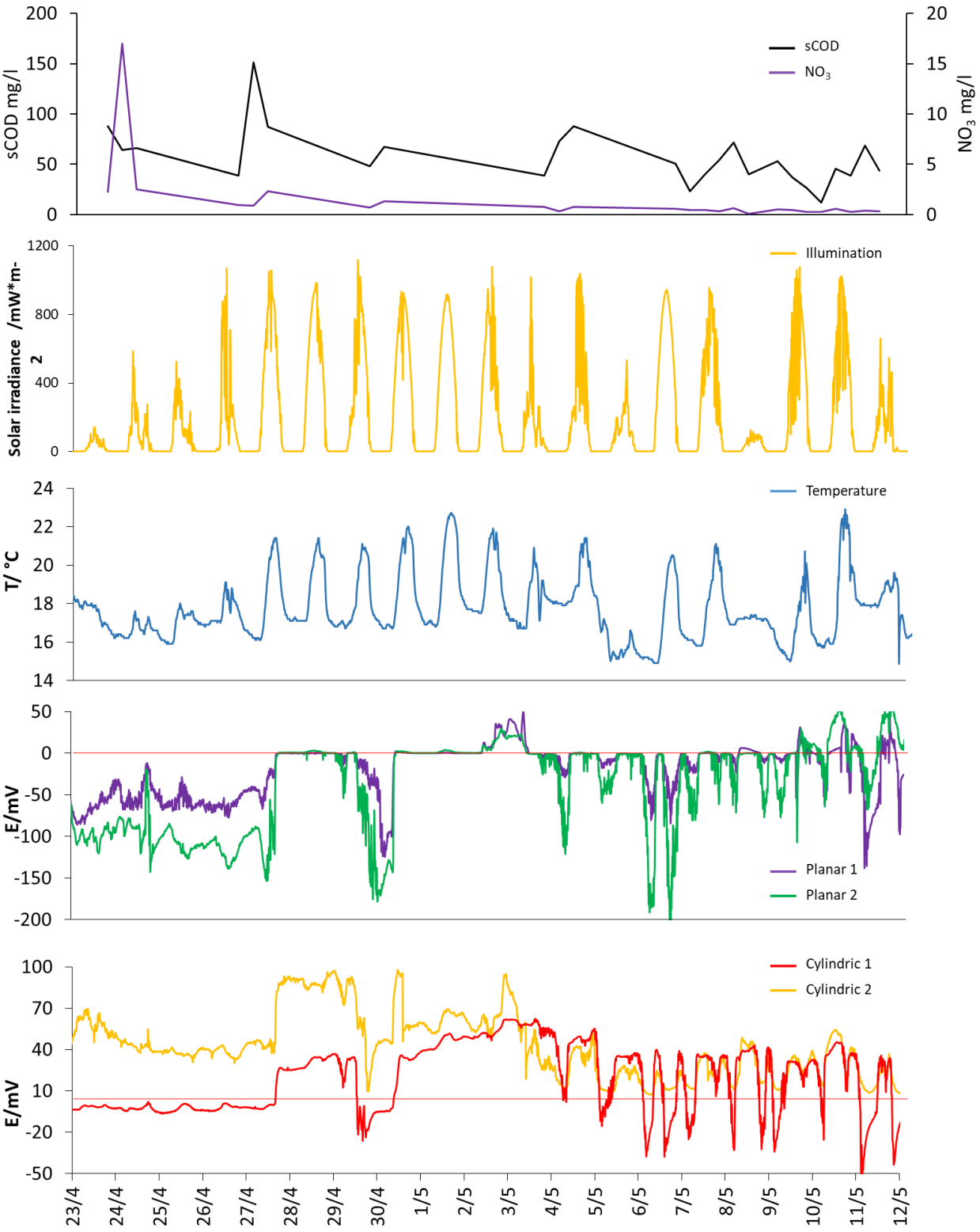

Figure 43 – Trends of solar irradiance, temperature, cell potential, nitrate and sCOD content in the wastewater over 20 days between the months of April and May 2019. The voltage is obtained as average of three replicates.

Microbial characterization

Taxonomic characterization of the bacterial communities present in the biofilm of anodes and cathodes of both prototypes and of the wastewater (Bulk) was performed by Illumina sequencing of the 16S rRNA gene (**Fig 44**).

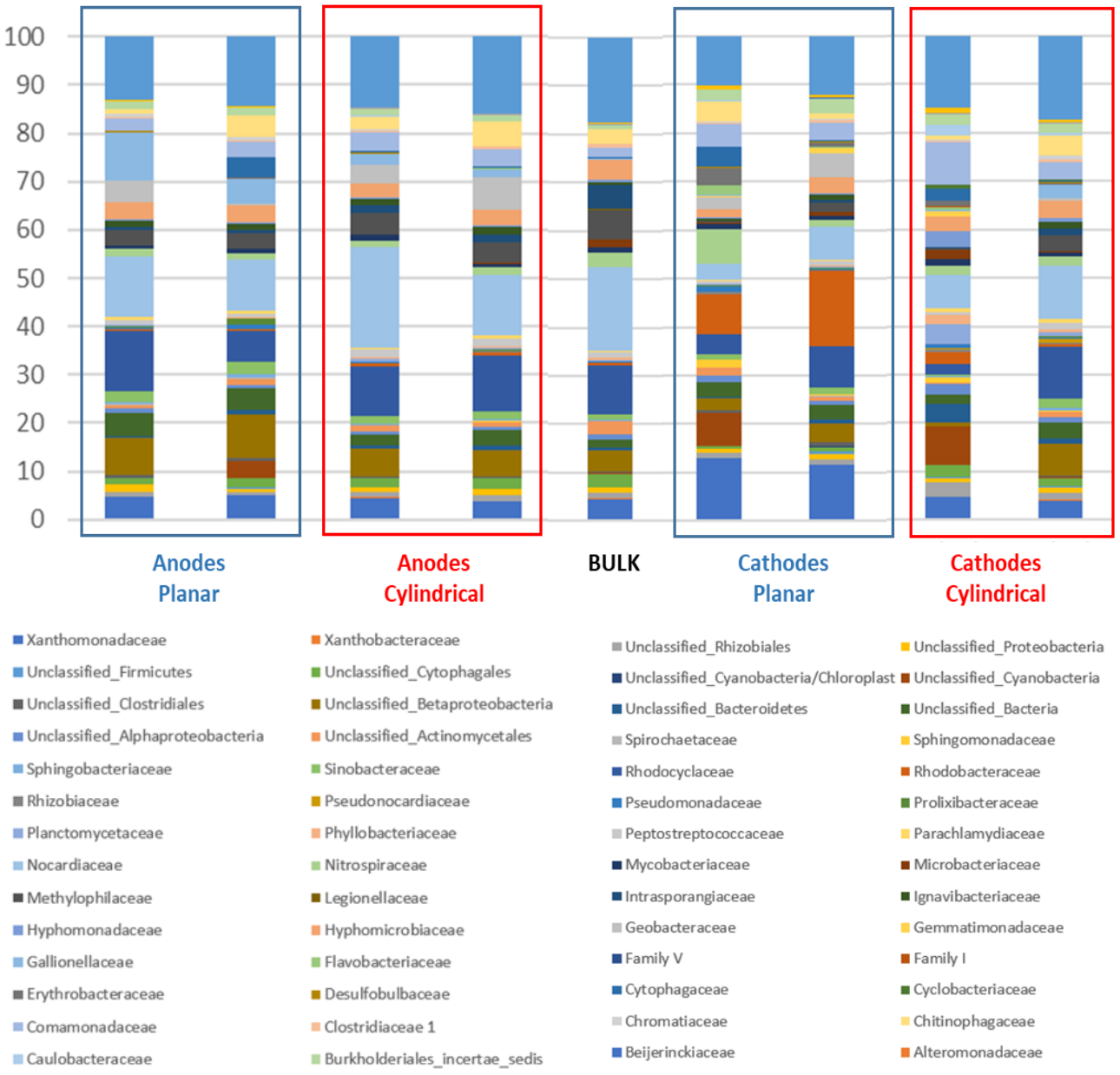

Figure 44 – Taxonomic composition at the family level of the microbial populations present in the anodic and cathodic biofilms for the two tested prototype and in the bulk solution of the wastewater. Each column refers to a group of three replicates.

The analysis of the bacterial communities underlines the influence of dissolved oxygen on the anodic biofilms. Indeed, bacteria belonging to the families *Nocardiaceae* and *Rhodocyclaceae,* which typically comprise aerobic species, were found on all the anodes of the tested MFCs. Bacteria

of such families have been previously found on the electrodes of microbial fuel cells [114,115], however, their presence indicates non-strictly anaerobic conditions.

The inversion phenomenon occurring to the planar MFCs could be explained with a cooperation between the families of *Rhodobacteraceae* and *Geobacteraceae*. The abundance of microorganisms belonging to those families on the cathodes was much higher in the case of planar MFCs as compared to the bulk and the cylindrical-type cathodes. The family of *Rhodobacteraceae* comprise species like *Rhodobacter capsulatus* and *Rhodobacter sphaeroides*, that are anoxigenic phothotrophs capable of photofermentation in which molecular hydrogen is produced [116,117]. As they need light to grow, it is reasonable that they are more abundant on the planar type's directly exposed cathodes. Within the family of *Geobacteraceae* is present the genus *Geobacter* [118,119], which is well known in the field of MES due to its ability to donate electrons to a solid metallic substrate via EET. Bacteria belonging to this family are strict anaerobes that can use H_2 as electron donor. Therefore, it is possible that *Rhodobacteraceae* bacteria used sunlight to produce hydrogen, which was then used by *Geobacteraceae* as a source of reducing power to drive their metabolism. *Geobacteraceae* then transferred electrons to the upper electrode (referred to as cathode in the text), thus using them as anode. The characteristics of these families are summarized in **table 3**.

Table 3 – Families found during the microbial characterization that have been previously found in the biofilms of MFCs

Family	Characteristics	Sample	References
Nocardiaceae	• Aerobic, Gram-positive actinomycetes commonly found in soil and water. • Previously found on anodes and cathodes of MFCs	All samples	[114,120,121]
Rhodocyclaceae	• Aerobic, Gram-negative • Previously found on cathodes of MFCs	All samples	[115]
Rhodobacteraceae	• Aquatic bacteria • aerobic photo and chemoheterotrophs but also purple non-sulphur bacteria which perform photosynthesis in anaerobic environments • Fermentation, hydrogen production • Previously found on anodes of MFCs	Planar type cathodes (>20% relative abundance)	[116,117,122]
Geobacteraceae	• Anaerobic, non-fermenting chemoorganotrophic mesophiles • Exoelectrogenic (nanowires) • Can use H2 as electron donor • Previously found on anodes of MFCs	Cylindrical type cathodes and bulk < 1%; Planar type cathodes and anodes ~ 6% (relative abundance)	[118,119]

In addition, the presence of algae was noted on the surface of the flat type MFCs, which may also have contributed to the oxygen diffusion towards their anodes (**Fig. 45**).

Figure 45 – Algal growth on the cathodes of the planar type MFCs

From the NMDS analysis of the microbial populations emerged that the anodic biofilms are very similar to each other and not very differentiated from the bulk (**Fig. 46**). Conversely, the ecologic distance between the cathodic populations types is much higher between the different groups of MFCs. This aspect is probably once more, the presence of oxygen in the first layer of wastewater impeded the formation of a mature anaerobic biofilm on the anodes, while the cathodic biofilms developed according to their exposure to air and light. Indeed, the presence of phototrophs seems to be the main difference between the planar and the cylindrical configuration.

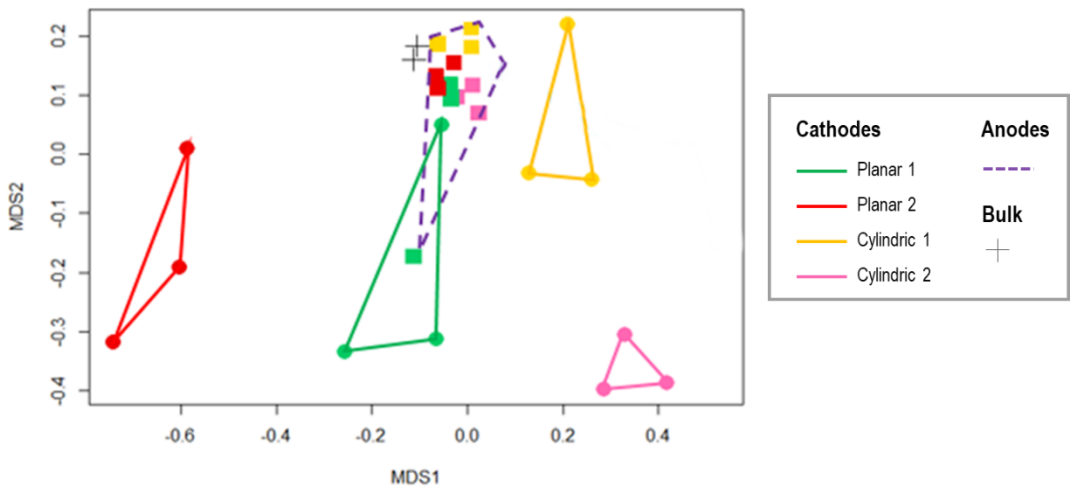

Figure 46 – Non-metric Multidimensional Scaling analysis of the microbial populations present on the electrodes of the different MFCs. The anodic biofilms (square marker, dotted line) show a high similarity between them and low differentiation from the microorganisms present in the bulk (+ markers), while the groups of different cathodes show a good level of differentiation between each other (round markers, continuous line).

To sum up the difference between the two configurations, the cylindrical type was less subjected to the inversion phenomenon due to the deeper position of the anodes in the wastewater, which reduced the impact of dissolved oxygen, and to the light-protected cathodes, that avoided the growth of photosynthetic species.

5.2.4 CONCLUSIONS

Two different kinds of floating MFC were tested in the denitrification tank of a wastewater treatment plant: planar and cylindrical. It was not possible to directly correlate the measured physical-chemical factors (i.e. temperature, illumination, nitrates and sCOD) with the voltage trends of the cells. However, the impact of light and dissolved oxygen on the cell performances was evidenced by the microbiologic analysis. In fact, all anodes populations showed a low level of differentiation from the wastewater and the presence of aerobic bacteria. In addition, a cooperation between *Rhodobacteraceae* and *Geobacteraceae* was identified as the probable cause of the inversion of potential occurring to the electrodes of planar MFCs. On the contrary, the cylindrical prototype was much less affected by the inversion due to the deeper position of the anodes and the protection from sunlight, therefore they showed better performances.

This study underlines the complexity of the factors that influence the signal of MFCs when applied in real field. Further research should address how to isolate the different contributions in order to build effective MFC-based monitoring system for wastewater treatment plants.

5.3.5 AKNOWLEDGEMENTS

The authors acknowledge WeMake s.r.l. (MI), and especially Ing. Paolo Bonelli, for the construction of the automatic sampler, and Gruppo CAP Amiacque for the possibility to work in the wastewater treatment plant of Bresso-Niguarda.

6 AMPEROMETRIC DETECTION OF HERBICIDES

6.1 Benzoquinone-based photo-bioelectrochemical sensor

From: M. Tucci, M. Grattieri, S. D. Minteer, A. Schievano, P. Cristiani. Microbial amperometric biosensor for online herbicide detection: Photocurrent inhibition of Anabaena variabilis, Electrochimica Acta 302 (2019) 102-108 [123]

6.1.1 SCIENTIFIC BACKGROUND

Herbicide pollution has become a serious threat for human health and ecosystems [124]. Photosynthesis inhibitors, such as urea, triazines and phenolics, are among the most used herbicides worldwide. These kinds of herbicides often damage non-target habitats, like neighbouring vegetation and freshwater ecosystems, due to spray drift, leaching, run-off or accidental spills [125]. Moreover, many photosynthetic herbicides are relatively recalcitrant to biodegradation and therefore persistent in the environment, especially in groundwater [97]. It has been proven that some herbicides can act as endocrine disruptors, especially in case of long-term exposure [94]. For example, the triazinic herbicide atrazine (6-chloro-4-N-ethyl-2-N-propan-2-yl-1,3,5-triazine-2,4-diamine) is one of the most extensively used pesticides in agriculture, and it is frequently found in soil, surface water and agriculture food products, due to its persistence, high mobility and slow degradation rate [126,127]. This compound can have negative effects on the reproductive system, endocrine system, central nervous system and immune system of freshwater fauna [128], while the effect on human health is still controversial [129]. The European Union (EU) banned atrazine in 2003 [130]. However, it is still broadly used in around sixty countries worldwide, including the United States, for the production of corn, sorghum and sugar cane etc. [131]. U.S. Environmental Protection Agency (EPA) sets 3 µg/l as the maximum concentration in drinking water for any member of the s-triazine class of pesticides [132]. Another widespread herbicide is diuron (3-(3,4-dichlorophenyl)-1,1-dimethylurea), belonging to the urea class. This compound is very persistent in soil due to its low solubility in water, where it can remain for up to 1 year [133]. Many different toxic symptoms have been associated with exposure to diuron, like eye and skin irritation, mutagenic, metabolic and carcinogenic effects [134]. Therefore, this herbicide arises serious environmental and human health concerns [135].

In this scenario, a constant monitoring of herbicides contamination in water and soil environmental compartments has become critical. Moreover, the availability of suitable diagnostic methods is crucial for maintaining an effective environmental management and analysis [124]. Despite their accuracy and precision, traditional analytical methods (i.e. high-performance liquid chromatography (HPLC), atomic absorption spectroscopy (AAS) and gas chromatography-mass spectrometry (GC-MS)) are usually quite expensive, are time-consuming, and involve sample pre-treatment, complex equipment and highly-trained operators [68].

As an alternative, many researchers are focusing on the development of low-cost biosensor for herbicides. A cost-effective approach is the use of biosensor based on cytotoxicity response (bacterial cells growth inhibition) [136]. Herbicides presence can be easily determined by a decrease of bacterial growth; however, this approach requires relatively long time for cell culture and growth analysis. Amperometric photobiosensors represent an interesting possibility for the fast and online monitoring of herbicides [21]. This classification of biosensor relies on amperometric measurements of the photocurrent generated by Photosystem II (PSII), a protein complex located in the thylakoid membrane of photosynthetic microorganisms. Within this complex, light energy starts a chain of electron transfer reactions, where oxygen is produced through water oxidation [137]. Photosynthesis-inhibiting herbicides can cause a decrease in the output current, by blocking the photosynthetic electron transport in a concentration-dependent manner [138]. In fact, herbicides competitively displace the plastoquinone complex from the Q_B binding pocket in the PSII (**Fig. 47**), thus blocking the electron transport chain [139,140]. The photocurrent generated by the PSII can be monitored directly or with the employment of artificial redox mediators. Among them, quinones are the most suitable compounds, as they have similar chemical properties as the plastoquinone complex and compete with the same binding site.

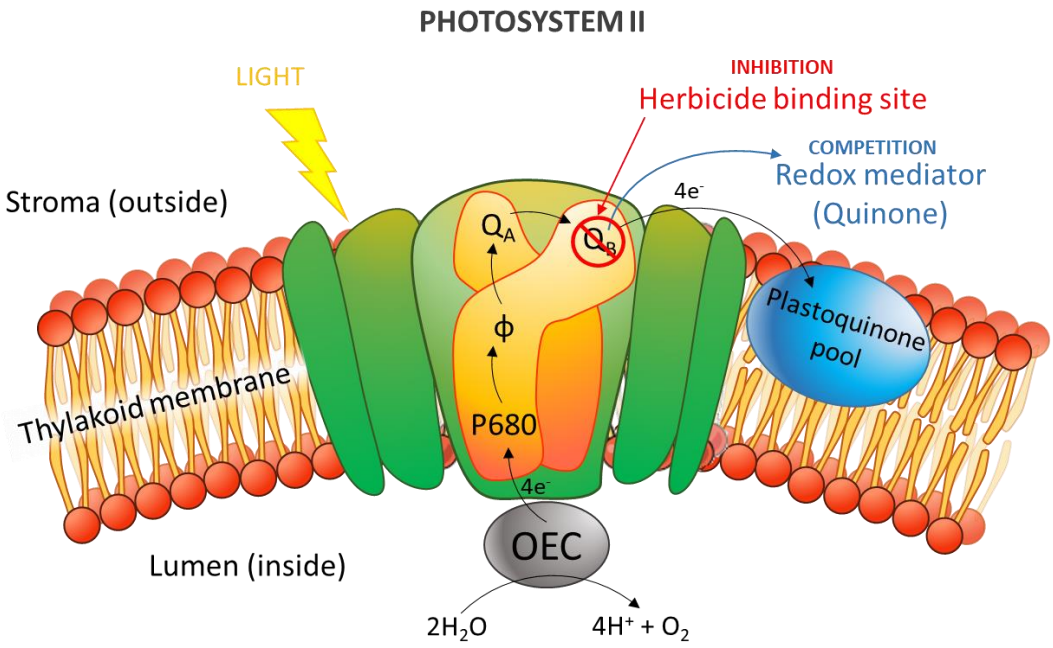

Figure 47 - Schematic representation of the mechanism of action for photosynthesis-inhibiting herbicides in the photosystem II. The plastoquinone pool is the natural electron acceptor for the electrons generated from water oxidation and transferred by the active site Q_B. Artificial quinones can also accept the electrons, thus competing with the plastoquinone complex. When photosynthesis inhibiting herbicides are present, they bind the active site and block the electron transport chain.

Different kinds of biological receptors have been employed for amperometric herbicide sensing, ranging from whole cells and organelles to purified PSII reaction centers [131]. Among these, an interesting class of biosensors utilizes thylakoid membranes [141,142], photosystems [125], and reaction centers proteins [131,143]. These bioreceptors have the advantage to be highly sensitive, as well as to have a fast response time and detection limits in the nM range [143]. However, one of the disadvantages of their application is the need of complex purification methods, and their higher fragility when isolated, making them less suitable for long-term operation [144]. Whole-cell based biosensors, on the other hand, are quite stable, and production of living cells is simple and cost-effective [145]. To date, this kind of sensor usually relied on the amperometric detection of photosynthetically-produced molecular oxygen [146–149], which is an indirect way of measuring the photocurrent. In fact, this measure can be influenced by environmental factors (e.g. temperature), making these biosensors not suitable for application in real conditions. Additionally, some of these biosensors employ selective membranes [138,146,147,149], which can be affected by fouling issues, particularly over long-term operation.

Herein, a novel amperometric biosensor based on direct inhibition of the photocurrent generated by an artificial biofilm of photosynthetic microorganisms is presented. The stability and operational simplicity related to the employment of whole-cells are coupled with the fast and accurate detection of the photocurrent inhibition. Photocurrent generated by living cells has been already studied for biophotovoltaic systems, where light energy is harvested in the absence of an organic feedstock [89], but this principle was never applied to biosensing. A very easy and low-cost preparation was experimented for building the biosensor: living cells were encapsulated in an alginate matrix, attached on a carbon felt electrode. Alginate is a natural biopolymer derived from seaweed, used for the entrapment of cells [150], drugs, and proteins [151]. Immobilization of bacterial cells in alginate capsules allows a high cell density, while enhancing the stability of bacterial communities [152] due to the fairly inert aqueous environment inside the matrix [145]. The encapsulation process involves mixing an aqueous solution of alginic acid with another solution rich in calcium ions (**Fig. 48**). When the dissolved alginic acid is in contact with Ca^{2+}, insoluble calcium alginate is obtained, resulting in the entrapment of bacterial cells. At the same time, the high porosity of the calcium alginate layer permits good diffusion rates of macromolecules and nutrients [145].

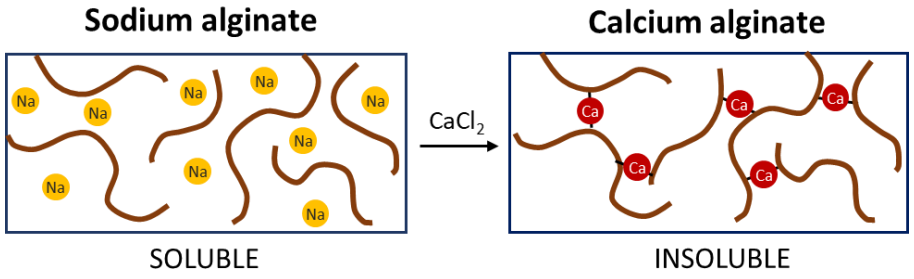

Figure 48 – Representation of the polimerization mechanism of alginate hydrogel: in presence of calcium ions, the soluble sodium alginate forms an insoluble polymer

p-Benzoquinone (BQ) was recently shown to enhance the extracellular electron transfer between purple photosynthetic bacteria and an electrode surface [91]. **Figure 49** shows the characteristic redox peaks associated with the activity of this compound. Accordingly, we utilized monomeric BQ as redox mediator also for this study. Since cytotoxic and genotoxic effects of quinone molecules can have a negative impact on the ecosystem[153], we aimed to entrap the redox mediator in the alginate matrix and compared biosensor performance with a configuration in which BQ was freely present in the electrolyte during the analysis. Activated carbon was employed

to create a conductive network inside the polymer [154], and its influence on the biosensor performance is discussed.

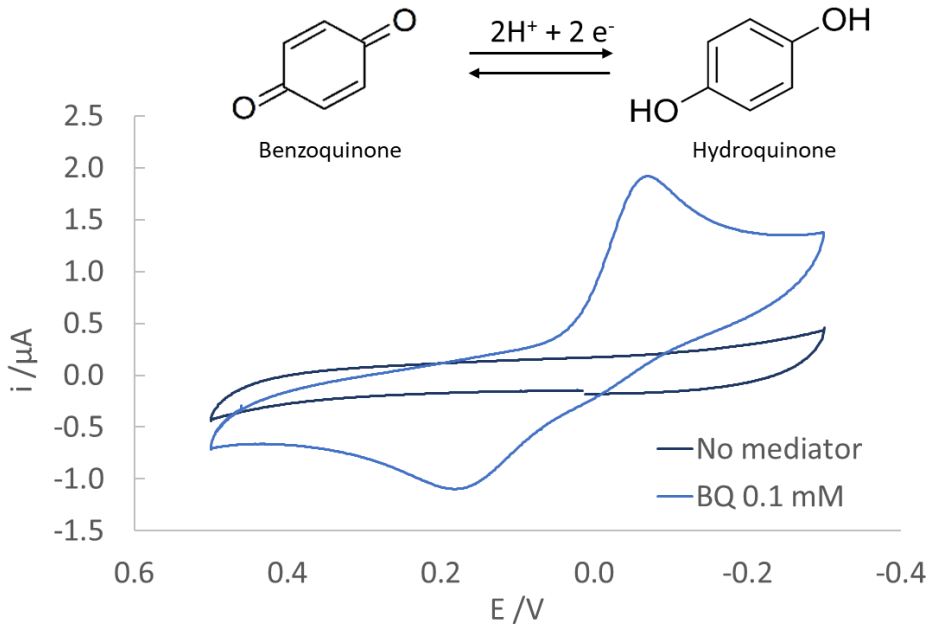

Figure 49 – Cyclic voltammogram obtained using a glassy carbon electrode in Tris/Hcl buffer + NaCl 0.1M: When benzoquinone is present, the characteristic redox peaks indicate a reversible

The cyanobacterium *Anabaena varibilis,* a filamentous heterocyst-forming cyanobacterium well-known for its numerous applications, was employed as bioreceptor of the sensor [155]. This particular species was chosen based on the available studies on its photocurrent generation ability present in literature [156–158]. Moreover, our group developed a consolidated knowledge in the growth and application of this bacterium for bioelectrocatalytic purposes [159].

The current generated by photo-bioelectrocatalytic oxidation of water was measured, and the relationship between inhibition of the photocurrent and concentration of herbicide was evaluated, using atrazine and diuron as model photosynthesis inhibitor herbicides.

6.1.2 MATERIALS AND METHODS

Reagents and solutions

Sodium carbonate and cupric sulfate 5-hydrate were obtained from Avantor (Macron Fine Chemicals). Citric acid monohydrate, activated carbon powder and boric acid were purchased from Fisher Scientific. Tris salt was obtained from Gold Biotechnology. All other reagents were purchased from Sigma Aldrich. They were of analytical grade and used without further purification. Ultra-pure water purified with a Millipore Milli-Q® Integral purification system was used for all the solutions. A standard solution of atrazine and a standard solution of diuron were prepared using water as solvent (concentration of 0.15mM).

***Anabaena variabilis* culture**

A 500mL culture of *A. variabilis* SA-1 was grown using BG-11 medium (ATCC Medium 616: Medium BG-11 for Blue-green Algae, pH 7.1) [160] with the addition of trace metal mix A5. It was constantly stirred at 140rpm and bubbled with air. Broad spectrum (400–700nm) fluorescent grow lights (10 $mWcm^{-2}$) were used as the light source. Temperature was maintained constant at 40°C. This setup was built as previously reported by Knoche et al. [159].

The culture was maintained in stationary phase by removing 20% of the culture and adding an equivalent amount of fresh medium once per week. The Optical Density (O.D.) of the culture at 750nm was 2.9±0.9.

Biosensor construction

In order to build the biosensor, *Anabaena variabilis* cells were harvested by centrifugation for 10 minutes at 7000 x g. The cells were re-suspended in a solution of fresh medium and sodium alginate $5gL^{-1}$, and the final concentration of bacterial cells was $25mgmL^{-1}$. For this study carbon felt electrodes with a geometrical area of 1 cm^2 were utilized as support for the construction of the working electrodes. The electrodes were placed for 10 min in the prepared alginate solution and then dipped for 1sec in a $CaCl_2$ $60mgL^{-1}$ solution to obtain a hardened capsule on the electrode surface. The redox mediator BQ was added in the electrolyte solution during the electrochemical analysis (**Fig. 50A**). To test the entrapment of BQ in the polymer, the biosensor was prepared adding 0.1 $mgmL^{-1}$ of BQ directly to the alginate solution containing bacterial cells, together with 0.1 $mgmL^{-1}$ of activated carbon (AC). The AC was added to ensure the electrical conductivity of the alginate

layer. In this configuration no redox mediator was added to the electrolyte during the electrochemical analysis (**Fig. 50B**). Control experiments were performed with a similar setup in absence of *Anabaena variabilis*.

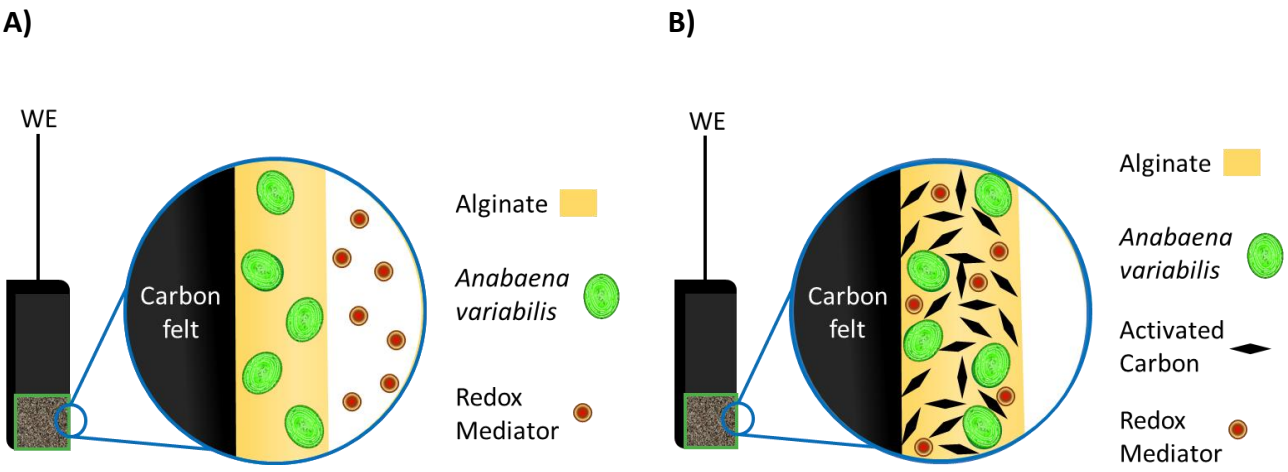

Figure 50 – Schematic representation of the electrode in cross section for the two configurations: A) with the mediator added to the electrolyte and B) with the mediator entrapped in the alginate matrix together with activated carbon

Scanning electron microscopy (SEM) was performed with a FEI Quanta 600 FEG microscope to study the surface and the section of the electrodes.

Electrochemical setup

A three-electrode setup was employed for all electrochemical analyses, where the biosensor was the working electrode, a platinum mesh was the counter electrode and a saturated calomel electrode (SCE) was used as the reference (**Fig. 51A**). All electrochemical characterizations were performed right after the construction of the biosensor. This allowed maximizing reproducibility of the results by limiting differences in the amount of active bacterial cells entrapped that could possibly account for different photocurrent generations. The experiments were performed with CHI 660E Electrochemical Workstation (CH Instruments) controlled by the manufacturer's software. The electrochemical analyses were conducted in 0.5M Tris/HCl buffer (pH 7.1) + 0.1M NaCl to ensure that additions of herbicide solutions did not influence pH or conductivity of the electrolyte. All the experiments were performed at room temperature (23±2°C). The solution was continuously stirred with a stir plate (300 rpm). A Dolan-Jenner Fiber-Lite lamp (Model 190-1) quartz–halogen

illumination system with an optical light guide providing a light intensity of 760 W m^{-2} was used to provide the illumination during the experiments. The light was set and maintained at a distance of 5.0±0.5 cm from the working electrode during operation. For the first type of sensor, 0.01 $mgmL^{-1}$ of BQ was added to the electrolyte at the beginning of the electrochemical analyses.

A) **B)**

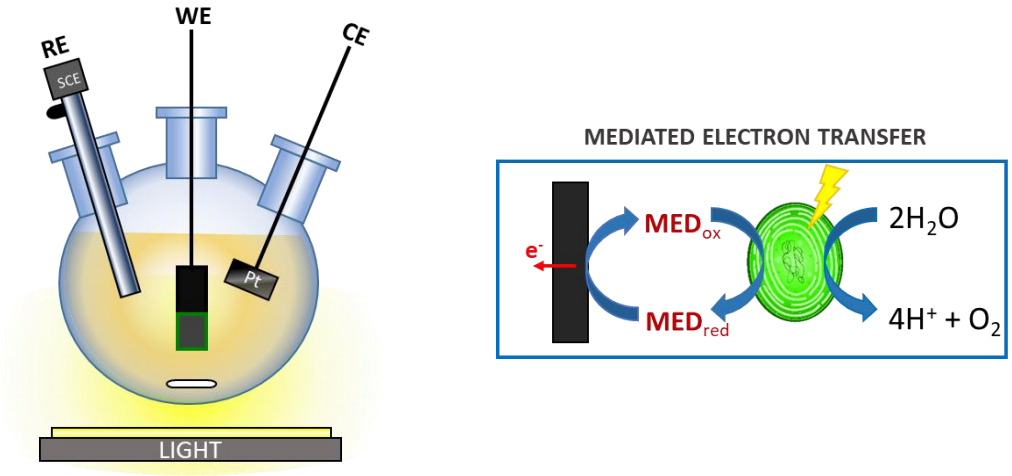

Figure 51 – A) Sketch of the electrochemical setup used for the experiments and B) scheme of the reactions occurring at the electrode surface

Cyclic voltammetry (CV) was performed between -0.3 and +0.5V vs. SCE at 1mV s^{-1}. The CVs were executed in the absence and the presence of light, in order to assess the photo-electrocatalytic activity of the biosensor. Chronoamperometry (CA) was conducted at an applied potential +0.5V vs. SCE. The imposed potential was selected in accordance with the CV results, to operate in a potential window where all BQ molecules were in the oxidized form. The current variation in the absence and the presence of light was evaluated. To study the inhibition effect of the herbicides, standard additions of atrazine or diuron were performed, and the consequent decrease of current was measured.

6.1.3 RESULTS AND DISCUSSION

Biosensor characterization and calibration

To confirm the successful deposition of the alginate layer on the electrode, the surface and the cross section of an electrode prepared as previously described were analyzed through scanning electron microscopy (SEM, **Fig. 52**). The obtained images show the distribution of the calcium alginate polymer on the carbon felt, with alginate mostly localized on the external surface of the carbon felt electrode (**Fig. 52B**), creating a layer with a thickness of approximately 100±20 µm (based on different measurements performed in different positions and different electrodes), which is permeable to the organic compounds present in solution. The cross section image indicates that no appreciable amount of polymer was formed inside the dense felt architecture. This could be explained with the limited and slow diffusion of Ca^{2+} ions into the fibers mat during the generation of the polymer, resulting in the alginate layer being localized only on the surface of the electrode.

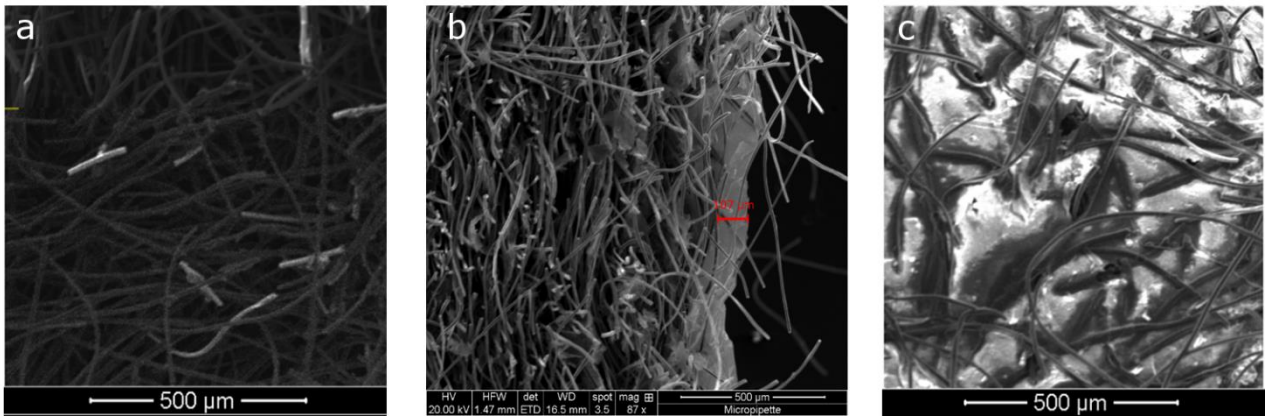

Figure 52 - SEM images of the carbon felt electrode: A) Carbon felt surface without alginate. B) Cross section of the electrode in which is visible the alginate layer. C) Electrode surface covered with alginate

Cyclic voltammetry revealed the electrochemical response of the biosensor in the absence and the presence of light. **Figure 53A** shows a clear increase of the oxidative current in presence of *Anabaena variabilis* under light exposure (blue line) compared to dark conditions (green line), as indicated by the red arrow. The oxidative current in control experiments was always lower, and no significant difference between light on/off conditions was obtained (red and black lines, respectively). The photocurrent generation was also analyzed by chronoamperometry, performed at +0.5V (**Fig. 53B**). In presence of *Anabaena variabilis*, an immediate increase of current can be noticed under illumination, while no variation in the current response occurs in all control experiments.

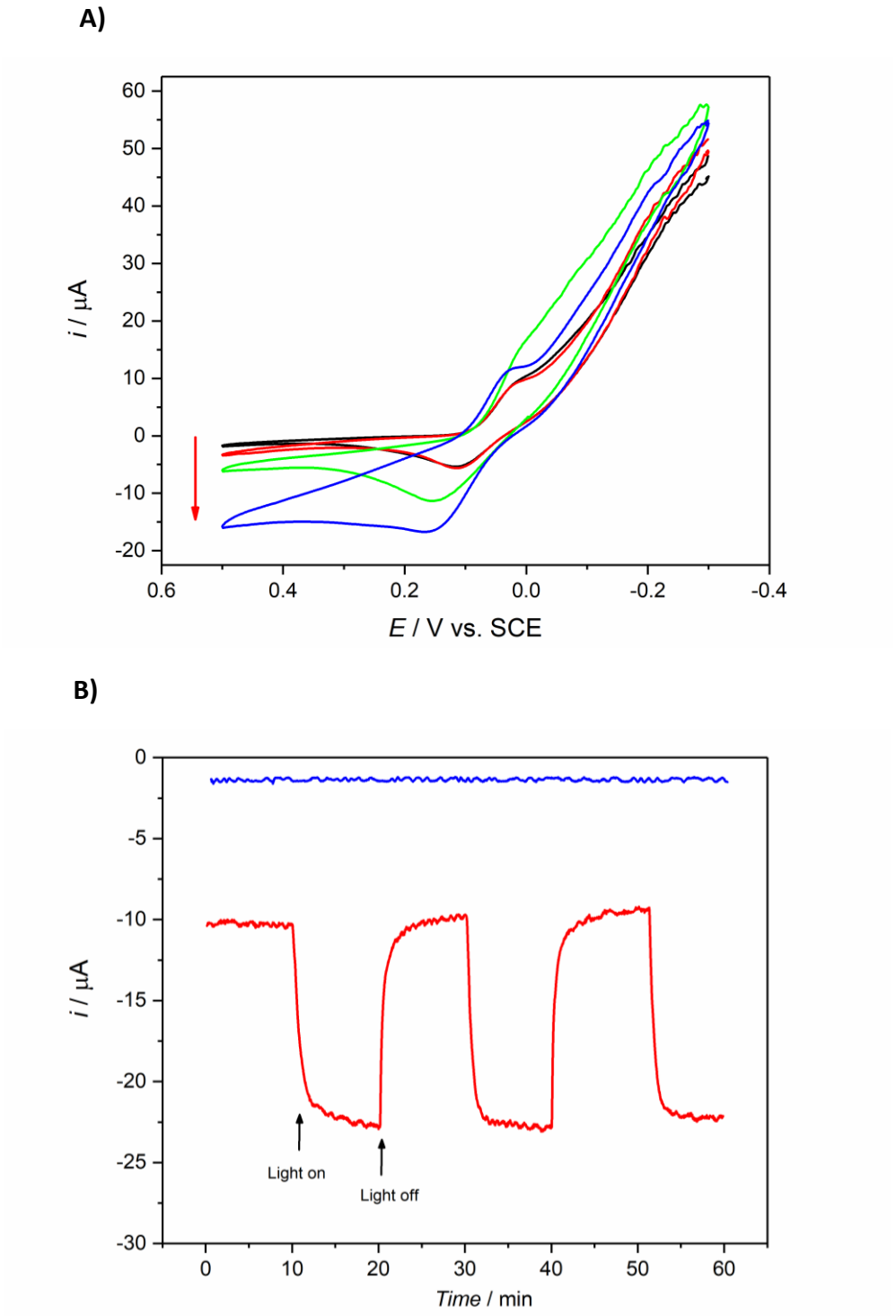

Figure 53 - Photocurrent generation of the biosensor with BQ dissolved into the electrolyter. A) Representative cyclic voltammograms in absence and presence of light: when Anabaena variabilis is present, the anodic current is higher under illumination (blue) than in dark conditions (green). In sterile conditions (control experiments), lower current with no significant difference between light (red) and dark conditions (black) was obtained. B) Amperometric i-t curves (applied potential +0.5V). When Anabaena variabilis is present (red), an immediate increase of the current can be noticed every time light is turned on. A sharp decrease of current is obtained when light is switched off. No variation can be noticed in the control experiments (blue).

The inhibiting effect of the model herbicides atrazine and diuron was evaluated by means of chronoamperometry performed at +0.5V vs. SCE. **Figure 54A** shows the influence of atrazine on the

biosensor. After reaching a steady photocurrent baseline, standard additions of atrazine into the electrolyte were performed. Every injection of atrazine resulted in an initial sharp decrease of the photocurrent, which then stabilized, reaching a steady state current only for the highest concentrations of herbicides. At low herbicide concentrations the steady state current was not completely reached, possibly due to limited diffusion of the analyte. Accordingly, a stabilization time of 15 min was selected prior to measure the current value and performing a new addition. The current response needed about to stabilize after each addition. For the highest concentration of inhibitor, the photocurrent drops almost to the background current obtained in dark condition.

Figure 54B reports the correlation between atrazine concentration and the decrease in associated current density *(Δj)*, calculated as the difference between the photocurrent baseline and the steady current reached after an addition. Each point is the average of three replicates, and the calculated standard deviation is displayed as an error bar on the graph. The linear part of the curve (R^2= 0.97) shows a good sensitivity of the biosensor in a sub-micromolar range (-24.6 µA μM^{-1} cm^{-2} up to 0.56µM). The aquatic life benchmarks set by EPA for chronic exposure of both fish and invertebrates to atrazine [161] fall within this range. Therefore, this biosensor could be suitable for quantitative environmental analysis of atrazine. Moreover, the obtained response is independent from the concentration of dissolved oxygen, which is a critical aspect for the field application of the biosensor as oxygen concentration in real water samples is subject to numerous variables. The same calibration procedure was performed in triplicate using diuron (**Fig. 55**). In this case, the concentration necessary for a comparable current drop was about an order of magnitude lower, proving that this herbicide is a much stronger PSII inhibitor than atrazine. A linear correlation was obtained up to 0.08µM (R^2 = 0.93), which is lower than the limits for chronic exposure of aquatic life set by EPA. Therefore, the biosensor seems suitable as an on/off sensor, for the early warning detection of this chemical. Accordingly, the biosensor is not selective towards any individual herbicide, as both compounds have an inhibiting effect on the photosynthetic bioprocess. However, the non-selectivity of the biosensor can be an advantage, allowing early detection of phytotoxic compounds when applied in solution of unknown composition. On the contrary, application of the biosensor in solutions where only atrazine or diuron are expected to be present will allow their preliminary quantification.

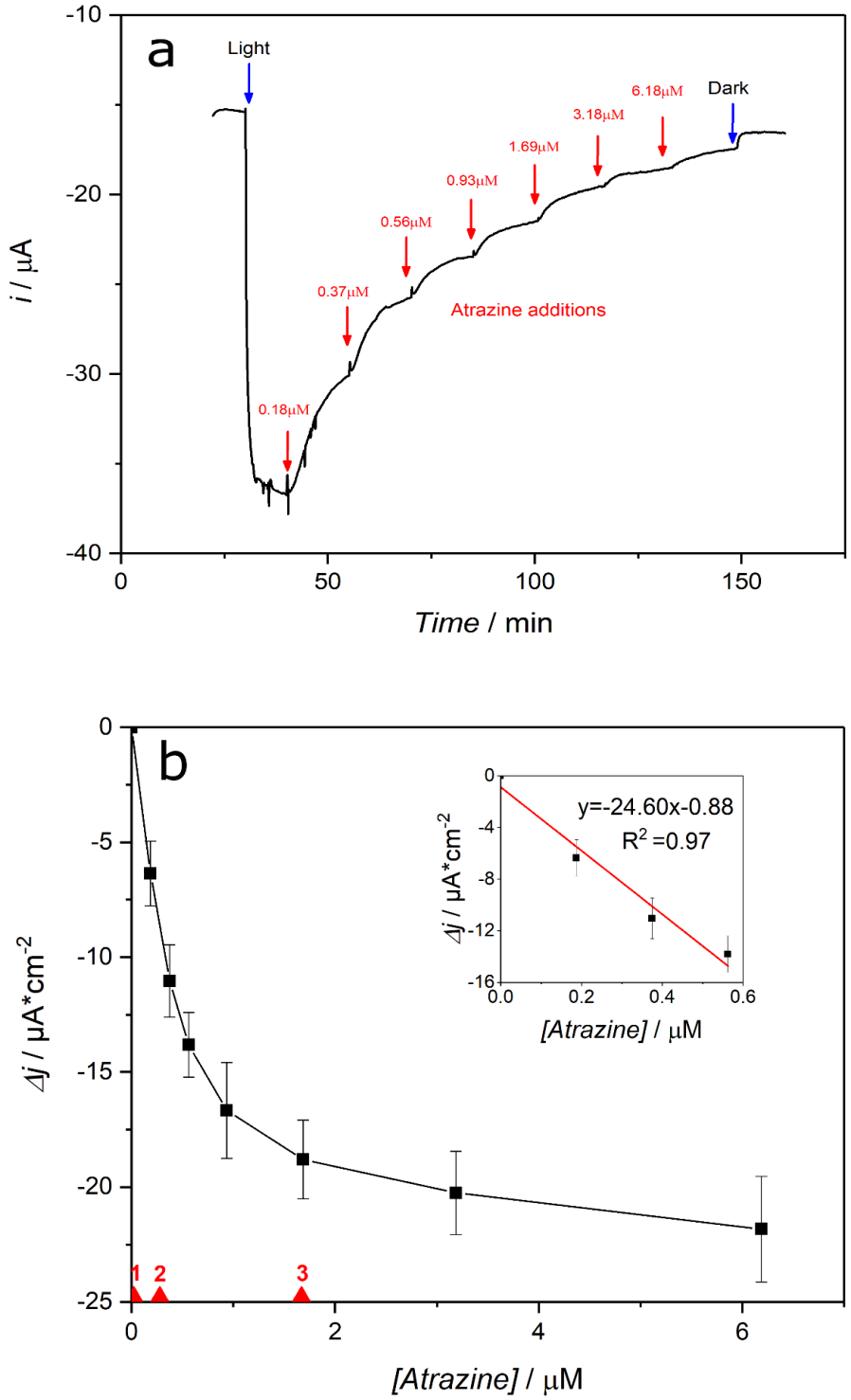

Figure 54 – Atrazine calibration of the biosensor with BQ dissolved into the electrolyte. Chronoamperogram showing the effect of atrazine on the photocurrent produced by the biosensor (applied potential +0.5V). Red numbers indicate atrazine concentration in μM. B) Concentration-current relationship. Aquatic life benchmarks set by EPA are represented with red triangles: 1) Chronic exposure concentration for invertebrates, 2) Chronic exposure concentration for fish, 3) Acute exposure concentration for invertebrates.

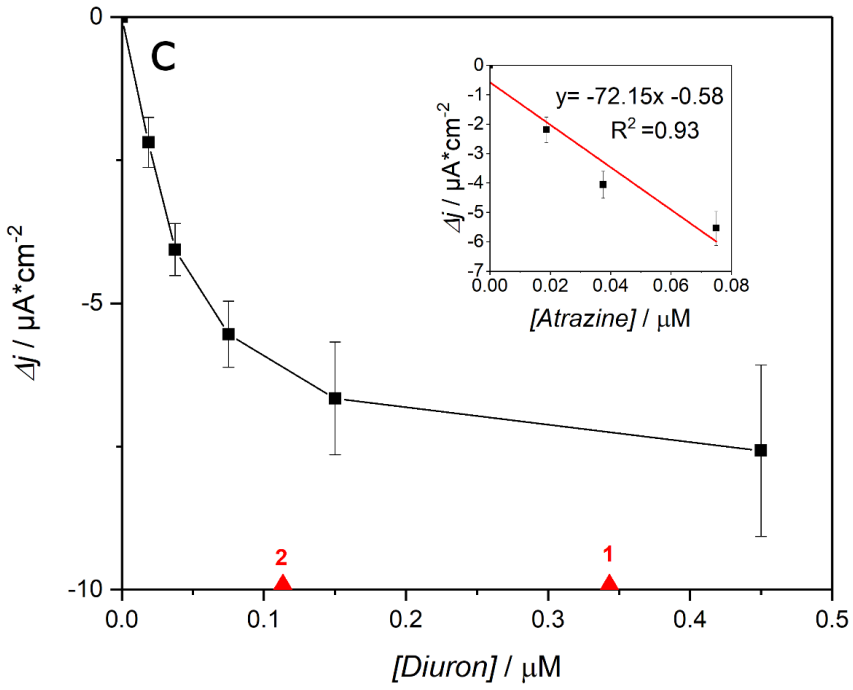

Figure 55 - Diuron calibration of the biosensor with BQ dissolved into the electrolyte. C) Concentration-current relationship for diuron. Insets show the linear range of the curves and the equations of the linear fitting. Aquatic life benchmarks set by EPA are represented with red triangles: 1) Chronic exposure concentration for invertebrates, 2) Chronic exposure concentration for fish

Alginate-encapsulated mediator

To avoid the release of mediator in solution, the entrapment of BQ in the polymer was tested. As mentioned before, activated carbon was necessary to create a conductive network inside the alginate matrix. Entrapment trials performed in the absence of activated carbon showed no response to light (data not shown). Partial adsorption of the mediator onto carbon granules is probably the main factor ensuring the electron transfer, allowing maintaining BQ in proximity of the conductive surface while limiting its isolation within the alginate matrix. It was demonstrated that quinones can be adsorbed on activated carbon with different strengths, depending on the crystalline structure [162].

With this configuration, it was possible to obtain a photocurrent of 9±3 μA, with immediate response to light. Even though the concentration of mediator inside the alginate layer was about ten times higher, the produced photocurrent was about 21±6 % lower when the mediator is entrapped in the polymer, meaning that a large portion of the mediator has been isolated by the alginate and was not able to shuttle electrons from the bacterial cells to the conductive material.

The efficacy of the mediator entrapment to avoid its release in solution was evaluated trough cyclic voltammetry. A carbon felt electrode prepared as previously described was kept into the electrolyte solution for 6h. Cyclic voltammograms were recorded using a glassy carbon electrode as the working electrode, both at the beginning and at the end of the experiment (6h exposure to the solution, Supporting information, **Fig. S56**). The voltammogram recorded after 6h was comparable with the one recorded immediately after exposing the modified carbon felt electrode to the electrolyte, and did not show the characteristic reversible redox peaks associated with BQ freely available in solution. Accordingly, diffusion of the redox mediator from the polymer to the electrolyte solution is strongly limited, remarking the effectiveness of the encapsulation.

Calibration experiments for this configuration are reported in the Supporting Information, (**Fig. S57**). It was possible to obtain a linear relationship between current and concentration up to 1.31µM of atrazine (sensitivity of -7.7 µA μM^{-1} cm^{-2}; $R^2 = 0.93$) and 0.13 µM of diuron (sensitivity of -34.5 µA μM^{-1} cm^{-2}; $R^2 = 0.95$). Therefore, the biosensor is able to monitor atrazine concentrations within the thresholds of chronic exposure for freshwater fauna set by EPA, while for diuron it allows only on/off detection. The response time was approximately 20 min. These results suggest that the biosensor can be used as a tool for freshwater quality monitoring.

Performance evaluation

The calibration curves were fitted to a sigmoidal function (**Eq. 11**), where max and min are maximal and minimal photocurrents normalized between 0% and 100%, and X is the concentration of inhibitor. The software GraphPad Prism 8 was used for the data fitting.

$$Y = min + \frac{max - min}{1 + (IC_{50}/X)^{Hill\ coefficent}} \qquad \text{(Equation 11)}$$

Using this model, the concentration necessary to inhibit 50% of the photocurrent (IC_{50}) was calculated. This value is inversely proportional to the sensitivity of the sensor: the lower the IC_{50}, the higher the sensitivity. The obtained values for the biosensor with BQ in solution were 0.34 and 0.04 µM for atrazine and diuron respectively, and for the biosensor with BQ entrapped were 1.05 and 0.10 µM.

Since the level of noise of the dark current was below 5% of the uninhibited photocurrent, the lower limit of detection (LLOD) was estimated as the concentration that inhibits 5% of the

photocurrent (IC_5) [131]. The obtained values are shown in **table 4**. In a similar manner, the upper limit of detection (ULOD) was estimated for 95% of photocurrent inhibition (**Tab. 4**). This parameter can be considered as the saturating concentration for the biosensor: above this value an increase in concentration generates a negligible increase of photocurrent.

Table 4 - Calculated values of Hill coefficients, IC_{50}, LLOD and ULOD

		Hill coefficent	**IC50 /µM**	**LLOD /µM**	**ULOD /µM**
Atrazine	BQ in solution	-1.10	0.34	0.023	4.85
	BQ entrapped	-1.05	1.05	0.064	17.28
Diuron	BQ in solution	-1.19	0.04	0.003	0.45
	BQ entrapped	-1.07	0.10	0.006	1.50

Comparing the two kinds of biosensor (**Tab. 4**), a loss of sensitivity can be noted with BQ entrapped in the polymer, as the calculated IC_{50} is higher. Moreover, the LLOD is lower when the mediator is dissolved in solution. This fact could be related to the adsorption capacity of activated carbon, resulting in a lower exposure of bacterial cells to the herbicide due to its decreased availability in solution. Indeed, this material has been employed for wastewater treatment as adsorbent for atrazine and other aromatic compounds [163–165].

On the other hand, this phenomenon can be the cause of the wider range of sensitivity: the linear range is broader when the mediator is entrapped, and the saturation concentration (ULOD) is increased of about four times. In conclusion, not only the entrapment prevented the release of BQ in the outer solution, but also improved the operating range of the sensor. The decrease of sensitivity is significant but it does not compromise the application of the biosensor. In fact, when compared with a whole-cell amperometric biosensors based on oxygen detection [146] and a biosensor based on the photocurrent generated by reaction centres [131], the present biosensor exhibits a better sensitivity towards atrazine (**Tab. 5**), and the estimated LLOD is comparable to the other two cases. The response time, however, is the highest among the three, possibly due to diffusional limitations caused by the alginate matrix. It is critical to underline that for our study

subsequent additions of inhibitor were performed, thus the concentration of contaminant was varying throughout the experiments. This condition is more representative of field operation compared to the single injection performed for each experiment in the other two cases. Accordingly, this comparison highlights once more that the presented biosensor can be a useful tool for quantitative online monitoring at low herbicide concentrations. It remains clear that the reported biosensor represents the first step for the development of self-powered devices capable of wireless data transmission at small-medium distance, which would facilitate their field application [14].

Table 5 - Comparison of a whole-cell amperometric biosensors based on oxygen detection [146] *and a biosensor based on reaction centers' photocurrent detection* [131]*, with the present biosensor in the configuration where BQ is entrapped in alginate. All values are referred to atrazine detection.*

Reference	Bioreceptor	IC_{50} / µM	LOD /µM	Response time /min
Present sensor -BQ entrapped	*Anabaena variabilis*	1.0	0.07	20
Shitanda et al. (2005)	*Chlorella vulgaris*	2.0	0.05	3,3
Swainsbury et al (2014)	*Rhodobacter sphaeroides* reaction centres	2.1	0.05	0.5

6.1.4 CONCLUSIONS

In this work, a biosensor based on the inhibition of photocurrent generated by the cyanobacteria *Anabaena variabilis* was built and successfully calibrated using atrazine and diuron as model compounds. The entrapment of the mediator in the polymer was successful, causing only a minor decrease of sensitivity, and increasing the operating range. The biosensor construction comprised only few steps, none of which involving complex procedures (e.g. purification of subcellular molecules or polymer synthesis). This aspect, together with the reported sensitivity, makes this biosensor a powerful tool for environmental analysis with reference to EPA aquatic life benchmarks for the tested herbicides. Future research should address the long-term operational stability of the biosensor and the capability to avoid BQ release. The selectivity toward different class of contaminants (e.g. heavy metals) is another aspect to be taken into account to elucidate biosensor response while applied in the field.

6.1.5 SUPPORTING INFORMATION

p-Benzoquinone entrapment test

The cyclic voltammograms performed to confirm p-Benzoquinone (BQ) entrapment in the alginate capsule are reported in **figure S56**. The voltammograms were recorded using a glassy carbon electrode as the working electrode, both at the beginning (blue line) and at the end (green line) of the experiment (6h exposure of the biosensor to the solution). The voltammogram recorded after 6h was comparable with the one recorded immediately after exposing the modified carbon felt electrode to the electrolyte, and did not show the characteristic reversible redox peaks associated with BQ (red line). Accordingly, diffusion of the redox mediator from the polymer to the electrolyte solution is strongly limited, remarking the effectiveness of the encapsulation.

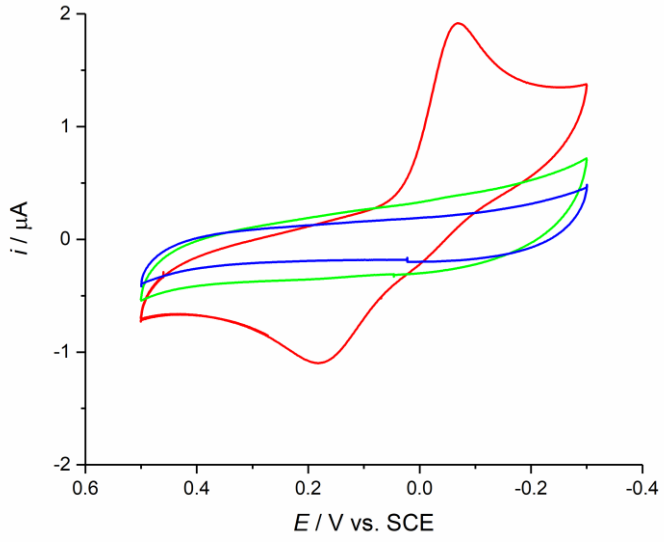

Figure S56. Cyclic voltammograms showing the efficacy of BQ entrapment. A carbon felt electrode constructed as described was placed in buffer solution for 6h. A voltammogram was recorded with a glassy carbon electrode at the beginning (blue line) and at the end (green line) of the experiment. The difference between the two cyclic voltammogram is negligible, and none of them show the characteristic redox peaks associated with BQ (red line).

Biosensor calibration with entrapped BQ

Figure S57 shows calibration obtained for the biosensor with entrapped BQ. It was possible to obtain a linear relationship between current and concentration up to 1.31µM of atrazine (sensitivity of -7.7 µA μM^{-1} cm^{-2}; R^2 = 0.93) and 0.13 µM of diuron (sensitivity of -34.5 µA μM^{-1} cm^{-2}; R^2 = 0.95).

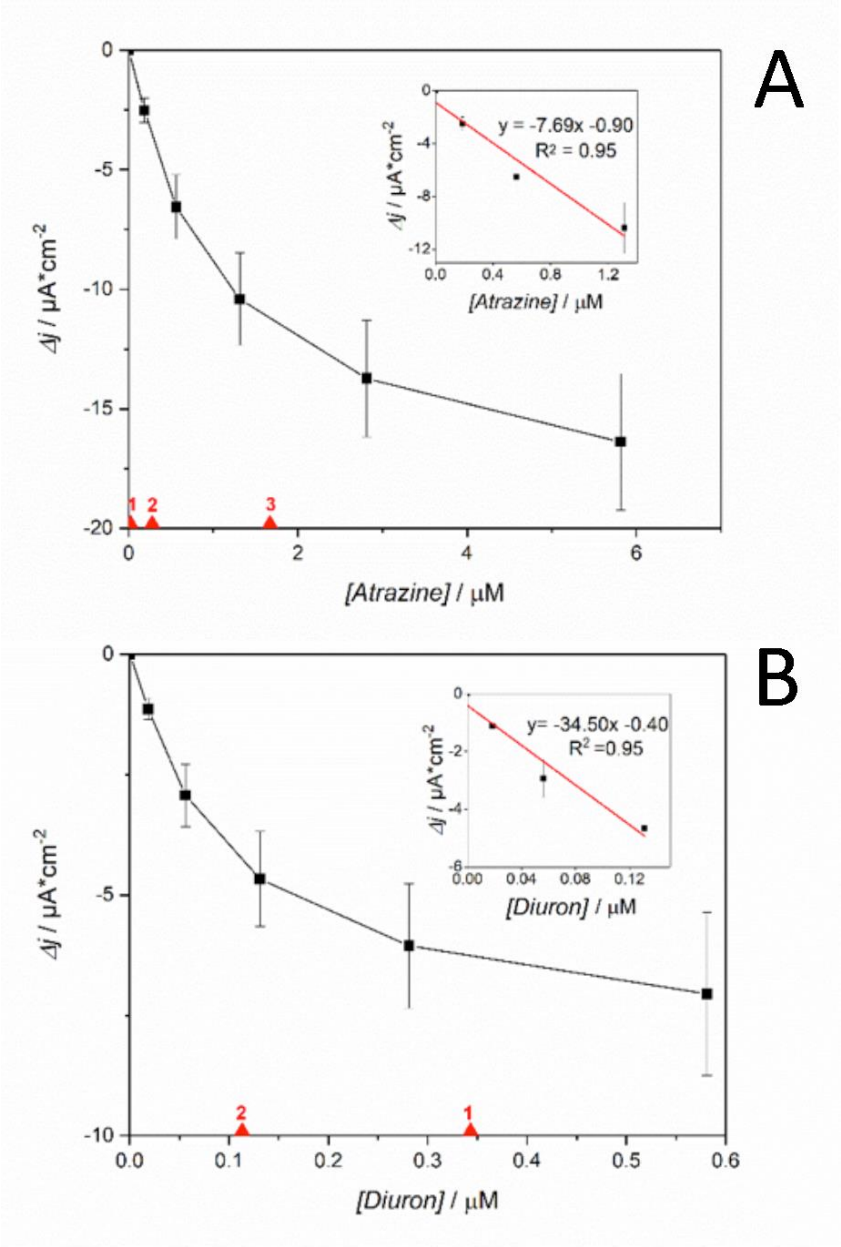

Figure S57. Calibration of the biosensor with BQ entrapped in alginate. A) Concentration-current relationship for atrazine. B) Concentration-current relationship for diuron. Insets show the linear range of the curves and the equation of the linear fitting. Aquatic life benchmarks set by EPA are represented with red triangles: 1) Chronic exposure concentration for invertebrates, 2) Chronic exposure concentration for fish, 3) Acute exposure concentration for invertebrates.

Table S6: Summary of the linear fitting parameters calculated from the calibration curves in the two configurations of the biosensor for both inhibitors

	Atrazine			Diuron		
	Sensitivity /µA µM^{-1} cm^{-2}	Range /µM	R^2	Sensitivity / µA µM^{-1} cm^{-2}	Range /µM	R^2
BQ in solution	-24.6	0 - 0.56	0.97	-72.1	0 – 0.08	0.95
BQ entrapped	-7.7	0 - 1.31	0.93	-34.5	0 – 0.13	0.95

6.2 Mediatorless photo-bioelectrochemical sensor

From: *M. Tucci, P. Bombelli, C. J. Howe, S. Vignolini, S. Bocchi, A. Schievano. A storable mediatorless electrochemical biosensor for herbicide detection, Microorganisms, 7, 630 (2019) 1-14* [166]

6.2.1 SCIENTIFIC BACKGROUND

Several synthetic herbicides interfere with the photosynthetic electron transport chain of photosynthetic organisms (cyanobacteria, algae, plants, etc.). Agrochemical companies have developed a variety of herbicides that exploit this to control weeds [167]. Most photosynthetic inhibitors can be categorized into one of two groups, those that inhibit Photosystem II (PSII) and those that inhibit Photosystem I (PSI).

Roughly a third of all the sales in the herbicide market are PSII inhibitors [168]. These compounds are able to block the plastoquinone binding site of PSII, hence precluding electron transfer to this intermediate [169]. Two common examples in this category are atrazine and diuron. Atrazine is a triazine herbicide widely used in sugarcane and maize agriculture [127]. Because of its persistence and extensive application, it tends to accumulate in surface and groundwater [170]. The chemical can act as an endocrine disruptor, interfering with the central nervous system and the immune system of animals and humans [171]. For this reasons, the European Union banned atrazine in 2003 [130], but it is still in use in many other countries, such as USA, Australia and China. Diuron is another herbicide commonly used for weed control in the culture of cotton, coffee, sugar cane and citrus [134]. Because of its widespread application, it is ubiquitous in the environment and causes serious risks to human and animals. Moreover, its main biodegradation product, 3,4-dichloroaniline, is persistent in soil, water and groundwater and has a higher toxicity [172].

Photosystem I inhibitors can accept electrons from PSI to form radicals, which are extremely dangerous for living cells because of their high reactivity [173]. Among them, paraquat (i.e. methyl viologen dichloride) is probably the most used, despite its high level of acute toxicity to humans and animals [174], which has led to its use even for suicide and murder [175]. In the environment, it can remain strongly adsorbed to soil particles, with a half-life up to 20 years [176]. As a consequence, this chemical was banned in the European Union [177] and several other nations. Unfortunately, it is still in use in many countries worldwide.

Given this situation, constant monitoring of these compounds in environmental compartments is crucial to ensure ecosystem and human health. Traditional analytical methods, such as high-performance liquid chromatography (HPLC), atomic absorption spectroscopy (AAS), capillary electrophoresis (CE) and mass spectrometry (MS), usually show good accuracy and precision. However, these techniques present several operational and economic limitations to their use for widespread field monitoring: high complexity, time-consuming procedures, and requirement for sample pre-treatment, expensive instrumentation and highly trained operators [178].

A novel approach to herbicide detection is represented by low-cost biosensors, which are based on the cytotoxicity response of photo-autotrophic microorganisms to concentrations of the target herbicide. A common approach is represented by optical biosensors, where the population's growth inhibition is analysed by means of a spectrophotometer over time [16]. This method was found effective in detecting several different herbicides, but requires a relatively long time for cell culture and growth analysis [21]. Conversely, amperometric photo-biosensors have the advantage of performing real-time monitoring of the process of inhibition [21]. This kind of sensor relies on measurement of the electron flow dependent on the bio-photocatalytic oxidation of water during the photosynthetic process. Two main types of biological materials have been employed in these systems: subcellular units and whole cells. Examples of the first type are thylakoid membranes [141,142], photosystems [125], and reaction centres [131], which have the advantages of being highly sensitive, having fast response time sand low detection limits [143]. On the other hand, these kinds of materials need complex and expensive purification techniques, are fragile after isolation and have no self-repairing capabilities. For this reason they seem less suitable for long-term field operations [144]. Whole-cells, instead, are robust, abundant and inexpensive to culture [145,179]. So far, amperometric biosensors based on whole-cells have mainly relied on the detection of photosynthetically-produced oxygen [146–149]. However, this is an indirect measure of the photocurrent, as it can be strongly influenced by environmental factors (e.g. temperature), making them ineffective for field applications. In addition, many biosensors of this type employ selective membranes [138,146,147,149], which over long application periods can be affected by fouling issues.

Recently, a novel whole-cell amperometric biosensor based on direct photocurrent monitoring was developed [123]. Unfortunately, despite the good performance achieved, it relied on p-benzoquinone to shuttle the electrons from the photosystems inside the cells to the electrode. Quinone-based compounds are frequently used as redox mediator in photo-bioelectrochemical

devices [91,143,180,181]. In fact, they have similar chemical properties to the plastoquinone complex, which is the natural electron acceptor in the photosynthetic electron transport chain [123]. Such compounds only temporarily increase the biofilm's photoresponse [179], as they also typically damage the biological structures [153]. Indeed, quinones are known to be good Michael acceptors: they are able to react with macromolecules like proteins, lipid and DNA and disrupt them [182]. In order to build long-lasting biosensors and to avoid genotoxic and cytotoxic effects caused by these chemicals, artificial mediators should be avoided. Extracellular Electron Transfer (EET) in absence of artificial redox mediators has been successfully obtained in the field of biophotovoltaics (BPVs), where photo-bioelectrochemical devices are used to produce electric power [179,183–185].

In this study, we designed and fabricated a novel photo-bioelectrochemical sensor for herbicide detection, operating in absence of any artificial electron mediators. The cyanobacterium *Synechocystis* PCC6803 (wild type). was chosen as photo-active component because of its proven electrogenic operation in BPV devices. [90,179,183–185]. A novel anodic material made by filter paper coated with carbon nanotubes and a titanium nanolayer was used. Living cyanobacterial cells were allowed to form a spontaneous biofilm on the surface of a carbon/titanium electrode. The biosensor photo-response for diuron, atrazine and paraquat was tested and compared. In addition, the stability of the biosensor was analysed to assess its durability under storage conditions.

6.2.2 MATERIALS AND METHODS

Reagents and solutions

All reagents were purchased from Sigma-Aldrich. The stock solutions of the herbicides were prepared as follows: atrazine (0.28 mM) in ethanol and water (ratio 1:7), diuron in pure ethanol (0.09 mM), and paraquat in ultra-pure water (0.23 mM). Ultra-pure water purified with a Millipore Milli-Q® Integral purification system was used for the stock solutions. Distilled water was used for the bacterial medium.

Synechocystis culture

Wild type *Synechocystis* PCC6803 was obtained from laboratory stocks. A Cryo-SEM image of *Synechocystis* cells is shown in **figure 58**. It was cultured at room temperature (22±2°C) in a 1.5 L flask using BG11 liquid medium [157]. The source of illumination was natural sunlight. Bubbling with sterile filtered air was continuously performed in the culture to provide stirring and facilitate

gas exchange. The culture was maintained at stationary phase by removing 10% of the volume and replacing it with fresh medium every week. The Optical Density of the culture at 750 nm (OD_{750}), measured with UV-Vis spectrometer (Agilent Cary 4000), was maintained at 7±2.

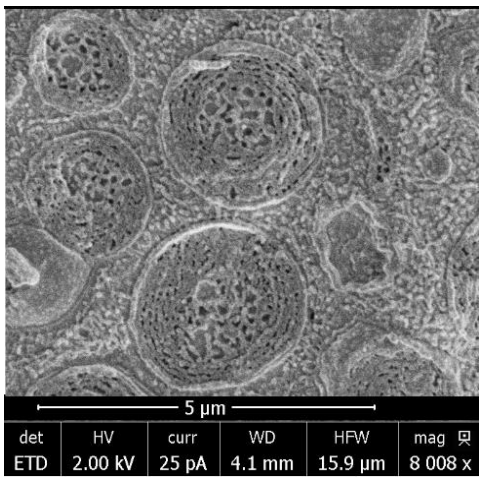

Figure 58 – Cryo-SEM image of Syncechocystis PCC6803 (wild type) cells

Electrode fabrication and biosensor construction

To build the electrode, a filter paper sheet was covered with 7 layers of single walled carbon nanotube paint (SWCNT ink, Sigma Aldrich, **Fig. 59C**). After each layer, the paint was allowed to dry for 1 h. The amount of nanotubes deposited for each layer was determined to be 1.12 ± 0.05 µg cm^{-2} by weighting. After that, a titanium nanolayer was deposited on the surface of the electrode by evaporation, using a four-crucible e-beam evaporator (Kurt J lesker PVD 75). A picture of the actual electrode is presented in **figure 59A**, and in **figure 59B** an image of the electrodic surface obtained with the optic microscope. To prepare the biosensor, the electrode was placed in a Petri dish and submerged in the cyanobacterial culture. The microbial cells were allowed to spontaneously settle on the surface under gravity for 48h. Finally, the bioelectrode was dried for 15 min before electrochemical analysis to assist the physical adsorption of the cells onto the electrode surface.

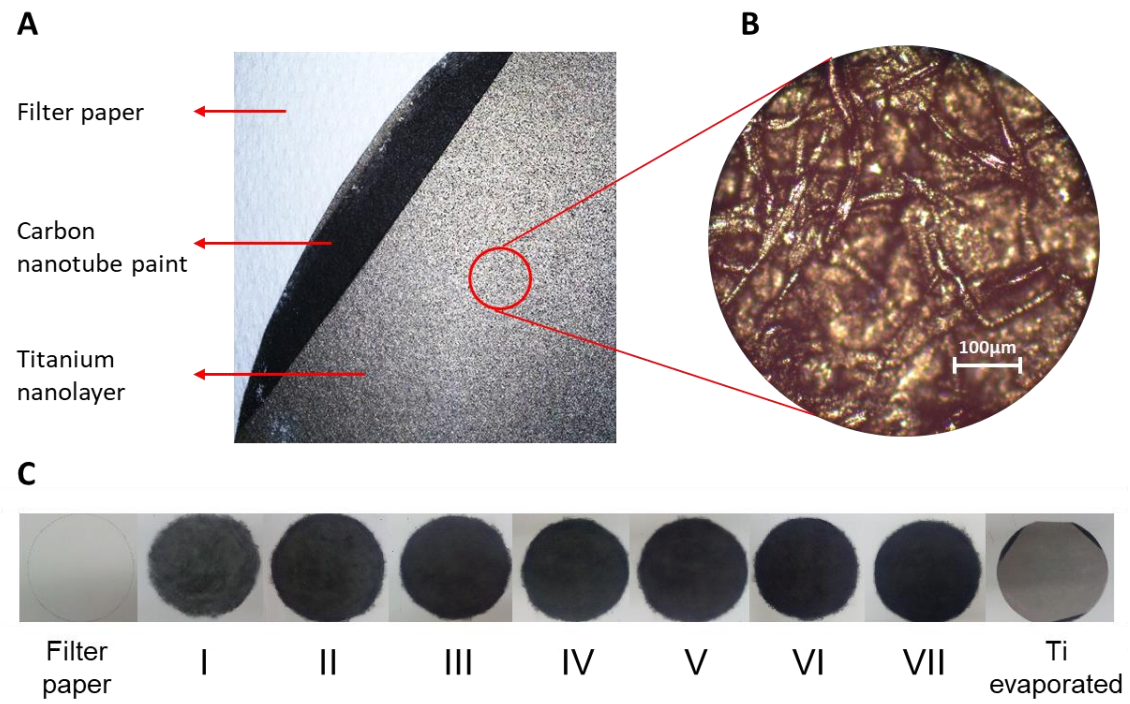

Figure 59 – A) Picture of the electrode surface B) Image of the surface obtained with optic microscope. C) electrode construction: filter paper (ø = 210mm) was coated with seven layers of carbon nanotube paint and a topmost layer of titanium was added by evaporation.

Electrochemical analysis

A three-electrode electrochemical setup was used for the analysis: the bioelectrode was the working electrode, a platinum wire (ø = 0.10mm Advent Research Materials Ltd) was used as counter electrode and Ag/AgCl electrode was used as reference electrode. The biosensor was clamped together with a stainless steel washer between two PTFE disks (**Fig. 60A and B**). The CE and the RE were held by the top part of the clamp. The experiments were performed using MultiEmStat 4-channel potentiostat (PalmSens) controlled by MultiTrace software. The electrochemical analyses were conducted using BG11 medium as electrolyte at room temperature (22±2°C) to maintain an optimal environment for the bacterial cells. A white LED lamp (4W, 3000K; Verbatim) lamp was used during the tests to provide illumination, at a distance of 20 cm resulting in the anodic surface being irradiated with ~450 µE m^{-2} s^{-1}. Chronoamperometry was performed at +0.4 V vs.Ag/AgCl, and light was switched on and off in order to assess the photocurrent production of the electrode. During the inhibition experiments, herbicide solutions were directly injected in the electrolyte. A diagram representing the electrochemical setup is shown in **figure 60C.**

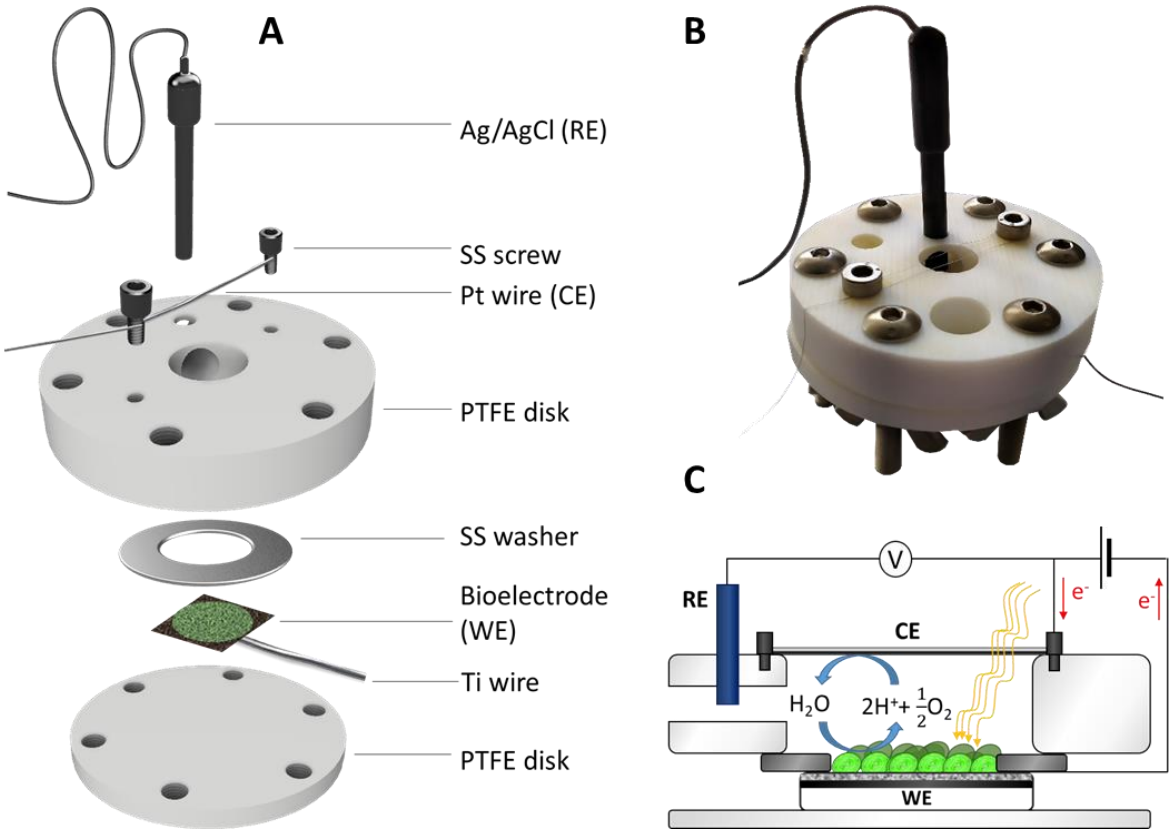

Figure 60 - A) Semi-exploded view, B) picture and C) electrochemical diagram of the setup used for the experiments: the bioelectrode (working electrode - WE) was clamped using two PTFE disks which also held the platinum wire (counter electrode - CE) and the Ag/AgCl reference electrode (RE). The stainless steel washer ensured electrical connection between the bioelectrode and the titanium wire.

Chlorophyll determination

Chlorophyll content of the biofilm present on the bioelectrodes for different days was determined by spectrophotometric measurement. Electrodes prepared as described above were kept at room temperature in BG11 medium. Chlorophyll was extracted in 99.8% (v/v) methanol at 4°C in absence of illumination for 15 min under agitation. The content of chlorophyll *a* was calculated according to Porra *et al.* [186].

Biosensor storage

In order to test its durability, several bioelectrodes prepared as previously described were placed in Petri dishes containing a sponge cloth (0.5cm thickness, Houseproud) on the bottom (**Fig. 65**). The sponge was moistened with BG11 medium to keep the humidity inside the plates. The Petri dish was sealed with Parafilm® and stored in a fridge at 4°C.

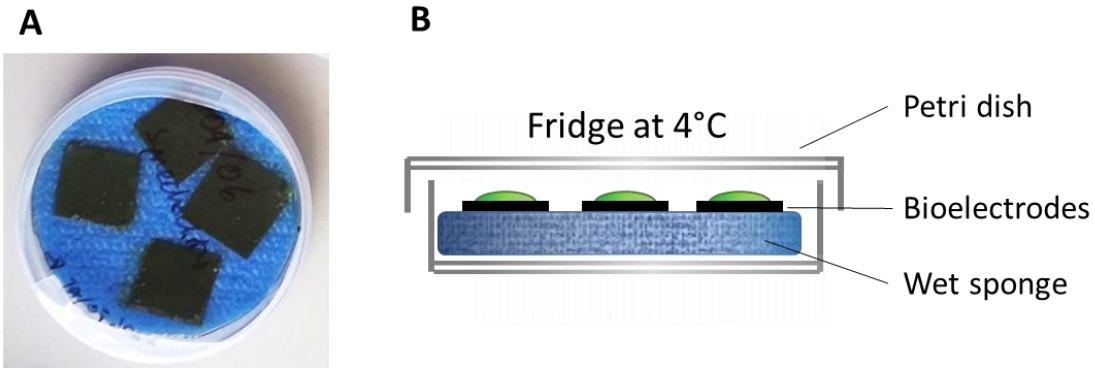

Figure 61 – Setup used for storing the bioelectrodes in the fridge: A) picture of the petri dish containing the bioelectrodes on top of the sponge, B) schematic representation of the setup

6.2.3 RESULTS

Biosensor design and photocurrent production

The novel electrochemical biosensor described here is shown in **Fig. 60.** The system includes an anode made by filter paper coated with carbon nanotubes and a titanium nanolayer (**Fig. 59A**). The roughness of the filter paper provides a suitable surface for the cyanobacterial cells to adhere to. The anode is clamped between two Teflon disks. The electrochemical setup is completed with a counter electrode made by Pt wire and an Ag/AgCl reference electrode located on the top Teflon disk (**Fig. 60A** and **B**). Cyanobacterial cells were allowed to sediment spontaneously on the anodic surface. More details on the fabrication of the anode are reported in the Material and Methods section.

The novel electrochemical biosensor was tested using chronoamperometry, by applying +0.4 V bias potential vs. Ag/AgCl. No artificial redox mediator was added during the electrochemical analysis. The anodic surface was irradiated with white LED light at ~450 µE m^{-2} s^{-1}.

As soon as the light was switched on **(Fig. 61A)**, a rapid increase in current (~0.4 µA) was observed for the biosensor operated with cyanobacterial cells. The increase in current on illumination is referred to as light response. Then, when the dark condition was restored, the current returned to its pre-illumination level. This basal level was termed the background current. As photocurrent is intended the difference between the light response and the background current.

The light response recorded during several cycles of illumination for the electrochemical biosensors operated with cyanobacterial cells was found to be stable over time and significantly higher than the abiotic control (**Fig.61B**, t-test p=0.01). Only a relatively small light-dependent increase in current (~0.03 µA) was recorded in the abiotic controls.

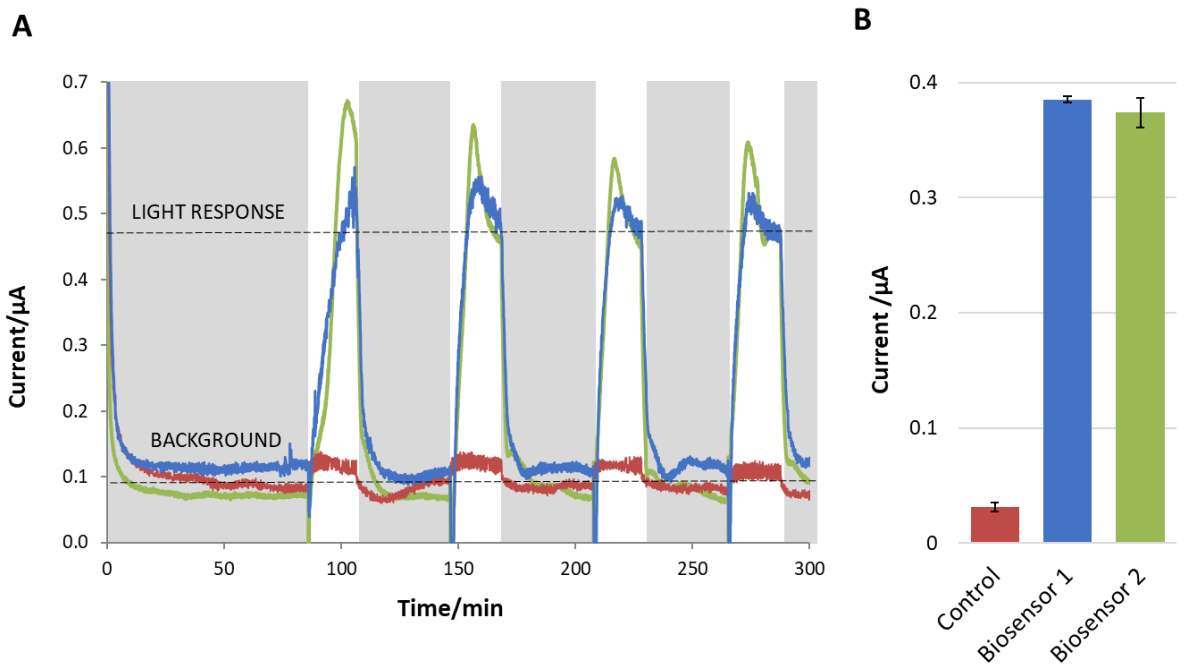

Figure 62 - A) Light effect on the biosensor in duplicate (blue and green lines) and on the abiotic control (red line). The periods of darkness are indicated with grey backgrounds. The biosensor showed a significant photocurrent (calculated as the difference between the stable light response current and the background current) production, which was stable during the different cycles. Only a very small change in current was observed in the control, where the biological material was not present. B) Histogram of the photocurrent produced by the biosensors (replicate 1 and 2) and the control. When Synechocystis was present, the photocurrent was about one order of magnitude higher than in the absence of Synechocystis. The error bars represent the standard deviation between the different illumination cycles of the same biosensor.

Detection of herbicides

In order to evaluate the sensing capabilities of this device, the effect of three commonly used herbicides was tested: diuron, atrazine and paraquat. In separate experiments the selected herbicides were injected into the cyanobacterial medium while performing chronoamperometry under cycles of dark and light. The percentage of inhibition was calculated by the equation 1.

$$\text{Phot. Inhibition (\%)} = (1 - (Ph_{after} / Ph_{before}))*100 \qquad \textbf{(Eq.1)}$$

In the equation Ph_{after} is the photocurrent measured after inhibition and Ph_{before} is the photocurrent measured before inhibition as shown in the **Fig. 62.**

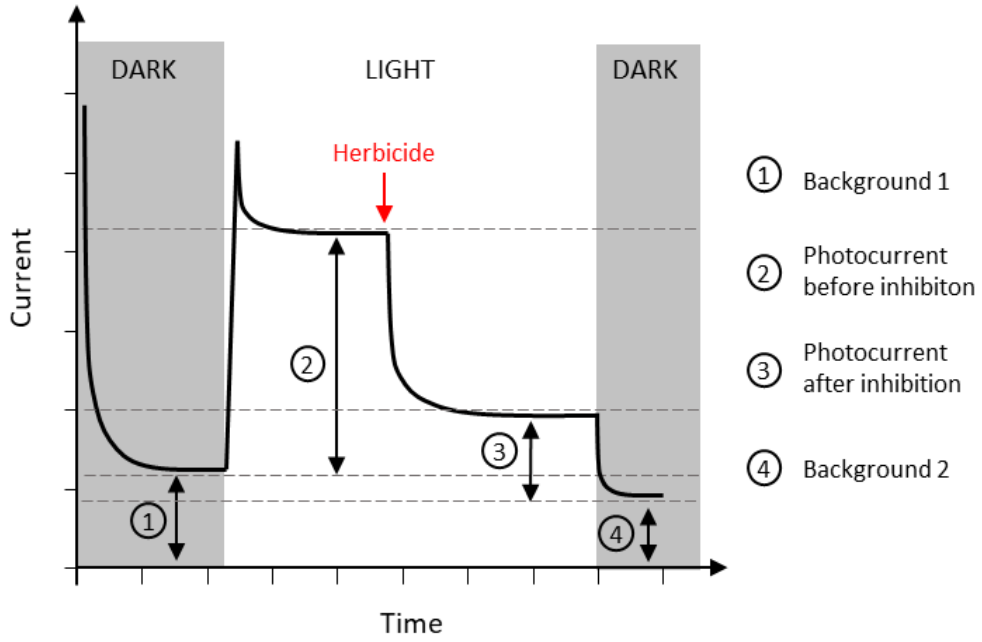

Figure 63 – Representation of a theoretical chronoamperometry in which are indicated the different phases of the photocurrent inhibition

Both diuron (**Fig. 63A**) and atrazine (**Fig. 63B**) caused an immediate drop in the light response, which decreased gradually until it reached a steady level. The experiments were conducted in triplicate, and the plots of the three replicates can be found in the Supporting Information (**Fig. S67)**. Even though the concentration used for diuron (0.5 µM) was more than one order of magnitude lower than that used for atrazine (10 µM), diuron caused a faster inhibition. Moreover, the inhibitory effect was significantly stronger in the case of diuron: atrazine was able to reduce the photocurrent by 76±7%, versus 91±4% of diuron. The photocurrent inhibition was calculated as the difference between uninhibited photocurrent and inhibited photocurrent. Since the background level is subjected to slight variations, the chosen background levels used to determine the different photocurrent values were selected as the ones just before light was switched on for each case.

In contrast, injection of paraquat resulted in an increase of the photocurrent 203±3% (**Fig. 64**), for a few hours. Then, the photocurrent started to decrease. Also, the background current tended to increase over time. This may indicate that paraquat was able to shuttle electrons originating from metabolic processes other than photosynthesis.

The calculated photocurrents and respective errors are reported in the supporting information (**Tab. S9, Fig. S68**)

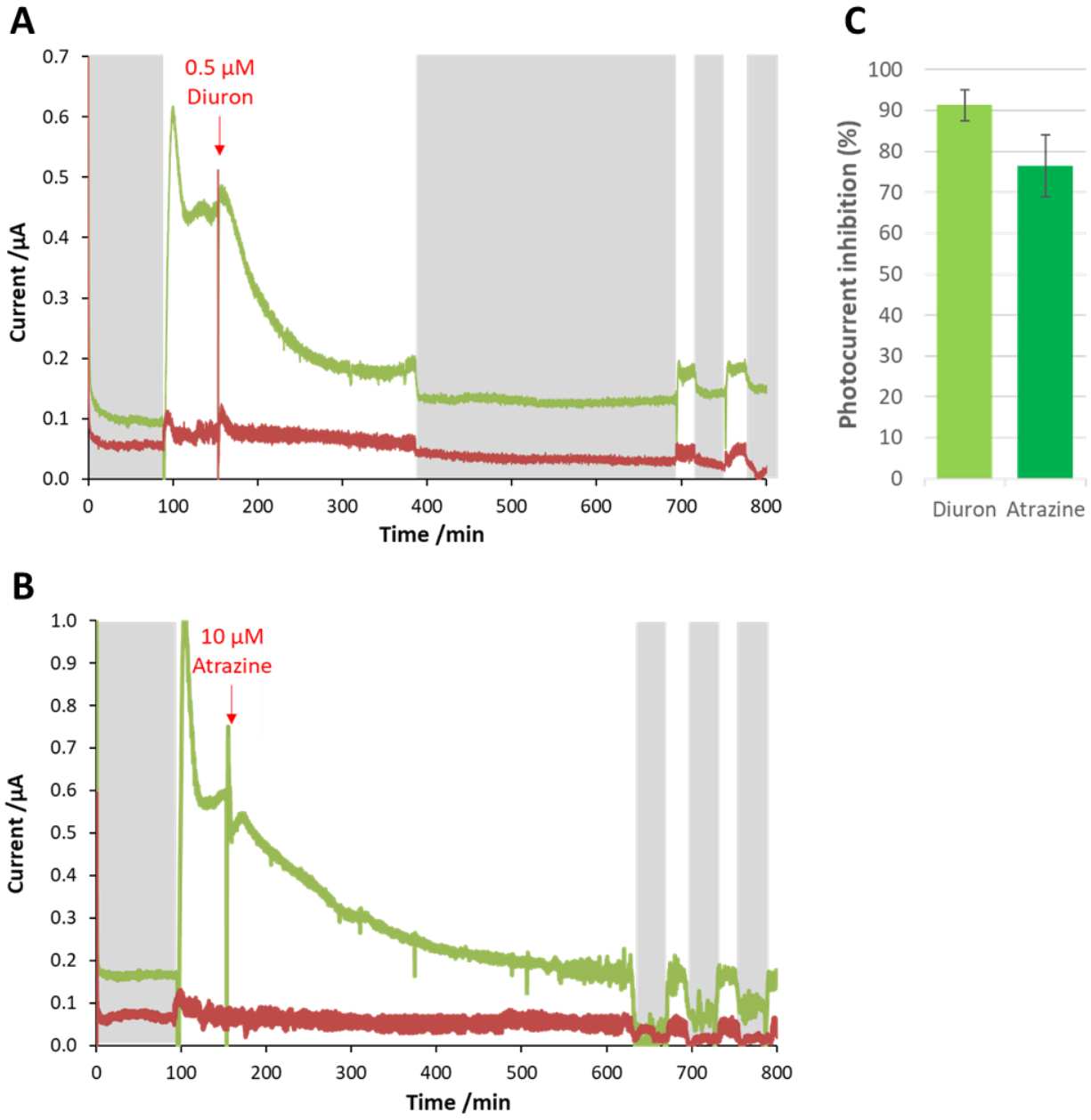

Figure 64 – Effect of diuron A) and atrazine B) on the light response of the biosensor (green lines). The periods of darkness are represented with grey backgrounds. Under illumination, the current under illimitation decreased as soon as the herbicide was injected. However, even if the concentration of atrazine was more than an order of magnitude higher, the inhibition process was slower compared to diuron. The current responses of the abiotic controls are shown with red lines. Figure C) shows the percentage of photocurrent inhibition in the two cases. The error bars represent the standard deviation for three different bioelectrodes.

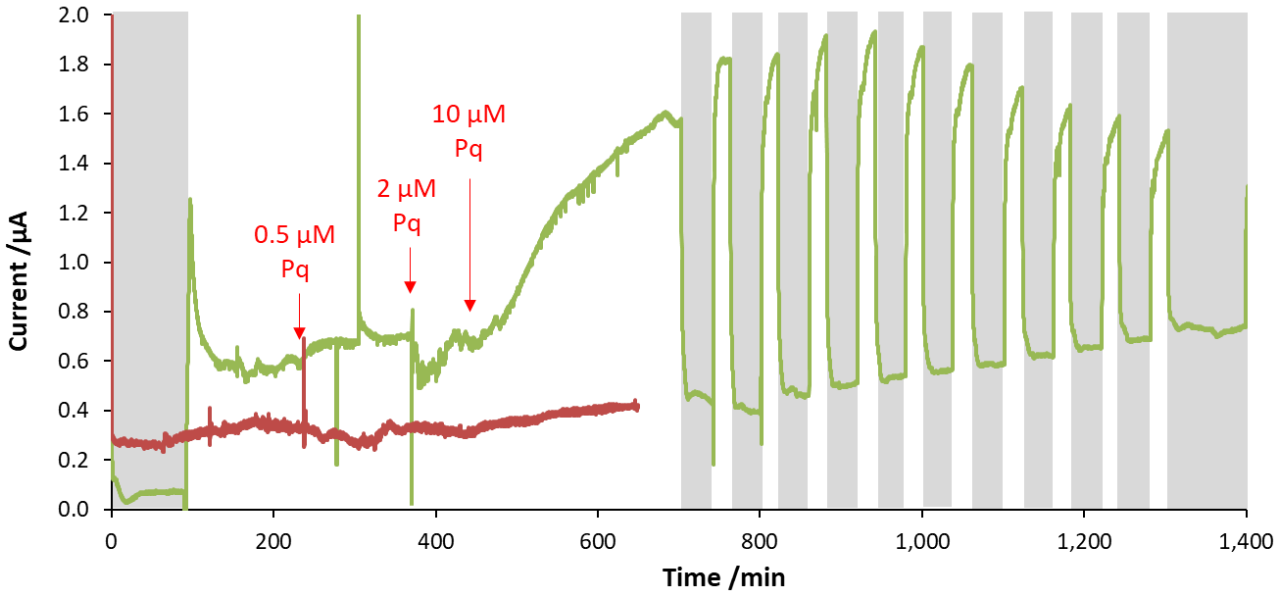

Figure 65 – Effect of paraquat on the light response (green line): when a low amount of the compound was injected (final concentration 0.5 µM) a subsequent increase in light response was seen. For higher concentrations the photocurrent increased further, and was more than doubled at 10 µM atrazine (final concentration). However, after a few cycles of illumination the light response decreased again to its initial level, while the dark current remained high. The current response of the abiotic control is shown with a red line.

Bioelectrode storage and stability

The durability of the biosensor under storage for up to 22 days was investigated. Several bioelectrodes (*i.e.,* anodes) were placed in Petri dishes containing a wet sponge to maintain humidity as shown in **Fig. 65** and stored in the fridge at 4 °C.

The viability and stability of the cyanobacterial biofilm on the electrode surface store at 4 °C was tested by measuring the amount of chlorophyll *a* [42] extracted from colonised electrodes at day 4, 8, 10 and 14 (**Fig. S69)** [186]. The amount of chlorophyll content was stable over a period of 14 days, indicating cellular stability and therefore that the cyanobacterial electrode described here might be suitable for future biotechnological applications.

Figure 66A shows a test conducted with a bioelectrode that was stored in this way for 22 days. The performance of this bioelectrode in terms of photocurrent and sensitivity towards diuron was slightly lower than for a freshly prepared biosensor. Indeed, only a loss of performance of ~20 % was obtained, calculated as the difference in percentage inhibition of photocurrent between the two cases (**Fig. 66B**).

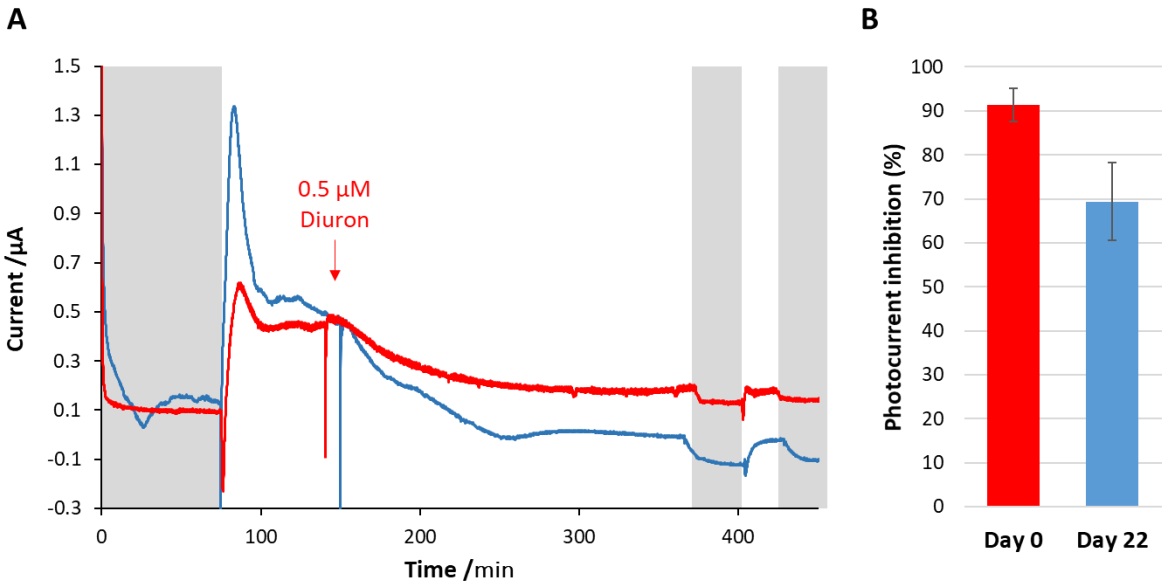

Figure 66 –. A) After being stored in the fridge for 22 days (blue line), the biosensor showed similar performances in terms of photocurrent production and diuron detection when compared with a fresh biosensor on day zero (red line). B) shows the average photocurrent inhibition caused by diuron obtained with three different bioelectrodes for day zero and three different ones for day 22. The error bars represent the standard deviation of the three replicates.

6.2.4 DISCUSSION

When compared with other whole-cell photosynthetic-based biosensors [138,145,147], the anode colonised by cyanobacteria displayed comparable storage stability to the cases reported in the literature (**Tab. 7**). However, the whole-cell photosynthetic-based biosensors previously published were mainly based on monitoring the oxygen produced by photosynthesis and not on the direct electrochemical measurement of the photocurrent. Because the concentration of dissolved oxygen can be affected by other environmental factors (e.g. temperature), the potential for such devices to be used in the field might be limited. Recently, Chouler *et al.* used a MFC-based sensor to detect atrazine in absence of photosynthetic bacteria [63]. However, the current output of MFCs is strongly influenced by the concentration of organic substrates fed to the anodic biofilm, which can mask or even overwhelm the response to the target toxicant [75].

Table 7 – Comparison of the storage stability of amperometric photo-biosensors found in literature and the present sensor.

Bioreceptor	Storage conditions	Storage time (days)	Loss of sensitivity (%)	Reference
Chlorella vulgaris	4°C in $CaCl_2$ solution	30	20	Shitanda et al. 2009 [147]
Chlorella vulgaris	4°C in Tris-HCl + $MgCl_2$	10	45	Ionescu et al. 2006 [145]

Chlamydomonas reinhardtii	25°C in storage buffer, light	25	40	Husu et al. 2013 [138]
Synechocystis 6803 wt.	4°C in BG11 medium, dark	22	22	Present study

The biosensor developed and tested in this study was able to detect the presence/absence of herbicide concentrations in the order of the micromolar. When compared with the benchmark for acute exposure of fish set by the Environmental Protection Agency of the United States [161], the detected concentrations are below the threshold for acute exposure of fish (**Tab. 8**). Therefore, the sensor could be applied to environmental monitoring. Further studies should be directed to obtain calibration curves for the herbicide concentration versus photocurrent.

Even though atrazine and diuron have the same mechanism of photocurrent inhibition, they showed different impacts on the photocurrent. Both compounds bind the QB pocket in PSII (**Fig. 21**), thus interrupting the electron transport chain [139,140]. Nevertheless, atrazine caused a much slower inhibition compared to diuron, even at 10-fold higher concentrations. In addition, the level of photocurrent inhibition caused by diuron was found to be higher than the inhibition caused by atrazine (t-test, p=0.05). These observations indicate that the biosensor is able to differentiate between the two substances to a certain extent. Indeed, diuron was previously reported as a stronger photosynthesis inhibitor than atrazine in terms of half maximal inhibitory concentration IC_{50} [123].

The response towards paraquat was completely different, as it temporarily enhanced the photocurrent. This is probably due to its ability to shuttle electrons between bacterial cells and the electrode. This compound is a well-known redox mediator, and for this reason it is used in microbial electrochemical systems under anoxic conditions [28,187]. However, the fact that the enhancement was only short term might be due to paraquat's cytotoxicity caused by the formation of peroxy radicals.

The electron transfer between *Synechocystis* and the electrode was achieved without adding any exogenous electron carrier. Under this condition, a net photocurrent production was obtained, with good reproducibility. This aspect gives several advantages to the biosensor: redox mediators are often toxic and can increase the operational cost and complexity. because of their cytotoxicity, the enhancement of the photocurrent with redox mediators is typically temporary [153]. Also,

quinone-based mediators may undergo photo-degradation when dissolved in aqueous media [188], thus their reactivity decreases overtime.

Our data suggest that, in absence of any exogenous electron carries, the biosensor could remain functional after over 20 days of inactivity at low temperature, with only a small loss in performances (~20%). The retention of activity was probably achieved thanks to the capacity of the cyanobacterial biofilm to regenerate and/or stay dormant. The capacity of this biosensor to recover after a cold season or other environmental prolonged stresses could be a key-advantage in field applications, such as in water bodies or agriculture.

However, further investigations should complete the present study, especially focusing on the durability of the cyanobacterial anodic biofilm over subsequent cycles of herbicide-inhibition and recovery. Also, native cyanobacteria kept in the dark tend to lose their photosynthetic activity [189]. The lifetime of the photoanodic population might represent a limiting factor for commercial application of this kind of devices.

Table 8 – Decrease in photocurrent upon treatment with the tested herbicide expressed as percentage (average for three replicates), concentrations used for the experiments and threshold of acute exposure for fish set by the Environmental Protection Agency of the United States (EPA- Aquatic life benchmarks [161]*). The biosensor could detect the presence of the selected compounds before it reached the threshold in all three cases.*

	Photocurrent variation (%)	**Conc. used (µM)**	**Acute exp. - Fish (µM)**
Atrazine	-76 ± 7	10.7	12.3
Diuron	-91 ± 4	0.5	0.9
Paraquat	+203 ± 3	0.7	23.3

6.2.5 CONCLUSIONS

A mediatorless electrochemical biosensor operating with wild type *Synechocystis* PCC6803 was developed and tested. The biosensor was able to detect the presence of diuron, atrazine at micromolar level, which are concentrations relevant to environmental analysis. Additionally, we showed that our cyanobacteria-colonised electrode could successfully recover after more than 20 days of low-temperature conditions. This concept opens up potential applications in the field of environmental monitoring. However, further research is needed, to assess the stability of the photosynthetic anodic biofilm over time and to enhance the sensitivity to different concentrations.

Also, further optimization of the storage conditions (e.g. temperature, light intensity, moisture) is needed in order to improve the storage stability of the bioreceptor.

6.2.6 AKNOWLEDGEMENTS

The authors acknowledge Christopher J. Valentine (Department of Engineering, University of Cambridge) for the titanium evaporation and Gea Van De Kerkhof (Department of Chemistry, University of Cambridge) for the cryo-SEM image of *Synechocystis*.

6.2.7 SUPPORTING INFORMATIONS

A)

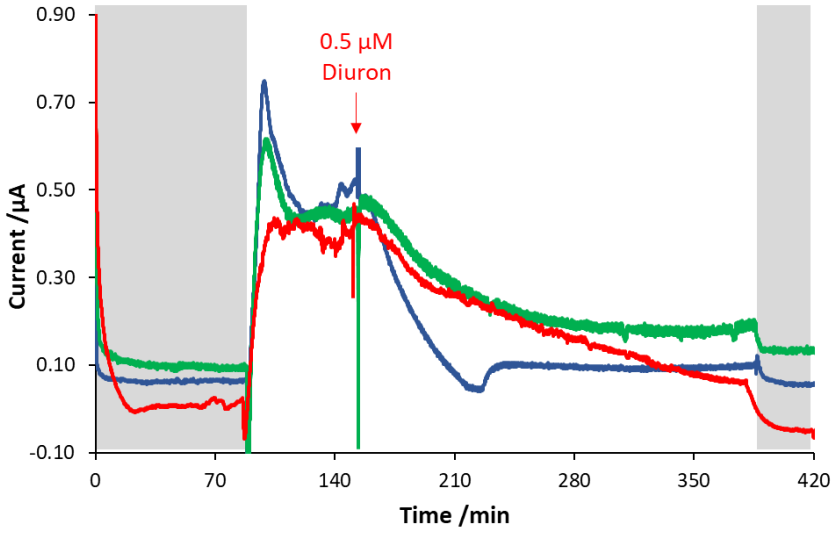

B)

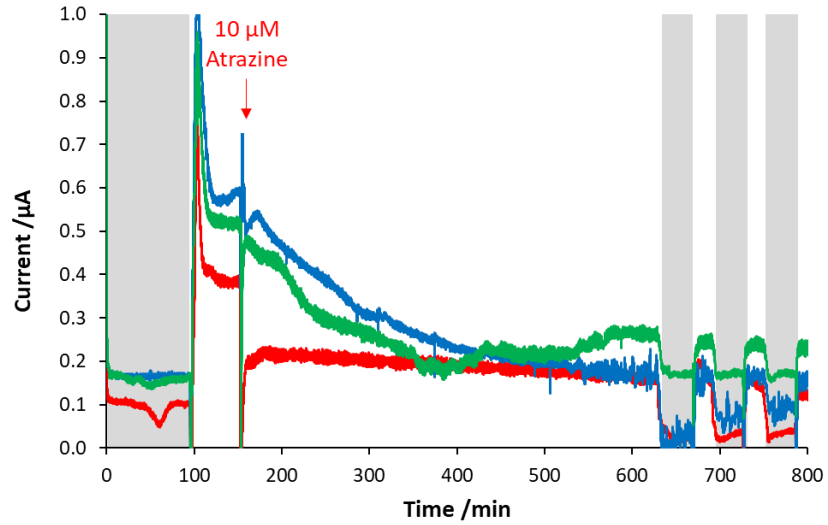

C

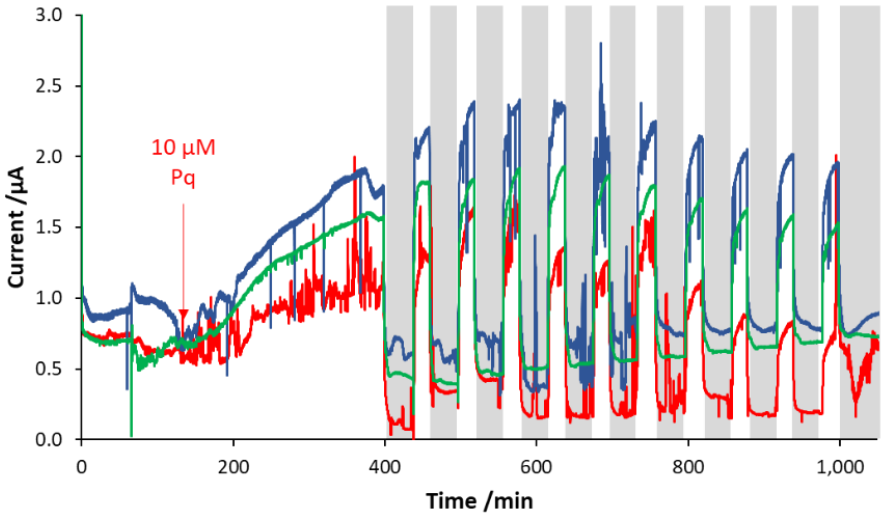

Figure S67 – Triplicates of the chronoamperometric detection of herbicides for A) diuron, B) atrazine and C) paraquat. The gray background indicates the periods of darkness. The applied potential was +0.4V vs. Ag/AgCl.

Table S9- Photocurrent production before and after the injection of the tested herbicides. The photocurrent is calculated as the difference between the current obtained during illumination and the current obtained in darkness.

	DIURON		ATRAZINE		PARAQUAT	
	Average	**St. Dev.**	**Average**	**St. Dev.**	**Average**	**St. Dev.**
Photocurrent (µA)	0.397	0.051	0.353	0.067	0.487	0.038
Photocurrent + Herbicide (µA)	0.033	0.012	0.080	0.010	1.477	0.124
Variation %	-91	4	-76	7	203	3

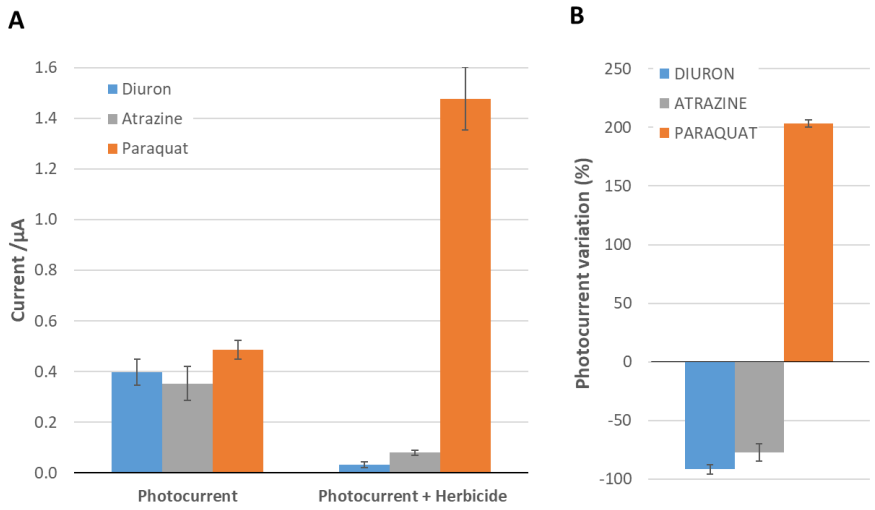

Figure S68 – A) photocurrent production before and after the injection of the tested herbicides. B) Variation of photocurrent after the injection of herbicide expressed as percentage.

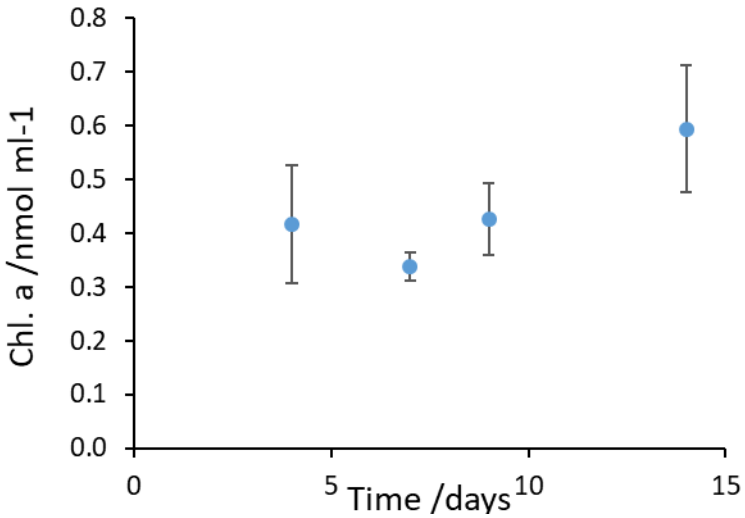

Figure S69 - The chlorophyll content of the biofilm on the electrode surface is stable over a period of 14 days

7 CONCLUSIONS AND OUTLOOK

In this dissertation, the application of microbial electrochemical systems as environmental sensing tools has been discussed. The great potential of MES-based biosensing has been proven, as it can allow to detect several different contaminants using low-tech devices constructed with cost-effective and sustainable materials. Moreover, fast and on-line response is obtained with low involvement of operators. Two main environmental sectors have been analysed: wastewater monitoring and herbicide detection.

7.1 Wastewater monitoring

Floating MFCs were employed as in-situ wastewater monitoring systems. A planar prototype was successfully calibrated in the lab using sodium acetate as carbon source. However, the trials conducted in the wastewater treatment plant underlined the strong impact of environmental factors and the influence of complex organic substrates on the signal. From the comparison with a cylindrical setup, together with a more detailed analysis of physical-chemical factors (i.e. temperature, illumination, nitrates and sCOD) and the characterization of the microbial communities present in the biofilms, some weaknesses of the design emerged. The main flows identified were two: the depth at which the anode is placed, and the exposure to light. Regarding the first one, anodes placed deeper in the wastewater reduced the contact with dissolved oxygen diffusing from the liquid/gas interface. Light exposure, on the other hand produces changes in temperature and allows development of photosynthetic microorganisms. Therefore, a setup in which the cathode is protected from sunlight is preferable, as it can avoid the noise associated with those factors.

These results prove that careful site-specific design is important to control the impact of environmental factors and obtain meaningful signals. In addition, a better understanding of the contributions of the different factors can be crucial to discern between them (e.g. using statistical tools). Furthermore, the employment of an array of various MFC-based sensors with different levels of sensitivity to the environmental factors can be an effective strategy to monitor the wastewater treatment process, as the combination of the data can give a complete assessment of the analysed sample.

7.2 Herbicide detection

Amperometric photo-biosensors based on the direct inhibition of the photocurrent produced by cyanobacteria has been tested. The first prototype developed involved the encapsulation of living cells in an alginate hydrogel and the use of p-benzoquinone as redox mediator. The sensor proved to be effective in detecting commonly used herbicides (i.e. atrazine and diuron) in concentrations suitable for environmental monitoring. However, since the redox compound has cytotoxic effects and photodegradation issues, the device was not able to operate for more than few hours. For this reason, a new prototype was built in absence of mediators. The new biosensor was stable over significantly longer periods (i.e. 22 days under storage conditions in the fringe), but this time it was not possible to obtain a concentration-current calibration curve, having only a presence/absence detection mechanism. Nevertheless, the improved stability of the device is crucial for implementation in field applications.

As general remark, a better understanding of the electron transfer between photosynthetic microorganisms can be of great help in designing effective mediatorless photo-bioelectrochemical sensors. Moreover, screening between different microorganisms is necessary in order to find the best candidate to be used as bioreceptor. Genetic engineering of the microorganisms could also bring substantial improvements for this device, by increasing the electron transfer rates, improve the sensitivity and the selectivity of microbial receptors. The electrode materials can also be optimized, for example using conductive hydrogels or functionalized surfaces to improve the electron exchange and the biofilm stability over time.

7.3 Relevance of the work and future challenges

In the recent years, microbial electrochemical sensors have been increasingly studied as means to detect of several different compounds. Nevertheless, the commercialization of this kind of biosensors is still not viable due to their current disadvantages compared to other kinds of sensors, like slow response, low sensitivity, and poor selectivity [21]. The results discussed in this dissertation represent a relevant step forward within this field, which can be summarized as the following achievements:

- Different innovative prototypes of low-cost and low-tech environmental biosensors have been successfully tested
- The impact of environmental factors on the current output and on the electrodic biofilms has been studied with a multiparametric approach in real field trials
- For the first time the photocurrent produced by whole cyanobacterial cells was employed for herbicide monitoring
- The possibility of amperometric detection using whole cyanobacterial cells as receptors in absence of artificial mediators has been demonstrated

These aspects provide new insights and strategies aimed at applying microbial electrochemical sensors as environmental sensors.

However, some important challenges still need to be addressed to actually implement microbial electrochemical sensors for field applications. The most urgent aspects that need to be tackled are the detection capabilities and the reliability of the devices. Indeed, improvements in sensitivity and selectivity may result in biosensors that outperform the commercial sensors for specific chemicals. This development could be obtained by either by genetic engineering of the microbial receptors, up-regulating or down-regulating with specific metabolic pathways, or building sensor arrays that provide a "fingerprint" (i.e. unique) response pattern for the selected contaminants [102]. Optimization of the operational stability and shelf-life is also key challenge for the commercialization of this kind of devices. For this reason, immobilization techniques must be improved, ensuring mechanical stability while preserving cell viability and functions.

To further advance microbial electrochemical devices, miniaturization could be of great interest as it can decrease the start-up times, enable their integration into existing facilities and reduce the chemicals and materials needed. Nanostructured materials and nanotechnologies can play a crucial role to this end, for example integrating microbes in microfluidic chips, going towards a Lab-on-Chip approach [102]. Another important feature that can be implemented is the integration of an on-line data transmission system, which would allow to create a diffuse environmental monitoring network able to collect data even in remote areas.

To conclude, both the technological and the scientific aspect require further studies in order explore the full potential of these devices, so that they can play an important role in environmental protection and health safety in the near future.

8 ACKNOWLEDGEMENTS

This achievement would not have been possible without the help and the encouragement of many people, that I would like to acknowledge here.

First of all, I would like to thank my supervisors Andrea Schievano and Pierangela Cristiani for the time that they dedicated to me during these three years, the guidance and the support. I thank you for the passion that you both demonstrate for research, which encouraged me to pursue my goals.

I would like to thank Shelley Minteer and Silvia Vignolini, who welcomed me in their respective labs in Salt Lake City and in Cambridge, for giving me the opportunity to have wonderful experiences abroad, and work in their amazing research groups. I received so much from these experiences both professionally and on a personal level.

A special thank goes to Matteo Grattieri and Paolo Bombelli for teaching me with patience and clearness and for inspiring me with their enthusiasm. Thank you for showing me how to address problems with a positive approach, to persevere in trying new strategies and never giving up. Thank you also for being such good guides during my experiences abroad, and showing me around the respective countries.

To my colleagues and friends Alessandra Colombo, Stefania Marzorati and Andrea Goglio I say thanks for being there in case of need, for the coffee (or better tea) times, and all the good moments inside and outside of the University that we spent together. It has been really nice to work with you guys!

I also thank all the people that gave me some of their time during this years, even if only for a moment, a good advice, a scientific explanation or showing me the way when I was lost: Kamrul Hasan, Sophiene Abedoullai, Bassam Alkotaini, David Hickey, Rong Cai, Kasha Lim, Mengwei Yuan, Alyssa Smith, Laura Caton, Clement Chan, Laura Rago, Rita Nasti and all the others that for sake of brevity I am not mentioning here.

Finally, I would like to thank mom and dad for their endless support.

BIBLIOGRAPHY

[1] P.K. Goel, Water Pollution: Causes, Effects and Control, New Age International, 2006. https://books.google.co.uk/books?id=4R9CYYoiFCcC.

[2] D.B. Walker, D.J. Baumgartner, C.P. Gerba, K. Fitzsimmons, Chapter 16 - Surface Water Pollution, in: M.L. Brusseau, I.L. Pepper, C.P. Gerba (Eds.), Environ. Pollut. Sci. (Third Ed., Third Edit, Academic Press, 2019: pp. 261–292. doi:https://doi.org/10.1016/B978-0-12-814719-1.00016-1.

[3] UNESCO, A. Azoulay, The United Nations World Water Development Report 2019: Leaving No One Behind, UNESCO, 2019.

[4] UN-WATER, Wastewater - The Untapped Resources, 2017. doi:10.1017/CBO9781107415324.004.

[5] FAO, Water pollution from agriculture: a global review, Food Agric. Organ. United Nations. (2017). http://www.fao.org/3/a-i7754e.pdf.

[6] M.T. Giardi, M. Koblízek, J. Masojídek, Photosystem II-based biosensors for the detection of pollutants., Biosens. Bioelectron. 16 (2001) 1027–33. doi:10.1016/S0956-5663(01)00197-X.

[7] United Nations, Transforming our world: the 2030 Agenda for Sustainable Development, United Nations Dep. Econ. Soc. Aff. (2015). doi:10.1080/02513625.2015.1038080.

[8] J.F. Artiola, M.L. Brusseau, Chapter 10 - The Role of Environmental Monitoring in Pollution Science, in: M.L. Brusseau, I.L. Pepper, C.P. Gerba (Eds.), Environ. Pollut. Sci. (Third Ed., Third Edit, Academic Press, 2019: pp. 149–162. doi:https://doi.org/10.1016/B978-0-12-814719-1.00010-0.

[9] Y.E. Chee, An ecological perspective on the valuation of ecosystem services, Biol. Conserv. 120 (2004) 549–565. doi:10.1016/j.biocon.2004.03.028.

[10] European Commission, Towards an EU Research and Innovation policy agenda for Nature-Based Solutions & Re-Naturing Cities. Final Report of the Horizon 2020 Expert Group on

"Nature-Based Solutions and Re-Naturing Cities" (full version), 2015. doi:10.2777/765301.

[11] S. Reis, E. Seto, A. Northcross, N.W.T. Quinn, M. Convertino, R.L. Jones, H.R. Maier, U. Schlink, S. Steinle, M. Vieno, M.C. Wimberly, Integrating modelling and smart sensors for environmental and human health, Environ. Model. Softw. 74 (2015) 238–246. doi:10.1016/j.envsoft.2015.06.003.

[12] G.W. Hunter, J.R. Stetter, P.J. Hesketh, C.-C. Liu, Smart Sensor Systems, Electrochem. Soc. Interface. 19 (2010) 29–34. doi:0.1149/2.F03104if.

[13] E. Martinucci, F. Pizza, D. Perrino, A. Colombo, S.P. Trasatti, A. Lazzarini Barnabei, A. Liberale, P. Cristiani, Energy balance and microbial fuel cells experimentation at wastewater treatment plant Milano-Nosedo, Int. J. Hydrogen Energy. 40 (2015) 14683–14689. doi:10.1016/j.ijhydene.2015.08.100.

[14] A. Schievano, A. Colombo, M. Grattieri, S.P. Trasatti, A. Liberale, P. Tremolada, C. Pino, P. Cristiani, Floating microbial fuel cells as energy harvesters for signal transmission from natural water bodies, J. Power Sources. 340 (2017) 80–88. doi:10.1016/j.jpowsour.2016.11.037.

[15] H. Liu, B.E. Logan, Electricity Generation Using an Air-Cathode Single Chamber Microbial Fuel Cell in the Presence and Absence of a Proton Exchange Membrane, Environ. Sci. Technol. 38 (2004) 4040–4046. doi:10.1021/es0499344.

[16] Y. V. Nancharaiah, S. Venkata Mohan, P.N.L. Lens, Metals removal and recovery in bioelectrochemical systems: A review, Bioresour. Technol. 195 (2015) 102–114. doi:10.1016/j.biortech.2015.06.058.

[17] S. Roy, A. Schievano, D. Pant, Electro-stimulated Microbial Factory for value added product synthesis, Bioresour. Technol. 213 (2016) 129–139. doi:10.1016/j.biortech.2016.03.052.

[18] P.T. Kelly, Z. He, Nutrients removal and recovery in bioelectrochemical systems: A review, Bioresour. Technol. 153 (2014) 351–360. doi:10.1016/j.biortech.2013.12.046.

[19] A. Kadier, Y. Simayi, P. Abdeshahian, N.F. Azman, K. Chandrasekhar, M.S. Kalil, A comprehensive review of microbial electrolysis cells (MEC) reactor designs and

configurations for sustainable hydrogen gas production, Alexandria Eng. J. 55 (2014) 427–443. doi:10.1016/j.aej.2015.10.008.

[20] Y. Kim, B.E. Logan, Microbial desalination cells for energy production and desalination, Desalination. 308 (2013) 122–130. doi:10.1016/j.desal.2012.07.022.

[21] M. Grattieri, K. Hasan, S.D. Minteer, Bioelectrochemical Systems as a Multipurpose Biosensing Tool: Present Perspective and Future Outlook, ChemElectroChem. 4 (2017) 834–842. doi:10.1002/celc.201600507.

[22] Z. Lu, D. Chang, J. Ma, G. Huang, L. Cai, L. Zhang, Behavior of metal ions in bioelectrochemical systems: A review, J. Power Sources. 275 (2015) 243–260. doi:10.1016/j.jpowsour.2014.10.168.

[23] M.C. Potter, Electrical Effects Accompanying the Decomposition of Organic Compounds . II . Ionisation of the Gases Produced during Fermentation Author (s): M . C . Potter Source : Proceedings of the Royal Society of London . Series A , Containing Papers of a Publish, Proc. R. Soc. London. 84 (1911) 260–276.

[24] C. Santoro, C. Arbizzani, B. Erable, I. Ieropoulos, Microbial fuel cells: From fundamentals to applications. A review, J. Power Sources. 356 (2017) 225–244. doi:10.1016/j.jpowsour.2017.03.109.

[25] J.R. Trapero, L. Horcajada, J.J. Linares, J. Lobato, Is microbial fuel cell technology ready? An economic answer towards industrial commercialization, Appl. Energy. 185 (2017) 698–707. doi:10.1016/j.apenergy.2016.10.109.

[26] S. Venkata Mohan, G. Velvizhi, J. Annie Modestra, S. Srikanth, Microbial fuel cell: Critical factors regulating bio-catalyzed electrochemical process and recent advancements, Renew. Sustain. Energy Rev. 40 (2014) 779–797. doi:10.1016/j.rser.2014.07.109.

[27] R.M. Donlan, Biofilms: Microbial life on surfaces, Emerg. Infect. Dis. 8 (2002) 881–890. doi:10.3201/eid0809.020063.

[28] B.E. Logan, Microbial fuel cells, John Wiley & Sons, Inc., 2008.

[29] C.M. Baicea, V.I. Luntraru, D.I. Vaireanu, E. Vasile, R. Trusca, Composite membranes with poly(ether ether ketone) as support and polyaniline like structure, with potential applications in fuel cells, Cent. Eur. J. Chem. 11 (2013) 438–445. doi:10.2478/s11532-012-0175-2.

[30] D. Pant, G. Van Bogaert, L. Diels, K. Vanbroekhoven, A review of the substrates used in microbial fuel cells (MFCs) for sustainable energy production, Bioresour. Technol. 101 (2010) 1533–1543. doi:https://doi.org/10.1016/j.biortech.2009.10.017.

[31] J.K. Nørskov, J. Rossmeisl, A. Logadottir, L. Lindqvist, J.R. Kitchin, T. Bligaard, H. Jónsson, Origin of the overpotential for oxygen reduction at a fuel-cell cathode, J. Phys. Chem. B. 108 (2004) 17886–17892. doi:10.1021/jp047349j.

[32] B. Erable, D. Féron, A. Bergel, Microbial catalysis of the oxygen reduction reaction for microbial fuel cells: A review, ChemSusChem. 5 (2012) 975–987. doi:10.1002/cssc.201100836.

[33] L. Rago, P. Cristiani, F. Villa, S. Zecchin, A. Colombo, L. Cavalca, A. Schievano, Influences of dissolved oxygen concentration on biocathodic microbial communities in microbial fuel cells, Bioelectrochemistry. 116 (2017) 39–51. doi:10.1016/j.bioelechem.2017.04.001.

[34] M. Daghio, I. Gandolfi, G. Bestetti, A. Franzetti, E. Guerrini, P. Cristiani, Anodic and cathodic microbial communities in single chamber microbial fuel cells., N. Biotechnol. 32 (2015) 79–84. doi:10.1016/j.nbt.2014.09.005.

[35] P. Cristiani, M.L. Carvalho, E. Guerrini, M. Daghio, C. Santoro, B. Li, Cathodic and anodic biofilms in Single Chamber Microbial Fuel Cells, Bioelectrochemistry. 92 (2013) 6–13. doi:10.1016/j.bioelechem.2013.01.005.

[36] E. Guerrini, M. Grattieri, S.P. Trasatti, M. Bestetti, P. Cristiani, Performance explorations of single chamber microbial fuel cells by using various microelectrodes applied to biocathodes, Int. J. Hydrogen Energy. 39 (2014) 21837–21846. doi:10.1016/j.ijhydene.2014.06.132.

[37] C. Santoro, A. Agrios, U. Pasaogullari, B. Li, Effects of gas diffusion layer (GDL) and micro porous layer (MPL) on cathode performance in microbial fuel cells (MFCs), Int. J. Hydrogen

Energy. 36 (2011) 13096–13104. doi:10.1016/j.ijhydene.2011.07.030.

[38] J. Xu, G.-P. Sheng, H.-W. Luo, W.-W. Li, L.-F. Wang, H.-Q. Yu, Fouling of proton exchange membrane (PEM) deteriorates the performance of microbial fuel cell, Water Res. 46 (2012) 1817–1824. doi:10.1016/j.watres.2011.12.060.

[39] E. Guerrini, M. Grattieri, A. Faggianelli, P. Cristiani, S.P. Trasatti, PTFE effect on the electrocatalysis of the oxygen reduction reaction in membraneless microbial fuel cells, Bioelectrochemistry. 106 (2015) 240–247. doi:10.1016/j.bioelechem.2015.05.008.

[40] U. Schröder, Anodic electron transfer mechanisms in microbial fuel cells and their energy efficiency, Phys. Chem. Chem. Phys. 9 (2007) 2619. doi:10.1039/b703627m.

[41] L. Shi, D.J. Richardson, Z. Wang, S.N. Kerisit, K.M. Rosso, J.M. Zachara, J.K. Fredrickson, The roles of outer membrane cytochromes of Shewanella and Geobacter in extracellular electron transfer, Environ. Microbiol. Rep. 1 (2009) 220–227. doi:10.1111/j.1758-2229.2009.00035.x.

[42] D.R. Lovley, Bug juice: harvesting electricity with microorganisms, Nat. Rev. Microbiol. 4 (2006) 497–508. doi:10.1038/nrmicro1442.

[43] D.R. Lovley, Electrically conductive pili: Biological function and potential applications in electronics, Curr. Opin. Electrochem. 4 (2017) 190–198. doi:10.1016/j.coelec.2017.08.015.

[44] N.S. Malvankar, D.R. Lovley, Microbial nanowires for bioenergy applications, Curr. Opin. Biotechnol. 27 (2014) 88–95. doi:10.1016/j.copbio.2013.12.003.

[45] G.M. Delaney, H.P. Bennetto, J.R. Mason, S.D. Roller, J.L. Stirling, C.F. Thurston, Electron-transfer coupling in microbial fuel cells. 2. performance of fuel cells containing selected microorganism—mediator—substrate combinations, J. Chem. Technol. Biotechnol. Biotechnol. 34 (1984) 13–27. doi:10.1002/jctb.280340104.

[46] K. Guo, A. Prévoteau, S.A. Patil, K. Rabaey, Engineering electrodes for microbial electrocatalysis, Curr. Opin. Biotechnol. 33 (2015) 149–156. doi:10.1016/j.copbio.2015.02.014.

[47] S. Kalathil, S.A. Patil, D. Pant, Microbial Fuel Cells: Electrode Materials, Elsevier Inc., 2018. doi:10.1016/b978-0-12-409547-2.13459-6.

[48] C. Santoro, K. Artyushkova, S. Babanova, P. Atanassov, I. Ieropoulos, M. Grattieri, P. Cristiani, S. Trasatti, B. Li, A.J. Schuler, Parameters characterization and optimization of activated carbon (AC) cathodes for microbial fuel cell application, Bioresour. Technol. 163 (2014) 54–63. doi:10.1016/j.biortech.2014.03.091.

[49] J.K. Jang, J. Kan, O. Bretschger, Y.A. Gorby, L. Hsu, B.H. Kim, K.H. Nealson, Electricity generation by microbial fuel cell using microorganisms as catalyst in cathode, J. Microbiol. Biotechnol. 23 (2013) 1765–1773. doi:10.4014/jmb.1310.10117.

[50] M. Kim, M. Sik Hyun, G.M. Gadd, H. Joo Kim, A novel biomonitoring system using microbial fuel cells, J. Environ. Monit. 9 (2007) 1323–1328. doi:10.1039/B713114C.

[51] M. Di Lorenzo, T.P. Curtis, I.M. Head, K. Scott, A single-chamber microbial fuel cell as a biosensor for wastewaters, Water Res. 43 (2009) 3145–3154. doi:10.1016/j.watres.2009.01.005.

[52] I.S. Chang, H. Moon, J.K. Jang, B.H. Kim, Improvement of a microbial fuel cell performance as a BOD sensor using respiratory inhibitors, 2005. doi:10.1016/j.bios.2004.06.003.

[53] B.H. Kim, I.S. Chang, G.C. Gil, H.S. Park, H.J. Kim, Novel BOD (biological oxygen demand) sensor using mediator-less microbial fuel cell, Biotechnol. Lett. 25 (2003) 541–545. doi:10.1023/A:1022891231369.

[54] A. Kumlanghan, J. Liu, P. Thavarungkul, P. Kanatharana, B. Mattiasson, Microbial fuel cell-based biosensor for fast analysis of biodegradable organic matter, Biosens. Bioelectron. 22 (2007) 2939–2944. doi:10.1016/j.bios.2006.12.014.

[55] M. Di Lorenzo, A.R. Thomson, K. Schneider, P.J. Cameron, I. Ieropoulos, A small-scale air-cathode microbial fuel cell for on-line monitoring of water quality, Biosens. Bioelectron. 62 (2014) 182–188. doi:10.1016/j.bios.2014.06.050.

[56] A. Franzetti, M. Daghio, P. Parenti, T. Truppi, G. Bestetti, S.P. Trasatti, P. Cristiani, Monod Kinetics Degradation of Low Concentration Residual Organics in Membraneless Microbial

Fuel Cells, J. Electrochem. Soc. 164 (2017) H3091–H3096. doi:10.1149/2.0141703jes.

[57] G. Pasternak, J. Greenman, I. Ieropoulos, Self-powered, autonomous Biological Oxygen Demand biosensor for online water quality monitoring, Sensors Actuators B Chem. 244 (2017) 815–822. doi:10.1016/j.snb.2017.01.019.

[58] Y. Zhang, I. Angelidaki, A simple and rapid method for monitoring dissolved oxygen in water with a submersible microbial fuel cell (SBMFC), Biosens. Bioelectron. 38 (2012) 189–194. doi:10.1016/j.bios.2012.05.032.

[59] X. Jin, I. Angelidaki, Y. Zhang, Microbial Electrochemical Monitoring of Volatile Fatty Acids during Anaerobic Digestion, Environ. Sci. Technol. 50 (2016) 4422–4429. doi:10.1021/acs.est.5b05267.

[60] A. Colombo, A. Schievano, S.P. Trasatti, R. Morrone, N. D'Antona, P. Cristiani, Signal trends of microbial fuel cells fed with different food-industry residues, Int. J. Hydrogen Energy. (2016). doi:10.1016/j.ijhydene.2016.09.069.

[61] N.E. Stein, H.V.M. Hamelers, G. van Straten, K.J. Keesman, Effect of toxic components on microbial fuel cell-polarization curves and estimation of the type of toxic inhibition, Biosensors. 2 (2012) 255–268. doi:10.3390/bios2030255.

[62] Y. Shen, M. Wang, I.S. Chang, H.Y. Ng, Effect of shear rate on the response of microbial fuel cell toxicity sensor to Cu(II), Bioresour. Technol. 136 (2013) 707–710. doi:10.1016/j.biortech.2013.02.069.

[63] J. Chouler, M. Di Lorenzo, Pesticides detection by a miniature microbial fuel cell under controlled operational disturbances, Water Sci. Technol. (2019) 1–11. doi:10.2166/wst.2019.207.

[64] M. Di Lorenzo, A.R. Thomson, K. Schneider, P.J. Cameron, I. Ieropoulos, A small-scale air-cathode microbial fuel cell for on-line monitoring of water quality, Biosens. Bioelectron. 62 (2014) 182–188. doi:10.1016/j.bios.2014.06.050.

[65] Y. Jiang, X. Yang, P. Liang, P. Liu, X. Huang, Microbial fuel cell sensors for water quality early warning systems: Fundamentals, signal resolution, optimization and future challenges,

Renew. Sustain. Energy Rev. 81 (2018) 292–305. doi:10.1016/j.rser.2017.06.099.

[66] G.S. Jadhav, M.M. Ghangrekar, Performance of microbial fuel cell subjected to variation in pH, temperature, external load and substrate concentration, Bioresour. Technol. 100 (2009) 717–723. doi:10.1016/j.biortech.2008.07.041.

[67] A. Larrosa-Guerrero, K. Scott, I.M. Head, F. Mateo, A. Ginesta, C. Godinez, Effect of temperature on the performance of microbial fuel cells, Fuel. 89 (2010) 3985–3994. doi:10.1016/j.fuel.2010.06.025.

[68] D.B. Curwin, J.M. Hein, B.D. Barr, C. Striley, Comparison of immunoassay and HPLC-MS/MS used to measure urinary metabolites of atrazine, metolachlor, and chlorpyrfos from farmers and non-farmers in Iowa, J. Expo. Sci. Environ. Epidemiol. 20 (2010) 2015–212. doi:1559-0631/10.

[69] K. Hiraoka, Microbe – surface interactions in biofouling and biocorrosion, (2005).

[70] T.E. Cloete, V.S. Brözel, A. Von Holy, Practical aspects of biofouling control in industrial water systems, Int. Biodeterior. Biodegrad. 29 (1992) 299–341. doi:10.1016/0964-8305(92)90050-X.

[71] A. Mollica, P. Cristiani, On-line biofilm monitoring by “BIOX” electrochemical probe, Water Sci. Technol. 47 (2003) 45–49.

[72] P. Cristiani, A. Franzetti, G. Bestetti, Monitoring of electro-active biofilm in soil, Electrochim. Acta. 54 (2008) 41–46. doi:10.1016/j.electacta.2008.01.107.

[73] F.F. Ajayi, P.R. Weigele, A terracotta bio-battery, Bioresour. Technol. 116 (2012) 86–91. doi:10.1016/j.biortech.2012.04.019.

[74] S. Rodriguez-Mozaz, M.J. Lopez De Alda, D. Barceló, Biosensors as useful tools for environmental analysis and monitoring, Anal. Bioanal. Chem. 386 (2006) 1025–1041. doi:10.1007/s00216-006-0574-3.

[75] Y. Jiang, X. Yang, P. Liang, P. Liu, X. Huang, Microbial fuel cell sensors for water quality early warning systems: Fundamentals, signal resolution, optimization and future challenges,

Renew. Sustain. Energy Rev. 81 (2018) 292–305. doi:10.1016/j.rser.2017.06.099.

[76] X.C. Abrevaya, N.J. Sacco, M.C. Bonetto, A. Hilding-Ohlsson, E. Cortón, Analytical applications of microbial fuel cells. Part II: Toxicity, microbial activity and quantification, single analyte detection and other uses, Biosens. Bioelectron. 63 (2015) 591–601. doi:10.1016/j.bios.2014.04.053.

[77] J. Winfield, I. Gajda, J. Greenman, I. Ieropoulos, A review into the use of ceramics in microbial fuel cells, Bioresour. Technol. 215 (2016) 296–303. doi:10.1016/j.biortech.2016.03.135.

[78] J. Winfield, L.D. Chambers, J. Rossiter, J. Greenman, I. Ieropoulos, Urine-activated origami microbial fuel cells to signal proof of life, J. Mater. Chem. A. 3 (2015) 7058–7065. doi:10.1039/C5TA00687B.

[79] J. Winfield, L.D. Chambers, J. Rossiter, J. Greenman, I. Ieropoulos, Towards disposable microbial fuel cells: Natural rubber glove membranes, Int. J. Hydrogen Energy. 39 (2014) 21803–21810. doi:10.1016/j.ijhydene.2014.09.071.

[80] S. Marzorati, A. Schievano, A. Colombo, G. Lucchini, P. Cristiani, Ligno-cellulosic materials as air-water separators in low-tech microbial fuel cells for nutrients recovery, J. Clean. Prod. (2017). doi:10.1016/j.jclepro.2017.09.142.

[81] S. Patil, F. Harnisch, U. Schröder, Toxicity response of electroactive microbial biofilms-a decisive feature for potential biosensor and power source applications, ChemPhysChem. 11 (2010) 2834–2837. doi:10.1002/cphc.201000218.

[82] Y. Jiang, P. Liang, P. Liu, Y. Bian, B. Miao, X. Sun, H. Zhang, X. Huang, Enhancing signal output and avoiding BOD/toxicity combined shock interference by operating a microbial fuel cell sensor with an optimized background concentration of organic matter, Int. J. Mol. Sci. 17 (2016) 1–8. doi:10.3390/ijms17091392.

[83] Y. Jiang, P. Liang, P. Liu, D. Wang, B. Miao, X. Huang, A novel microbial fuel cell sensor with biocathode sensing element, Biosens. Bioelectron. 94 (2017) 344–350. doi:10.1016/j.bios.2017.02.052.

[84] L.C. Clark, Monitor_and_Control_of_Blood_and_Tissue_Oxygen.7.pdf, Am. Soc. Artif. Intern. Organs. 2 (1956) 41–48.

[85] S.J. Sadeghi, Amperometric Biosensors, in: G.C.K. Roberts (Ed.), Encycl. Biophys., Springer Berlin Heidelberg, Berlin, Heidelberg, 2013: pp. 61–67. doi:10.1007/978-3-642-16712-6_713.

[86] D. Thevenot, K. Toth, R. Durst, G. Wilson, D. Thevenot, K. Toth, R. Durst, G. Wilson, Electrochemical biosensors : recommended definitions and classification, Pure Appl. Chem. 71 (2014) 2333–2348.

[87] A.J. Bard, L.R. Faulkner, Electrochemical methods: fundamentals and applications, 2nd ed., Austin, 2001. doi:10.1038/nprot.2009.120.Multi-stage.

[88] C. de Blasio, Overview of the main mechanisms of photosynthesis, Green Energy Technol. (2019) 47–56. doi:10.1007/978-3-030-11599-9_4.

[89] A.J. McCormick, P. Bombelli, R.W. Bradley, R. Thorne, T. Wenzel, C.J. Howe, Biophotovoltaics: oxygenic photosynthetic organisms in the world of bioelectrochemical systems, Energy Environ. Sci. 8 (2015) 1092–1109. doi:10.1039/C4EE03875D.

[90] A. Cereda, A. Hitchcock, M.D. Symes, L. Cronin, T.S. Bibby, A.K. Jones, A bioelectrochemical approach to characterize extracellular electron transfer by synechocystis sp. PCC6803, PLoS One. 9 (2014). doi:10.1371/journal.pone.0091484.

[91] M. Grattieri, Z. Rhodes, D.P. Hickey, K. Beaver, S.D. Minteer, Understanding Biophotocurrent Generation in Photosynthetic Purple Bacteria, ACS Catal. 9 (2019) 867−873. doi:10.1021/acscatal.8b04464.

[92] K.P. Sokol, D. Mersch, V. Hartmann, J.Z. Zhang, M.M. Nowaczyk, M. Rögner, A. Ruff, W. Schuhmann, N. Plumeré, E. Reisner, Rational wiring of photosystem II to hierarchical indium tin oxide electrodes using redox polymers, Energy Environ. Sci. 9 (2016) 3698–3709. doi:10.1039/c6ee01363e.

[93] USEPA, Pesticides Industry Sales and Usage 2008 - 2012 Market Estimates, U.S. Environ. Prot. Agency. (2017).

[94] Y. Combarnous, Endocrine Disruptor Compounds (EDCs) and agriculture: The case of pesticides, Comptes Rendus - Biol. 340 (2017) 406–409. doi:10.1016/j.crvi.2017.07.009.

[95] P.K. Gupta, Herbicides and fungicides, Biomarkers Toxicol. (2011) 409–431. doi:10.1016/B978-0-12-404630-6.00024-5.

[96] R.H. Marrs, A.J. Frost, A microcosm approach to the detection of the effects of herbicide spray drift in plant communities, J. Environ. Manage. 50 (1997) 369–388. doi:10.1006/jema.1996.9984.

[97] L. Wackett, M. Sadowsky, B. Martinez, N. Shapir, Biodegradation of atrazine and related s-triazine compounds: From enzymes to field studies, Appl. Microbiol. Biotechnol. 58 (2002) 39–45. doi:10.1007/s00253-001-0862-y.

[98] I. Heap, The International Survey of Herbicide Resistant Weeds, (n.d.). http://www.weedscience.org/summary/SOADescription.aspx (accessed September 3, 2019).

[99] M. Tucci, Electrochemical micro biosensor for glucose analysis, (2016).

[100] A Review of Techniques for Electrochemical Analysis, Princet. Appl. Res. (n.d.) 1–15. www.princetonappliedresearch.com.

[101] A. Hulanicki, S. Glab, F. Ingman, Chemical sensors: definitions and classification, Pure Appl. Chem. 63 (1991) 1247–1250. doi:10.1351/pac199163091247.

[102] L. Su, W. Jia, C. Hou, Y. Lei, Microbial biosensors: A review, Biosens. Bioelectron. 26 (2011) 1788–1799. doi:10.1016/j.bios.2010.09.005.

[103] F.-G. Bănică, CHEMICAL SENSORS AND BIOSENSORS: Fundamentals and Applications, Jhon Wiley and Sons, 2012.

[104] E. Desimoni, B. Brunetti, About Estimating the Limit of Detection by the Signal to Noise Approach, Pharm. Anal. Acta. 6 (2015). doi:10.4172/2153-2435.1000355.

[105] W.J. Peveler, M. Yazdani, V.M. Rotello, Selectivity and Specificity: Pros and Cons in Sensing, ACS Sensors. 1 (2016) 1282–1285. doi:10.1021/acssensors.6b00564.

[106] A. Menditto, M. Patriarca, B. Magnusson, Understanding the meaning of accuracy, trueness and precision, Accredit. Qual. Assur. 12 (2007) 45–47. doi:10.1007/s00769-006-0191-z.

[107] M. Tucci, A. Goglio, A. Schievano, P. Cristiani, Floating mfc for BOD monitoring in real time: field test in a wastewater treatment plant, Proc. 7th Eur. Fuel Cell Piero Lunghi Conf. (2017).

[108] M. Grattieri, S.D. Minteer, K. Hasan, Bio-Electrochemical Systems as A Multipurpose Biosensing Tool: Present Perspective and Future Outlook, ChemElectroChem. (2013). doi:10.1016/j.future.2015.08.005.

[109] J.K. Jang, T.H. Pham, I.S. Chang, K.H. Kang, H. Moon, K.S. Cho, B.H. Kim, Construction and operation of a novel mediator- and membrane-less microbial fuel cell, Process Biochem. 39 (2004) 1007–1012. doi:10.1016/S0032-9592(03)00203-6.

[110] M. Daghio, V. Tatangelo, A. Franzetti, I. Gandolfi, M. Papacchini, A. Careghini, E. Sezenna, S. Saponaro, G. Bestetti, Hydrocarbon degrading microbial communities in bench scale aerobic biobarriers for gasoline contaminated groundwater treatment, Chemosphere. 130 (2015) 34–39. doi:10.1016/j.chemosphere.2015.02.022.

[111] R.C. Edgar, UPARSE: highly accurate OTU sequences from microbial amplicon reads, Nat. Methods. 10 (2013) 996. https://doi.org/10.1038/nmeth.2604.

[112] Q. Wang, G.M. Garrity, J.M. Tiedje, J.R. Cole, Naïve Bayesian classifier for rapid assignment of rRNA sequences into the new bacterial taxonomy, Appl. Environ. Microbiol. 73 (2007) 5261–5267. doi:10.1128/AEM.00062-07.

[113] N.C. Kenkel, L. Orloci, Applying Metric and Nonmetric Multidimensional Scaling to Ecological Studies: Some New Results, Ecology. 67 (1986) 919–928. doi:10.2307/1939814.

[114] G. Zhang, Q. Zhao, Y. Jiao, K. Wang, D.J. Lee, N. Ren, Biocathode microbial fuel cell for efficient electricity recovery from dairy manure, Biosens. Bioelectron. 31 (2012) 537–543. doi:10.1016/j.bios.2011.11.036.

[115] P. Cristiani, A. Franzetti, I. Gandolfi, E. Guerrini, G. Bestetti, Bacterial DGGE fi ngerprints of biofilms on electrodes of membraneless microbial fuel cells, Int. Biodeterior. Biodegradation. 84 (2013) 211–219. doi:10.1016/j.ibiod.2012.05.040.

[116] J.P. Magnin, J. Deseure, Hydrogen generation in a pressurized photobioreactor: Unexpected enhancement of biohydrogen production by the phototrophic bacterium Rhodobacter capsulatus, Appl. Energy. 239 (2019) 635–643. doi:10.1016/j.apenergy.2019.01.204.

[117] X. Zheng, H. Ma, H. Yang, The effect of cycA overexpression on hydrogen production performance of Rhodobacter sphaeroides HY01, Int. J. Hydrogen Energy. 43 (2018) 13842–13851. doi:10.1016/j.ijhydene.2018.02.017.

[118] C. Koch, F. Harnisch, Is there a Specific Ecological Niche for Electroactive Microorganisms ?, (2016) 1282–1295. doi:10.1002/celc.201600079.

[119] B.R. Dhar, J.H. Park, H.D. Park, H.S. Lee, Hydrogen-based syntrophy in an electrically conductive biofilm anode, Chem. Eng. J. 359 (2019) 208–216. doi:10.1016/j.cej.2018.11.138.

[120] M. Zeppilli, M. Villano, F. Aulenta, S. Lampis, G. Vallini, M. Majone, Effect of the anode feeding composition on the performance of a continuous-flow methane-producing microbial electrolysis cell, Environ. Sci. Pollut. Res. 22 (2015) 7349–7360. doi:10.1007/s11356-014-3158-3.

[121] Y. Song, L. Xiao, I. Jayamani, Z. He, A.M. Cupples, A novel method to characterize bacterial communities affected by carbon source and electricity generation in microbial fuel cells using stable isotope probing and Illumina sequencing, J. Microbiol. Methods. 108 (2015) 4–11. doi:10.1016/j.mimet.2014.10.010.

[122] P. Cristiani, A. Franzetti, I. Gandolfi, E. Guerrini, G. Bestetti, Bacterial DGGE fingerprints of biofilms on electrodes of membraneless microbial fuel cells, Int. Biodeterior. Biodegrad. 84 (2013). doi:10.1016/j.ibiod.2012.05.040.

[123] M. Tucci, M. Grattieri, A. Schievano, P. Cristiani, S.D. Minteer, Microbial amperometric biosensor for online herbicide detection : Photocurrent inhibition of Anabaena variabilis, Electrochim. Acta. 302 (2019) 102–108. doi:10.1016/j.electacta.2019.02.007.

[124] C. Tortolini, P. Bollella, R. Antiochia, G. Favero, F. Mazzei, Inhibition-based biosensor for atrazine detection, Sensors Actuators, B Chem. 224 (2015) 552–558. doi:10.1016/j.snb.2015.10.095.

[125] J. Masojídek, S. Pavel, M. Jana, F. Jan, K. Karel, M. Jan, Detection of photosynthetic herbicides : Algal growth inhibition test vs . electrochemical photosystem II biosensor Jiˇ, Ecotoxicol. Environ. Saf. 74 (2011) 117–122. doi:10.1016/j.ecoenv.2010.08.028.

[126] X. Liu, W.J. Li, L. Li, Y. Yang, L.G. Mao, Z. Peng, A label-free electrochemical immunosensor based on gold nanoparticles for direct detection of atrazine, Sensors Actuators, B Chem. 191 (2014) 408–414. doi:10.1016/j.snb.2013.10.033.

[127] S. Sagarkar, S. Mukherjee, A. Nousiainen, K. Björklöf, H.J. Purohit, K.S. Jorgensen, A. Kapley, Monitoring bioremediation of atrazine in soil microcosms using molecular tools, Environ. Pollut. 172 (2013) 108–115. doi:10.1016/j.envpol.2012.07.048.

[128] R.M. Zaya, Z. Amini, A.S. Whitaker, S.L. Kohler, C.F. Ide, Atrazine exposure affects growth, body condition and liver health in Xenopus laevis tadpoles, Aquat. Toxicol. 104 (2011) 243–253. doi:10.1016/j.aquatox.2011.04.021.

[129] G. MendaŠ, M. Vuletić, N. Galić, V. Drevenkar, Urinary metabolites as biomarkers of human exposure to atrazine: Atrazine mercapturate in agricultural workers, Toxicol. Lett. 210 (2012) 174–181. doi:10.1016/j.toxlet.2011.11.023.

[130] E.U. Health & Consumer Protection Directorate General, Review report for the active substance atrazine- SANCO/10496/2003-final, 2003.

[131] D.J.K. Swainsbury, V.M. Friebe, R.N. Frese, M.R. Jones, Evaluation of a biohybrid photoelectrochemical cell employing the purple bacterial reaction centre as a biosensor for herbicides, Biosens. Bioelectron. 58 (2014) 172–178. doi:10.1016/j.bios.2014.02.050.

[132] - US Environmental Protection Agency, National survey of pesticides in drinking water wells. Phase II report, Springfield, 1992.

[133] R.D. Wauchope, T.M. Buttler, A.G. Hornsby, P.W.M. Augustijn-Beckers, J.P. Burt, The SCS/ARS/CES Pesticide Properties Database for Environmental Decision-Making, in: G.W. Ware (Ed.), Rev. Environ. Contam. Toxicol. Contin. Residue Rev., Springer New York, New York, NY, 1992: pp. 1–155. doi:10.1007/978-1-4612-2862-2_1.

[134] M. da Silva Simões, L. Bracht, A.V. Parizotto, J.F. Comar, R.M. Peralta, A. Bracht, The

metabolic effects of diuron in the rat liver, Environ. Toxicol. Pharmacol. 54 (2017) 53–61. doi:10.1016/j.etap.2017.06.024.

[135] J. da S. Coelho-Moreira, T. Brugnari, A.B. Sá-Nakanishi, R. Castoldi, C.G.M. de Souza, A. Bracht, R.M. Peralta, Evaluation of diuron tolerance and biotransformation by the white-rot fungus Ganoderma lucidum, Fungal Biol. 122 (2018) 471–478. doi:10.1016/j.funbio.2017.10.008.

[136] E. Farkas, A. Szekacs, B. Kovacs, M. Olah, R. Horvath, I. Szekacs, Label-free optical biosensor for real-time monitoring the cytotoxicity of xenobiotics : A proof of principle study on glyphosate, J. Hazard. Mater. 351 (2018) 80–89. doi:10.1016/j.jhazmat.2018.02.045.

[137] D.G. Varsamis, E. Touloupakis, P. Morlacchi, D.F. Ghanotakis, M.T. Giardi, D.C. Cullen, Development of a photosystem II-based optical microfluidic sensor for herbicide detection, Talanta. 77 (2008) 42–47. doi:10.1016/j.talanta.2008.05.060.

[138] I. Husu, G. Rodio, E. Touloupakis, M.D. Lambreva, K. Buonasera, S.C. Litescu, M.T. Giardi, G. Rea, Insights into photo-electrochemical sensing of herbicides driven by Chlamydomonas reinhardtii cells, Sensors Actuators, B Chem. 185 (2013) 321–330. doi:10.1016/j.snb.2013.05.013.

[139] S. Wilski, U. Johanningmeier, S. Hertel, W. Oettmeier, Herbicide binding in various mutants of the photosystem II D1 protein of Chlamydomonas reinhardtii, Pestic. Biochem. Physiol. 84 (2006) 157–164. doi:10.1016/j.pestbp.2005.07.001.

[140] A. Halmschlager, J. Tandori, M. Trotta, L. Rinyu, I. Pfeiffer, A mathematical model for quinone-herbicide competition in the reaction centres of Rhodobacter sphaeroides, Funct. Plant Biol. 29 (2002) 1–7.

[141] E. Touloupakis, L. Giannoudi, S.A. Piletsky, L. Guzzella, F. Pozzoni, M.T. Giardi, A multi-biosensor based on immobilized Photosystem II on screen-printed electrodes for the detection of herbicides in river water, Biosens. Bioelectron. 20 (2005) 1984–1992. doi:10.1016/j.bios.2004.08.035.

[142] M. Rasmussen, A. Wingersky, S.D. Minteer, Comparative study of thylakoids from higher

plants for solar energy conversion and herbicide detection, Electrochim. Acta. 140 (2014) 304–308. doi:10.1016/j.electacta.2014.02.121.

[143] M. Chatzipetrou, F. Milano, L. Giotta, D. Chirizzi, M. Trotta, M. Massaouti, M.R. Guascito, I. Zergioti, Functionalization of gold screen printed electrodes with bacterial photosynthetic reaction centers by laser printing technology for mediatorless herbicide biosensing, Electrochem. Commun. 64 (2016) 46–50. doi:10.1016/j.elecom.2016.01.008.

[144] L. Croisetière, R. Rouillon, R. Carpentier, A simple mediatorless amperometric method using the cyanobacterium Synechococcus leopoliensis for the detection of phytotoxic pollutants, Appl. Microbiol. Biotechnol. 56 (2001) 261–264. doi:10.1007/s002530100652.

[145] R.E. Ionescu, K. Abu-Rabeah, S. Cosnier, C. Durrieu, J.M. Chovelon, R.S. Marks, Amperometric algal Chlorella vulgaris cell biosensors based on alginate and polypyrrole-alginate gels, Electroanalysis. 18 (2006) 1041–1046. doi:10.1002/elan.200603506.

[146] I. Shitanda, K. Takada, Y. Sakai, T. Tatsuma, Compact amperometric algal biosensors for the evaluation of water toxicity, Anal. Chim. Acta. 530 (2005) 191–197. doi:10.1016/j.aca.2004.09.073.

[147] I. Shitanda, S. Takamatsu, K. Watanabe, M. Itagaki, Amperometric screen-printed algal biosensor with flow injection analysis system for detection of environmental toxic compounds, Electrochim. Acta. 54 (2009) 4933–4936. doi:10.1016/j.electacta.2009.04.005.

[148] A. Tsopela, A. Lale, E. Vanhove, O. Reynes, I. Séguy, P. Temple-boyer, Integrated electrochemical biosensor based on algal metabolism for water toxicity analysis, Biosens. Bioelectron. 61 (2014) 290–297. doi:10.1016/j.bios.2014.05.004.

[149] L. Campanella, F. Cubadda, M.P. Sammartino, A. Saoncella, An algal biosensor for the monitoring of water toxicity in estuarine environments, Water Res. 35 (2001) 69–76. doi:10.1016/S0043-1354(00)00223-2.

[150] G. Simó, E. Fernández-Fernández, J. Vila-Crespo, V. Ruipérez, J.M. Rodríguez-Nogales, Research progress in coating techniques of alginate gel polymer for cell encapsulation, Carbohydr. Polym. 170 (2017) 1–14. doi:https://doi.org/10.1016/j.carbpol.2017.04.013.

[151] W.R. Gombotz, S.F. Wee, Protein release from alginate matrices, Adv. Drug Deliv. Rev. 64 (2012) 194–205. doi:10.1016/j.addr.2012.09.007.

[152] B. Alkotaini, S.L. Tinucci, S.J. Robertson, K. Hasan, S.D. Minteer, M. Grattieri, Alginate-Encapsulated Bacteria for the Treatment of Hypersaline Solutions in Microbial Fuel Cells, ChemBioChem. (2018) 1162–1169. doi:10.1002/cbic.201800142.

[153] J.L. Bolton, M.A. Trush, T.M. Penning, G. Dryhurst, T.J. Monks, Role of quinones in toxicology, Chem. Res. Toxicol. 13 (2000) 135–160. doi:10.1021/tx9902082.

[154] H.Y. Tran, M. Wohlfahrt-mehrens, S. Dsoke, In fl uence of the binder nature on the performance and cycle life of activated carbon electrodes in electrolytes containing Li-salt, J. Power Sources. 342 (2017) 301–312. doi:10.1016/j.jpowsour.2016.12.056.

[155] H. Nordberg, M. Cantor, S. Dusheyko, S. Hua, A. Poliakov, I. Shabalov, T. Smirnova, I.V. Grigoriev, I. Dubchak, The genome portal of the Department of Energy Joint Genome Institute, (2014). https://genome.jgi.doe.gov/portal/anava/anava.home.html (accessed October 16, 2018).

[156] K. Tanaka, N. Kashiwagi, T. Ogawa, Effects of light on the electrical output of bioelectrochemical fuel-cells containing Anabaena variabilis M-2: Mechanism of the post-illumination burst, J. Chem. Technol. Biotechnol. 42 (1988) 235–240. doi:10.1002/jctb.280420307.

[157] N. Sekar, Y. Umasankar, R.P. Ramasamy, Photocurrent generation by immobilized cyanobacteria via direct electron transport in photo-bioelectrochemical cells, Phys. Chem. Chem. Phys. 16 (2014) 7862. doi:10.1039/c4cp00494a.

[158] T. Yagishita, S. Sawayama, K.-I. Tsukahara, T. Ogi, Performance of photosynthetic electrochemical cells using immobilized Anabaena variabilis M-3 in discharge/culture cycles, J. Ferment. Bioeng. 85 (1998) 546–549. doi:https://doi.org/10.1016/S0922-338X(98)80106-2.

[159] K.L. Knoche, E. Aoyama, K. Hasan, S.D. Minteer, Role of Nitrogenase and Ferredoxin in the Mechanism of Bioelectrocatalytic Nitrogen Fixation by the Cyanobacteria Anabaena

variabilis SA-1 Mutant Immobilized on Indium Tin Oxide (ITO) Electrodes, Electrochim. Acta. 232 (2017) 396–403. doi:10.1016/j.electacta.2017.02.148.

[160] R.Y. Stanier, J. Deruelles, R. Rippka, M. Herdman, J.B. Waterbury, Generic Assignments, Strain Histories and Properties of Pure Cultures of Cyanobacteria, Microbiology. 111 (1979) 1–61. doi:10.1099/00221287-111-1-1.

[161] O. US EPA, OCSPP, Aquatic Life Benchmarks and Ecological Risk Assessments for Registered Pesticides, (2016). https://www.epa.gov/pesticide-science-and-assessing-pesticide-risks/aquatic-life-benchmarks-and-ecological-risk#ref_4 (accessed October 16, 2018).

[162] H.J. Kim, Y.K. Han, How can we describe the adsorption of quinones on activated carbon surfaces?, Curr. Appl. Phys. 16 (2016) 1437–1441. doi:10.1016/j.cap.2016.08.009.

[163] N. Liu, A.B. Charrua, C.H. Weng, X. Yuan, F. Ding, Characterization of biochars derived from agriculture wastes and their adsorptive removal of atrazine from aqueous solution: A comparative study, Bioresour. Technol. 198 (2015) 55–62. doi:10.1016/j.biortech.2015.08.129.

[164] X. Wei, Z. Wu, Z. Wu, B.C. Ye, Adsorption behaviors of atrazine and Cr(III) onto different activated carbons in single and co-solute systems, Powder Technol. 329 (2018) 207–216. doi:10.1016/j.powtec.2018.01.060.

[165] J. Lladó, C. Lao-Luque, B. Ruiz, E. Fuente, M. Solé-Sardans, A.D. Dorado, Role of activated carbon properties in atrazine and paracetamol adsorption equilibrium and kinetics, Process Saf. Environ. Prot. 95 (2015) 51–59. doi:10.1016/j.psep.2015.02.013.

[166] M. Tucci, P. Bombelli, C.J. Howe, S. Vignolini, S. Bocchi, A Storable Mediatorless Electrochemical Biosensor for Herbicide Detection, Microorganisms. 7 (2019) 1–14. doi:10.3390/microorganisms7120630.

[167] R.R. Teixeira, J.L. Pereira, W.L. Pereira, Photosynthesis inhibitors, in: M. Najafpou (Ed.), Appl. Photosynth., IntechOpen, London (UK), 2012: pp. 2–22.

[168] W. Draber, T. Fujita, Rational approaches to structure, activity, and ecotoxicology of agrochemicals., CRC Press, Boca Raton, Florida, USA, 1992.

[169] J.G. Metz, H.B. Pakrasi, M. Seibert, C.J. Arntzer, Evidence for a dual function of the herbicide-binding D1 protein in photosystem II, FEBS Lett. 205 (1986) 269–274. doi:10.1016/0014-5793(86)80911-5.

[170] T. Hayes, K. Haston, M. Tsui, A. Hoang, C. Haeffele, A. Vonk, Atrazine-induced hermaphroditism at 0.1 ppb in American leopard frogs (Rana pipiens): Laboratory and field evidence, Environ. Health Perspect. 111 (2003) 568–575. doi:10.1289/ehp.5932.

[171] J.-P. Lasserre, F. Fack, D. Revets, S. Planchon, J. Renaut, L. Hoffmann, A.C. Gutleb, C.P. Muller, T. Bohn, Effects of the Endocrine Disruptors Atrazine and PCB 153 on the Protein Expression of MCF-7 Human Cells, J. Proteome Res. 8 (2009) 5485–5496. doi:10.1021/pr900480f.

[172] S. Giacomazzi, N. Cochet, Environmental impact of diuron transformation: a review, Chemosphere. 56 (2004) 1021–1032. doi:https://doi.org/10.1016/j.chemosphere.2004.04.061.

[173] K. Al-Khatib, Photosystem I (PSI) Electron Diverter, Univ. Calif. (n.d.). http://herbicidesymptoms.ipm.ucanr.edu/MOA/Photosystem_I_PSI_Electron_Diverter/ (accessed August 4, 2019).

[174] J.S. Bus, S.D. Aust, J.E. Gibson, Paraquat toxicity: proposed mechanism of action involving lipid peroxidation, Environ. Health Perspect. Vol.16 (1976) 139–146.

[175] S.J. Seok, H.W. Gil, D.S. Jeong, J.O. Yang, E.Y. Lee, S.Y. Hong, Paraquat intoxication in subjects who attempt suicide: Why they chose paraquat, Korean J. Intern. Med. 24 (2009) 247–251. doi:10.3904/kjim.2009.24.3.247.

[176] M.F. Zaranyika, S. Nyoni, Degradation of Paraquat in the Aquatic Environment: A proposed Enzymatic Kinetic Model that takes into account adsorption/desorption of the Herbicide by Colloidal and Sediment Particles, Int. J. Res. Chem. Environ. 3 (2013) 26–35.

[177] Court of First Instance of the European Communities, The court of first instance annuls the directive authorizing paraquat as an active plant protection substance, (2007).

[178] R. Zamora-sequeira, R. Starbird-p, O. Rojas-carillo, C. Rica, What are the Main Sensor

Methods for Quantifying Pesticides in Agricultural Activities ? A Review, (2019) 1–26.

[179] J.Z. Zhang, P. Bombelli, K.P. Sokol, A. Fantuzzi, A.W. Rutherford, C.J. Howe, E. Reisner, Photoelectrochemistry of Photosystem II in Vitro vs in Vivo, J. Am. Chem. Soc. 140 (2018) 6–9. doi:10.1021/jacs.7b08563.

[180] G. Longatte, F. Rappaport, F.A. Wollman, M. Guille-Collignon, F. Lemaître, Electrochemical Harvesting of Photosynthetic Electrons from Unicellular Algae Population at the Preparative Scale by Using 2,6-dichlorobenzoquinone, Electrochim. Acta. 236 (2017) 337–342. doi:10.1016/j.electacta.2017.03.124.

[181] J.M. Pisciotta, Y. Zou, I. V. Baskakov, Light-dependent electrogenic activity of cyanobacteria, PLoS One. 5 (2010). doi:10.1371/journal.pone.0010821.

[182] G. Longatte, A. Sayegh, J. Delacotte, F. Rappaport, F.A. Wollman, M. Guille-Collignon, F. Lemaître, Investigation of photocurrents resulting from a living unicellular algae suspension with quinones over time, Chem. Sci. 9 (2018) 8271–8281. doi:10.1039/c8sc03058h.

[183] T. Wenzel, D. Härtter, P. Bombelli, C.J. Howe, U. Steiner, Porous translucent electrodes enhance current generation from photosynthetic biofilms, Nat. Commun. 9 (2018) 1–9. doi:10.1038/s41467-018-03320-x.

[184] M. Sawa, A. Fantuzzi, P. Bombelli, C.J. Howe, K. Hellgardt, P.J. Nixon, Electricity generation from digitally printed cyanobacteria, Nat. Commun. 8 (2017) 1–9. doi:10.1038/s41467-017-01084-4.

[185] K.L. Saar, P. Bombelli, D.J. Lea-Smith, T. Call, E.M. Aro, T. Müller, C.J. Howe, T.P.J. Knowles, Enhancing power density of biophotovoltaics by decoupling storage and power delivery, Nat. Energy. 3 (2018) 75–81. doi:10.1038/s41560-017-0073-0.

[186] R.J. Porra, W.A. Thompson, P.E. Kriedemann, Determination of accurate extincton coefficients and simultaneous equations for assaying chlorophylls a and b extracted with four different solvents: verification of the concentration of chlorophyll standards by atomic adsorption spectroscopy, Biochim. Biophys. Acta. (1989) 384–394.

[187] K.J.J. Steinbusch, H.V.M. Hamelers, J.D. Schaap, C. Kampman, C.J.N. Buisman,

Bioelectrochemical ethanol production through mediated acetate reduction by mixed cultures, Environ. Sci. Technol. 44 (2010) 513–517. doi:10.1021/es902371e.

[188] P.A. Leighton, G.S. Forbes, The photochemical decomposition of benzoquinone in water and in alcohol, J. Am. Chem. Soc. 51 (1929) 3549–3559. doi:10.1021/ja01387a006.

[189] R. Rouillon, M. Tocabens, R. Carpentier, A photoelectrochemical cell for detecting pollutant-induced effects on the activity of immobilized cyanobacterium Synechococcus sp . PCC 7942, Enzyme Microb. Technol. 25 (1999) 230–235.

LIST OF FIGURES

LIST OF TABLES

APPENDIX

A.1 List of publications

A.1.1 Peer-reviewed papers:

M. Tucci, P. Bombelli, C. J. Howe, S. Vignolini, S. Bocchi, A. Schievano. A storable mediatorless electrochemical biosensor for herbicide detection, Microorganisms, 7, 630 (2019) 1-14

M. Tucci, M. Grattieri, S. D. Minteer, A. Schievano, P. Cristiani. Microbial amperometric biosensor for online herbicide detection: Photocurrent inhibition of *Anabaena variabilis, Electrochimica Acta 302 (2019) 102-108*

Andrea Schievano, Bruno Rizzi, Andrea Goglio, Giovanni Rusconi Clerici, Rosaria Tizzani, Matteo Tucci, Matteo Broggi, Matteo Lucchini, Antonino Idà. E-Biopond® – Copuling Microbial Electrochemical Technologies to raceway ponds to recover added value from biowaste lechates, *Detritus* 04 (2018) / I-II

A. Goglio, M. Tucci, B. Rizzi, A. Colombo, P. Cristiani, A. Schievano. Microbial recycling cells (MRCs): A new platform of microbial electrochemical technologies based on biocompatible materials, aimed at cycling carbon and nutrients in agro-food systems, *Science of the Total Environment* 649 (2019) 1349–1361.

A.1.2 Conference papers:

M. Tucci, E. Barontini, A. Schievano, M. Papacchini, A. Espinoza-Tofalos, A. Franzetti, P. Cristiani. Influence of environmental factors on MFC-based sensor for wastewater monitoring. *Proceedings of the 8th European Fuel Cell Piero Lunghi Conference* (2109)

P. Cristiani, P. Bonelli, A. Liberale, M. Tucci, M. Papacchini, S. P. Trasatti. Field Testing of Floating Microbial Fuel Cells and Energy Harvesting Related Power Systems. *ECS Meeting Abstracts* (2018) 2258-2258.

M. Tucci, A. Goglio, A. Schievano, P. Cristiani. Floating MFC for BOD monitoring in real time: field test in a wastewater treatment plant. *Proceedings of the 7th European Fuel Cell Piero Lunghi Conference* (2107)

A.2 Congresses and symposia

A.2.1 Oral presentations

M. Tucci, E. Barontini, A. Schievano, M. Papacchini, A. Espinoza-Tofalos, A. Franzetti, P. Cristiani. Influence of environmental factors on MFC-based sensor for wastewater monitoring. *8th European Fuel Cell Piero Lunghi Conference (EFC),* Naples (IT), 8-11December, 2109

M. Tucci, E. Barontini, A. Schievano, M. Papacchini, A. Espinoza-Tofalos, A. Franzetti, P. Cristiani. Light Influence on the Performances of Air-Cathode Floating MFC for Wastewater Monitoring, *The Electrochemical Conference on Energy and the Environment: Bioelectrochemistry and Energy Storage* (ECEE 2019), Glasgow (UK), 21-26 July, 2019

M. Tucci. Floating MFC for real-time wastewater monitoring: Field application, *IUKWC Workshop: Safe and Sustainable Technologies and Strategies for Integrated Freshwater Resource Management*, Mysuru (IND), 25-28 June, 2019

M. Tucci, M. Grattieri, S. D. Minteer, A. Schievano, P. Cristiani. Bioelectrochemical herbicide sensor based on photocurrent inhibition of Anabaena variabilis. *XXV International Symposium on Bioelectrochemistry and Bioenergetics*, Limerick, (IRL) 26-30 May, 2019

M. Tucci, M. Grattieri, S. D. Minteer, A. Schievano, P. Cristiani. Amperometric herbicide biosensor based on photocurrent inhibition of *Anabaena variabilis. International Society for Microbial Electrochemistry and Technology, 4th European Meeting,* Newcastle (UK), 12-14 September 2018

P. Cristiani, P. Bonelli, A. Liberale, M. Tucci, M. Papacchini, S. P. Trasatti. Field Testing of Floating Microbial Fuel Cells and Energy Harvesting Related Power Systems. *233rd ECS Meeting,* Seattle (WA), 13 -17 May 2018

M. Tucci, A. Goglio, P. Cristiani. Wastewater treatment plant field application of a real time MFC-

based BOD sensor. *General Meeting of the International Society for Microbial Electrochemistry and Technology*, Lisbon (PL), 3-6 October 2017

M. Tucci, A. Colombo, A. Goglio, A. Schievano, P. Cristiani. Shock-sensors as a tool for online monitoring of Anaerobic Digestion process. *XXIV International Symposium on Bioelectrochemistry and Bioenergetics*, Lion, (FR), 3-7 July 2017

P. Cristiani, A. Schievano, M. Tucci, G. D'Ippolito, L. Dipasquale, A. Fontana. Electrochemical stimulation of *Thermotoga neapolitana* cultures. *3rd European Meeting of the International Society for Microbial Electrochemistry and Technology*, Rome (IT), 26-28 September 2016

A.2.2 Poster presentations:

M. Tucci, A. Goglio, A. Schievano, P. Cristiani. Floating MFC for BOD monitoring in real time: field test in a wastewater treatment plant. *European Fuel Cell Technology & Applications Conference - Piero Lunghi Conference*, Napoli (IT), 12-15 December 2017

M. Tucci, M. Grattieri, P. Cristiani. Layer-by-layer Glucose microsensor: application in MFC. *3rd European Meeting of the International Society for Microbial Electrochemistry and Technology*, Roma (IT), 26-28 September 2016

A.3 Tutoring

Co-supervisor for MSc thesis: Enrico Barontini "Celle a combustibile microbiche per il monitoraggio ambientale dell'acqua reflua", University of Milan-Bicocca (2019)

A.4 Schools and workshops

A.3.1 Schools:

- 8th European Summer School on Electrochemical Engineering, *Université Paul Sabatier*, 27-31 August 2018
- Prima scuola nazionale sensori chimici, *Società Chimica Italiana*, 24-27 May 2017

- Statistic applied to environmental engineering, Politecnico di Milano, 16 Feb. – 02 Mar. 2017

A.3.2 Workshops:

- Safe and Sustainable Technologies and Strategies for Integrated Freshwater Resource Management, *India UK Water Centre,* Mysore, 25-28 June 2019

A.4 Patents

Patent pending: A. Schievano A. Idà, A. Goglio, M. Tucci. "Sistema integrato di processi bioelettrochimici e fotobioreattori per la coltivazione di microrganismi fotosintetizzatori con il recupero di carbonio e nutrienti da fonti organiche o da acque reflue" (102018000010683 - 29/11/2018) *Electrochemical system for coupling nutrient recovery and wastewater treatment in a microalgal photobioreactors*